

1 Highlights

2 **Amount of carbon fixed, transit time and fate of harvested wood**
3 **products define the climate change mitigation potential of boreal**
4 **forest management - A model analysis**

5 Holger Metzler, Samuli Launiainen, Giulia Vico

- 6 • We evaluate wood production and climate change mitigation potential
7 of boreal forests
- 8 • We combine an ecophysiological growth model with ~~tree-allometries~~
9 ~~from forest inventories~~ forest inventory tree allometries
- 10 • ~~We evaluate wood production and~~ Integrated carbon stocks account for
11 transit times, in contrast to net carbon gain
- 12 • Higher carbon sequestration does not ensure higher climate change mit-
13 igation potential
- 14 • Potential climate change mitigation depends on carbon time away from
15 the atmosphere ~~This is affected by management, including mixing species~~
16 ~~and ages~~ ~~Assessing management options requires following carbon in~~
17 ~~ecosystem and wood products~~

18 Amount of carbon fixed, transit time and fate of
19 harvested wood products define the climate change
20 mitigation potential of boreal forest management - A
21 model analysis

22 Holger Metzler^{a,c,*}, Samuli Launiainen^b, Giulia Vico^a

^a*Department of Crop Production Ecology, Swedish University of Agricultural Sciences
(SLU), PO Box 7043, Uppsala, 750 07, Sweden*

^b*Natural Resources Institute Finland, Latokartanonkaari 9, Helsinki, 00790, Finland*

^c*Present address: Department of Forest Ecology and Management, Swedish University of
Agricultural Sciences (SLU), Skogsmarksgränd 17, Umeå, 901 83, Sweden*

23 **Abstract**

24 Boreal forests are often managed to maximize wood production, but other
25 goals, among which climate change mitigation, are increasingly important.
26 ~~Examining~~ Hence, it is necessary to examine synergies and trade-offs be-
27 tween forest production and its potential for carbon sequestration and cli-
28 mate change mitigation in forest stands ~~requires explicitly accounting for how~~
29 ~~long forest ecosystems and wood products retain carbon from the atmosphere~~
30 ~~(i.e., the carbon transit time)~~. We propose. To this aim, we develop a novel
31 mass-balanced process-based compartmental model that allows following the
32 carbon path from its ~~photosynthetical~~ photosynthetic fixation until its return
33 to the atmosphere by autotrophic or heterotrophic respiration, or by being
34 burnt as wood product. We investigate Following carbon in the system allows
35 to account for how long forest ecosystems and wood products retain carbon
36 from the atmosphere (i.e., the carbon transit time). As example, we apply the
37 model to four management scenarios: i.e., mixed-aged pine, even-aged pine,
38 even-aged spruce, and even-aged mixed forest. ~~The even-aged clear-cut based~~
39 ~~scenarios reduced the carbon amount in the system by one third in the first~~

*Corresponding author: holger.metzler@slu.se

40 18 yr. Considering only the amount of carbon stored in the ecosystem, these
41 initial losses are compensated after 42–45 yr. At , and contrast metrics of
42 performance relative to wood production, carbon sequestration, and climate
43 change mitigation potential. While at the end of an 80 yr rotation, the even-
44 aged forests ~~hold~~ held up to 31 % more carbon than the ~~the~~ mixed-aged forest.
45 However, the mixed-aged forest ~~management is superior to even-aged forest~~
46 ~~management was superior~~ during almost the entire rotation when factoring
47 in the carbon retention time away from the atmosphere, i.e., in terms of
48 climate change mitigation potential. Importantly, scenarios that maximize
49 production or amount of carbon stored in the ecosystems are not necessarily
50 the most beneficial for carbon retention away from the atmosphere. These
51 results underline the importance of considering carbon transit time when
52 evaluating forest management options for potential climate change mitigation
53 ~~and hence explicitly tracking carbon in the system, e.g. via models like~~
54 ~~the one developed here.~~

55 *Keywords:* boreal forest ~~management~~, wood production, carbon
56 sequestration, transit time, climate change mitigation, process-based
57 modelling

58 Statements and Declarations

59 **Competing Interests:** The authors have no relevant financial or non-
60 financial interests to disclose.

61 **Code Repository:** The Python code to reproduce the figures used in the
62 manuscript is available as a documented package at <https://github.com/goujou/BFCPM/tree/revision2>.

64 In case of publication this repository will be transformed into a permanent
65 repository with DOI.

66 **1. Introduction**

67 Boreal forests are one of the largest biomes on Earth and strongly reg-
68 ulate global climate through land-surface energy, water and carbon cycles
69 (Bonan, 2008, Chapin III et al., 2000, Baldocchi et al., 2000). These forests
70 are in large part managed (Högberg et al., 2021), often to maximize tim-
71 ber production and economic income (Millennium Ecosystem Assessment,
72 2005). They comprise approximately 45 % of the global stock of growing
73 timber (Vanharen et al., 2012), contributing to the economic well-being and
74 cultural heritage of the Nordic societies (Millennium Ecosystem Assessment,
75 2005, Vanhanen et al., 2012) and providing numerous ecosystem services
76 (Maes et al., 2016, Vihervaara et al., 2010). Nevertheless, the focus on pro-
77 duction has led to degradation of other important ecosystem services, among
78 which climate regulation, collectable goods, recreation, water regulation and
79 purification, maintenance of soil productivity and air-quality regulation (Po-
80 hjanmies et al., 2017).

81 There is an increasing commitment to more sustainable forest manage-
82 ment and ~~preserving~~preservation of ecosystem services (Larsen et al., 2022,
83 Kellomäki, 2022). There is also an increasing interest in carbon sequestration
84 by boreal forests ~~to~~ support the rapid net emission reductions required to
85 avoid exceeding global tipping points of the climate system (Lenton et al.,
86 2008). Indeed, boreal forests have potential for climate change mitigation by
87 holding CO₂ away from the atmosphere ~~stored as carbon for long periods~~
88 (Pan et al., 2011). To which extent carbon retention potential and wood
89 production clash is a key question when planning management strategies for
90 the future.

91 ~~To evaluate the potential for climate change mitigation of forest managements~~
92 ~~we need to quantify the forest's wood production and subsequent fate of~~
93 ~~harvested wood products and the associated carbon.~~

94 A commonly employed metric of carbon sequestration and climate change
95 mitigation potential is the net ecosystem carbon gain over a certain amount of

time (Pukkala, 2020, Sterek et al., 2021)(Pukkala, 2020). This metric ignores the carbon transit time outside the atmosphere, i.e., however, ignores the time span between the carbon fixation via photosynthesis and its release back to the atmosphere. Yet, the transit time is the period during which this carbon does not contribute to the radiative effects, later referred to as *transit time* (Bolin and Rodhe, 1973, Sierra et al., 2017). Together with the amount of carbon stored, the time the photosynthesized CO₂ remains stored in living plants, residues, soil or wood products determines the *avoided radiative effect* (Sierra et al., 2021) of greenhouse gases emitted to in the atmosphere (i.e., the Global Warming Potential; Shine et al. 1990). Knowing both the amount and time the carbon spends outside the atmosphere is key to quantify the *avoided radiative effect* (Sierra et al., 2021) by storing the carbon in ecosystems or wood products, and hence the climate change mitigation potential. Also the fate of harvested carbon and of legacy carbon, i.e., carbon already in the ecosystem and wood products at the beginning of the forest management cycle, and of harvested carbon needs to be considered. Harvested carbon does not immediately return to the atmosphere but spends considerable time as wood products (Schulze et al., 2020), potentially defining whether ultimately a managed forest is a carbon source or sink (Liski et al., 2001). when evaluating climate change mitigation potential of alternative management regimes. The fate of legacy carbon is of particular relevance to climate change mitigation potential when management is applied to old-growth forests (Luyssaert et al., 2008). Despite their (Luyssaert et al., 2008, Schulze et al., 2020). Despite its importance for climate change mitigation, these aspects have so far not been jointly and systematically quantified the role of transit time of carbon outside the atmosphere when assessing alternative forest management scenarios in their climate-performance has not been systematically analyzed.

Forest management strategies differ in their synergies and trade-offs among economic, biodiversity, and climate change mitigation targets (Pohjanmies et al., 2017). Currently, the predominant approach to timber production

126 ~~in boreal forests is even-aged~~ Even-aged forestry with one to three thin-
127 nings to promote tree growth, followed by a clear cut at the end of the
128 rotation and subsequent regeneration (Pohjanmies et al., 2017). Selection
129 harvesting to maintain has been the prevailing management regime in the
130 boreal zone (Pohjanmies et al., 2017). In the recent decades, there has been
131 increasing interest and pressure to move towards selection harvests. The
132 maintenance of a continuous forest cover of mixed-age, mixed-size, and multi-
133 species stands have been suggested as alternatives has been suggested to
134 better address environmental and societal concerns stemming from even-aged
135 management (Kuuluvainen et al., 2012, Larsen et al., 2022, Kellomäki, 2022).
136 Selection harvesting (also called mixed-aged/uneven-aged management or
137 continuous-cover management) better mimics natural disturbances than clear-cut
138 based harvesting, in regions where stand-replacing natural disturbances are
139 uncommon (e.g., in Fennoscandia) (Gromtsev, 2002, Shorohova et al., 2009, Kuuluvainen et al., 20
140 . Even where stand-replacing disturbances (e.g., wildfires) occur, clear-cut
141 based harvesting does not ensure a suitable share of late-successional forest
142 (Bergeron et al., 2004).

143 The consequences of age and species diversity for production are site- and
144 species-specific (Pukkala et al., 2009, Mikola, 1984, Lähde et al., 2010, Huuskonen et al., 2021, Ho
145 . Results are also mixed regarding ecological and economical outcomes, and
146 dependent on spatial and temporal timescales considered and the quantification
147 approach (Kuuluvainen et al., 2012). Furthermore, how The climate change
148 mitigation potentials in even-aged and mixed-aged, and mixed-species man-
149 agement strategies differ in their climate change mitigation potential remains
150 unclear if considering and their trade-offs with productivity remain unclear,
151 particularly if considering not only the amount of carbon sequestered and not
152 also the transit time during a fixed rotation period but also the carbon transit
153 time and the timescale of interest. Importantly, we do not know whether and
154 to what extent ensuring both short- and long-term carbon sequestration and
155 climate change mitigation reduces biomass and/or wood production Pohjan-

156 mies et al. (2017).

157 The ~~decade-long time scales typical for boreal forest rotation make long~~
158 ~~60 to 100-yr rotation periods make process-based~~ modelling a powerful tool
159 to evaluate the ~~effects of management choices on specific services ecosystem~~
160 ~~services provided by boreal forests differing in age, species distribution, and~~
161 ~~management~~. Most ecological growth and yield models ~~of boreal forests developed~~
162 ~~for boreal forests, however~~ focus mainly on wood production (SORTIE,
163 Pacala et al. 1996; CROBAS, Mäkelä 1997; ~~3PG3-PG~~, Landsberg and War-
164 ing 1997) and less frequently on carbon sequestration (Pukkala 2014, Pukkala
165 2020). Furthermore, most existing models are conceptualized for even-aged
166 ~~management (Kuuluvainen et al., 2012)~~ and do not allow to explore mixed-species
167 ~~or mixed-aged stands (e.g. Hynynen et al., 2002)~~. Models of forest growth
168 ~~applicable to both even- and mixed-aged stands generally compute diameter~~
169 ~~increment or distribution without accounting for carbon fluxes between tree~~
170 ~~organs (Kolström, 1993, Martin-Bollandsås et al., 2008, Pukkala et al., 2009)~~
171 ~~– Importantly, none of these models allows to track carbon and compute the~~
172 ~~transit time, i.e., the time that the carbon spends away from the atmosphere;~~
173 ~~including the role of the fate of flows through trees, soil, and harvested~~
174 wood products. For an effective quantification of climate change mitigation
175 potential, we need a model that describes the carbon stocks and fluxes
176 in the forest during the entire rotation and beyond, including the legacy
177 carbon from before the beginning of the rotation and wood product use
178 after harvest. The model also needs to allow the exploration of a variety of
179 management scenarios, including mixed-aged and mixed-species ones. These
180 carbon flows are essential to compute the carbon transit times and to evaluate
181 the importance of legacy carbon and wood-product use when comparing
182 climate performances of alternative management strategies. The available
183 analyses of the effects of legacy carbon, wood products, and fossil fuel substitution
184 on carbon sinks (Wutzler, 2008, Böttcher et al., 2008a,b) have not included
185 the transit time aspect.

186 Here, we develop a ~~model that follows~~ process-based mass-balanced forest
187 and forest-product model to compute carbon transit times for even-aged,
188 mixed-aged, or mixed-species stands. The model enables following the carbon
189 path from ~~the moment of its photosynthetic fixation from the atmosphere~~
190 ~~its fixation via photosynthesis~~, through its fate in the forest ~~stand affected by~~
191 ~~competition and management~~, until the moment ~~it returns of its return~~ to
192 the atmosphere by respiration or wood-product burning. ~~With the help~~
193 ~~of this model~~, we quantify We use the model to quantify four metrics of
194 performance: wood production, carbon sequestration, and ~~the two alternative~~
195 ~~estimates of~~ climate change mitigation potential~~based on carbon transit time~~.
196 We. We demonstrate how these different metrics of performance lead to
197 contrasting conclusions. We consider four idealized management scenarios
198 during an 80-yr rotation: a continuous-cover, mixed-aged pine forest and
199 even-aged mono- (pine or spruce), or mixed-species (pine and spruce) stands
200 established after clear cutting, and ask:

- 201 • How do ~~management scenarios rank differently when considering transit~~
202 ~~time-based~~ metrics of carbon sequestration and climate change mitigation
203 potential ~~vs carbon sequestration~~ compare in different management
204 scenarios?
- 205 • How important is the fate of harvested wood products when assessing
206 carbon sequestration and climate change mitigation potential?
- 207 • Are there trade-offs ~~across management scenarios~~ between the capacity
208 of forests to produce biomass and sequester carbon and keep it away
209 from the atmosphere?

210 While our model is general, we here We focus on pure and mixed Scots pine
211 (*Pinus sylvestris*) and Norway spruce (*Picea abies*) stands under current
212 ~~climate~~ climatic conditions for southern Finland. As examples, we consider
213 four management scenarios during an 80 yr rotation: a continuous-cover,

214 mixed-age pine forest and even-aged mono- (pine or spruce), or mixed-species
215 (pine and spruce) stands established after clear-cutting.

216 2. Materials and methods

217 We Our primary aim is to compare and contrast different metrics of
218 carbon sequestration and climate change mitigation potential, and to analyze
219 whether these goals are in conflict with wood production. Based on the
220 general mathematical framework for compartmental models (Section 2.1), we
221 introduce different metrics of stand performance representing wood production,
222 carbon sequestration, and climate change mitigation potential (Section 2.2).
223 To determine these metrics, we develop and parameterize a mass-balanced,
224 process-based compartmental model , where the forest and wood-product
225 carbon cycle is described by a (Section 2.3) that allows us to track the carbon
226 path through the trees, soil, and wood products, as needed by one of the
227 climate change mitigation potential metrics. We compare the performance
228 metrics relative to four scenarios of forest management, differing in age- and
229 species composition (Section 2.5).

230 2.1. Mathematical framework for compartmental models

231 Compartmental models are mass-balanced, nonnegative dynamical systems
232 that describe the flow of a material (here carbon) into, through, and out of a
233 set interconnected and well-mixed compartments or, equivalently, pools (here
234 tree organs, soil, and wood products) (Anderson, 1983, Jacquez and Simon, 1993, Luo and Weng,
235 . They can be described mathematically by a d -dimensional system of non-
236 linear and nonautonomous ordinary differential equations .

$$\begin{aligned} \frac{d}{dt} \mathbf{x}(t) &= \mathbf{B}(\mathbf{x}(t), t) \mathbf{x}(t) + \mathbf{u}(\mathbf{x}(t), t), \quad t > 0, \\ \mathbf{x}(0) &= \mathbf{x}^0. \end{aligned} \tag{1}$$

237 Here $\mathbf{x}(t) \in \mathbb{R}^d$ (gC m^{-2}) is the vector of the carbon pools considered at time
 238 $t \geq 0$ (Section 2.3) yr), \mathbf{x}^0 gives their initial sizes (at time $t = 0$) and the
 239 vector-valued function \mathbf{u} ($\text{gC m}^{-2} \text{yr}^{-1}$) represents the input to the system
 240 (in our case via photosynthesis, i.e., the gross primary production of all
 241 trees in the system). The matrix-valued function \mathbf{B} (compartmental matrix)
 242 governs the internal carbon cycling and the release of carbon from the system
 243 (in our case to the atmosphere). The matrix entry B_{mj} (yr^{-1}) denotes the
 244 rate of carbon transferred from pool j to pool m . The dimension d of the
 245 equation system is the number of considered pools that describe the carbon
 246 in the trees, soil, and wood products.

247 The fluxes ($\text{gC m}^{-2} \text{yr}^{-1}$) from pool j to pool m at time t are given by

$$F_{mj}(t) = B_{mj}(\mathbf{x}(t), t) x_j(t), \quad t \geq 0. \quad (2)$$

248 The solution of Eq. (2.3.5) is given by (Brockett, 2015, Theorem 1.6.1)

$$\mathbf{x}(t) = \Phi(t, 0) \mathbf{x}^0 + \int_0^t \Phi(t, \tau) \mathbf{u}(\tau) d\tau, \quad (3)$$

249 where the first term on the right hand side is the part of legacy carbon that
 250 has not yet left the system until time t , and the second term is the amount
 251 of carbon that has entered the system and remained since the beginning of
 252 the simulation. Legacy carbon, given by \mathbf{x}^0 , is the initial amount of carbon
 253 in the tree biomass, the soil, and the wood products at time $t = 0$. The
 254 matrix-valued function Φ denotes the state-transition operator given as the
 255 numerical solution of the matrix equation

$$\begin{aligned} \frac{d}{dt} \Phi(t, s) &= \mathbf{B}(t) \Phi(t, s), \quad 0 < s \leq t, \\ \Phi(s, s) &= \mathbf{I}, \end{aligned} \quad (4)$$

256 where I is the identity matrix. For a vector $\mathbf{x}(s)$ of carbon stocks in different
 257 pools at time s , the vector $\Phi(t, s)\mathbf{x}(s)$ describes the remaining mass (not yet
 258 returned to the atmosphere) and its distribution over the pools at time $t \geq s$.

259

260 This mathematical framework enables us to compute the *transit times*
 261 of carbon through the system (Rasmussen et al., 2016, Metzler et al., 2018)
 262 which are at the basis of the climate change mitigation potential of the
 263 system (Sierra et al., 2021) (see Section 2.2.2). To demonstrate the model
 264 capabilities, we compare four boreal forest management scenarios (Section 2.5),
 265 with reference to their wood production and

266 2.2. Stand performance metrics

267 We assess the performance of forest stands relative to four metrics: wood
 268 production, carbon sequestration as net carbon gain. We also evaluate the
 269 and two climate change mitigation potential estimates. The climate change
 270 mitigation potential estimates are based on the carbon transit time, i.e., the
 271 time during which the fixed carbon remains in the system and hence away
 272 from the atmosphere (Section 2.2).

273 2.2.1. Wood production

274 The wood-product yields till time T are quantified as the integrated
 275 carbon fluxes entering the wood-product pools (WP_S and WP_L , since we
 276 consider short- and long-lasting wood products Y_S and Y_L , respectively; see
 277 Section 2.3.4). Let S and L be the indices of WP_S and WP_L in the carbon
 278 content vector \mathbf{x} , i.e., $x_S = WP_S$ and $x_L = WP_L$. Then

$$Y_S(T) = \int_0^T \sum_{j \neq S} B_{Sj}(t) x_j(t) dt \quad \text{and} \tag{5}$$

$$Y_L(T) = \int_0^T \sum_{j \neq L} B_{Lj}(t) x_j(t) dt.$$

279 *2.2.2. Carbon sequestration and climate change mitigation potential*

280 We quantify carbon sequestration and the potential for climate change
 281 mitigation via three metrics. We contrast the results relative to the entire
 282 system (including wood products) with those for the forest stand only, because
 283 the wood products can be a crucial factor for whether a forest stand subject to
 284 a specific management scenario is a carbon sink or source (Liski et al., 2001)

285 ~

286 As metric of carbon sequestration we use the Integrated Net Carbon
 287 Balance, INCB(T), i.e., the net carbon gain or loss over the time interval
 288 $[0, T]$, defined as the integrated carbon inputs to the system minus the
 289 integrated outputs from the system. Note that INCB(T) does not consider
 290 when the carbon uptake or release have taken place. Mathematically,

$$290 \text{INCB}(T) = \int_0^T \|\mathbf{u}(t) - \mathbf{r}(t)\| dt = \|\mathbf{x}(T)\| - \|\mathbf{x}^0\|, \quad (6)$$

291 where the carbon inputs at a generic time t are given by $\|\mathbf{u}(t)\|$, with
 292 $\|\mathbf{u}(t)\| = \sum_m |u_m(t)|$, and the carbon outputs from pool j are given by

$$290 r_j(t) = - \sum_m B_{mj}(t) x_j(t). \quad (7)$$

293 INCB is closely related to integrated net ecosystem production(NEP, Randerson et al. 2002
 294), with the difference that INCB includes wood-product carbon. INCB has
 295 dimensions of mass, because it is the result of integrating fluxes (which have
 296 dimension mass/time) over time. INCB can also be described as the total
 297 carbon stocks at time $t = T$ minus the total stocks at time $t = 0$. Hence,
 298 to compute INCB over the rotation, only the total carbon stocks at the
 299 beginning and end of the rotation are needed.

300 As first metric of climate change mitigation potential we use the Integrated

301 Inputs Transit Time (IITT), originally named Carbon Sequestration (CS) by
 302 Sierra et al. (2021). IITT accounts for both the amount of carbon entering
 303 the system during the period of interest (via photosynthesis in our case) and
 304 the time that it spends in the system. IITT for the time period $[0, T]$ is
 305 given by

$$IITT(T) = \int_0^T \int_0^t \|\Phi(t, \tau) \mathbf{u}(\tau)\| d\tau dt. \quad (8)$$

306 Computing IITT requires the time each atom of carbon has spent inside
 307 the system, i.e., in practice a compartmental model (Section 2.1), whose
 308 state transition operator Φ allows us to track all carbon fluxes in the system
 309 during the rotation. Hence, the time spent by newly fixed carbon inside
 310 the system makes IITT. As such, IITT is a measure of climate change
 311 mitigation potential rather than simply carbon sequestration. Nevertheless,
 312 IITT neglects the legacy carbon, i.e., the carbon that was in the system at
 313 the beginning of the period.

314 To overcome the limitation of IITT not considering legacy carbon, we use
 315 an additional metric of climate change mitigation potential, the Integrated
 316 Carbon Stocks (ICS). This metric is based on the same transit-time concept
 317 as IITT but additionally includes the fate of the legacy carbon already in
 318 the system at $t = 0$. The ICS for the period $[0, T]$ is computed as

$$ICS(T) = \int_0^T \|\Phi(t, 0) \mathbf{x}^0\| dt + IITT(T) = \int_0^T \|\mathbf{x}(t)\| dt. \quad (9)$$

319 As follows from the second part of Eq. (9), the computation of ICS merely
 320 requires the time series of total carbon stocks included in all pools during the
 321 rotation. Hence, taking legacy carbon into account, somewhat surprisingly,
 322 simplifies the computation compared with IITT, because ICS emerges to be
 323 the integral of the total carbon stocks in the system over the rotation. The

324 dimension of both IITT and ICS is mass \times time, because they are integrals
325 of mass over time.

326 *2.3. Model description*

327 ~~The model describes~~ To compute the introduced performance metrics,
328 particularly IITT, we developed a tree and stand level model describing
329 the carbon dynamics in a horizontally homogeneous forest stand comprising
330 *n* different *MeanTrees* tree cohorts competing for light. ~~Each *MeanTree* *i*~~
331 ~~represents a cohort~~ The stand structure is affected by growth, mortality, and
332 management decisions. Furthermore, we describe dynamics of carbon in the
333 soil and in the wood products (Fig. 1).

334 The stand comprises several cohorts of trees of density N_i (ha^{-1}), identical
335 in species, age, and size. ~~Different *MeanTrees* can differ in these properties,~~
336 ~~allowing~~, each represented by a *MeanTree* *i*. This allows to describe not only
337 even-aged mono-specific forest stands, but also mixed-aged and/or mixed-
338 species stands. The carbon dynamics and growth of each *MeanTree* are
339 modeled combining a physiologically-based carbon fixation and statistical
340 descriptions of ~~the~~ tree allometry. For the ~~allometry~~ latter, we developed
341 an extension of the Allometrically Constrained Growth and Carbon Alloc-
342 ation model (ACGCA, Ogle and Pacala, 2009). ~~Compared with the original~~
343 ~~formulation, our novel allometric desription explicitly considers to explicitly~~
344 ~~consider~~ the carbon allocation to tree organs based on statistical allometries
345 derived from large experimental data (Lehtonen, 2005, Repola, 2009, Repola
346 and Ahnlund Ulvcrona, 2014). The model describes carbon stocks and fluxes
347 entering the system via photosynthetic CO_2 fixation and then exchanged
348 among the carbon pools within each *MeanTree*, three soil carbon pools and
349 two wood-product carbon pools, and eventually released back to the atmo-
350 sphere. The key state variables of the model are the carbon contents of each
351 pool (Table 1).

352 The model consists of four inter-linked modules: 1) a photosynthesis
353 module, computing the annual gross primary productivity of each *MeanTree*

354 (GPP_i), based on the Atmosphere-Plant Exchange Simulator (APES, Lau-
355 niainen et al. 2015); 2) a tree module, allocating GPP_i to the organs of
356 *MeanTree* i as structural and nonstructural biomass, describing tree-internal
357 and -external fluxes such as growth and maintenance respiration and tissue
358 turnover based on the ~~Allometrically Constrained Growth and Allocation~~
359 ~~Model (ACGCA, Ogle and Pacala 2009)~~ but with ACGCA-model (Ogle and Pacala, 2009)
360 but with an improved carbon allocation driven by statistical allometries de-
361 rived from forest inventory data; 3) a soil carbon module; and 4) a for-
362 est management module, describing the rules for planting and harvesting of
363 *MeanTrees* (Fig. 1) in specific ~~scenarios and the fate sample scenarios and~~
364 allocation of harvested wood as wood products. The photosynthesis mod-
365 ule is solved at half-hourly ~~timescale time step~~, while the other modules have
366 annual time step. The complete model description and its parameterization
367 ~~is are~~ provided in the Supplementary Information (SI, Section A): ~~only the~~
368 ~~most salient features are discussed here. Environmental~~. The environmental
369 conditions (model forcing) ~~and carbon dynamics parameters~~ are provided in
370 SI, Section B.

371 In order to calculate the stand performance metrics Y_S , Y_L , INCB, IITT,
372 and ICS (Eqs. (5)–(9)) with this model, the involved integrals are computed
373 as sums over yearly time steps through the rotation. For the computation of
374 Y_S , Y_L , and IITT we are required to reconstruct the compartmental matrix
375 $B(t_k)$ in each yearly time step t_k . This is done using a discretized version of
376 the analogous continuous-time approach presented in Metzler et al. (2020).
377 Transit-time related computations involving the state-transition matrix Φ are
378 supported by the Python package “CompartmentalSystems” (freely available
379 at <https://github.com/goujou/CompartmentalSystems>).

380 2.3.1. Photosynthesis module

381 The photosynthesis module (SI, Section A.1) computes carbon and wa-
382 ter fluxes in the forest stand, considering competition for light among the
383 *MeanTrees*. The module provides the *MeanTree* annual GPP_i - the carbon

Tree carbon pools

E	transient, available for growth and maintenance
B_L	leaf biomass
C_L	labile, stored as leaf glucose
B_R	fine root biomass
C_R	labile, stored as <u>fine</u> root glucose
B_{OS}	“other” sapwood
B_{OH}	“other” heartwood
B_{TS}	trunk sapwood
B_{TH}	trunk heartwood
C_S	labile, stored as sapwood glucose

Soil carbon pools

Litter	fast litter
CWD	coarse woody debris
SOC	soil organic carbon

Wood-product carbon pools

WP_S	short-lasting wood products
WP_L	long-lasting wood products

Table 1: State variables of the different model components (gC m^{-2}).

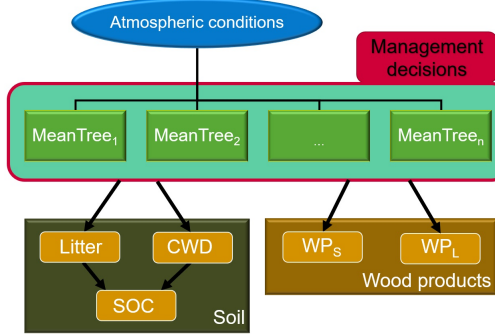


Figure 1: Scheme of the model. Several *MeanTrees* (green boxes) interact with the soil components (dark green box) and the wood product (wood-product) components (brown box). The atmospheric conditions are the forcing of the carbon dynamics. The photosynthesis module quantifies for each *MeanTree* i the annual GPP_i to be distributed to ten tree carbon compartments (carbon pools shown in Fig. 2). Management decisions (i.e., planting, thinning, and cutting) are applied to each *MeanTree* and affect the stand composition and tree carbon distribution to soil and wood-product pools.

384 input to the tree module. The stand structure, i.e., the maximum leaf-area
 385 index (LAI) and leaf-area density profiles and heights of each *MeanTree*,
 386 are provided by the tree module (Section 2.3.2) at the beginning of each
 387 year. The light environment and leaf photosynthesis and transpiration rates
 388 are solved separately for the sunlit and shaded parts of each canopy layer
 389 (1 m height each), using well-established biogeochemical models (model and
 390 stomatal optimality principles (Farquhar et al., 1980, Medlyn et al., 2012,
 391 Launiainen et al., 2015). The photosynthesis module includes sub-models
 392 to account for the seasonal leaf-area dynamics and photosynthetic acclima-
 393 tion (Launiainen et al., 2015, 2019), and the feedback of restricted soil water
 394 availability in the root zone to leaf gas-exchange (Launiainen et al., 2022).
 395 The root zone is described as a single water storage and is equally accessible
 396 to each *MeanTree*.

397 *2.3.2. Tree module*

398 The tree module (SI, Section A.2) describes the partitioning of the annual
 399 $GPP = \sum_{i=1}^n GPP_i$ to maintenance and growth of a *MeanTree*'s organs

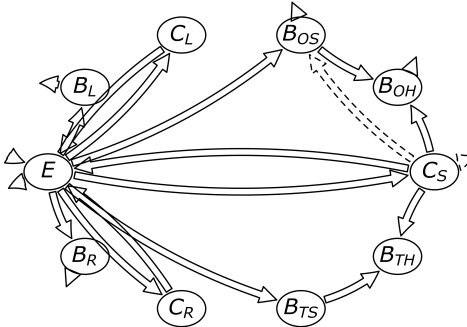


Figure 2: ~~Complete carbon model of Carbon budget and flows in a *MeanTree*~~. Symbols inside the pools are the state variables of the ~~model's~~-tree module (Table 1). In the “static” and “shrinking” states, there is an additional flux from the labile carbon storage (C_S) to B_{OS} to support the regrowth of “other” wood. The ~~the~~-associated growth respiration flux leaves from C_S (dashed arrows).

400 (Fig. 2). All tree module variables are shown in SI, Table A.2.

401 Each *MeanTree* has ten carbon pools, representing structural (B) and
 402 nonstructural (C) carbon in leaves (B_L, C_L), fine roots (B_R, C_R), coarse
 403 roots and branches (~~subscript O, i.e., sapwood (B_{OS} , subscript “O” stands for~~
 404 “other”) sapwood (B_{OS}), and heartwood (B_{OH}), as well as the trunk (~~subscript~~
 405 T) sapwood (B_{TS}) and heartwood (B_{TH}). Coarse roots and branches and the
 406 trunk share a single nonstructural labile storage pool C_S , and carbon input
 407 from photosynthesis is temporarily stored in a transient pool E (Fig. 2).

408 At the beginning of ~~the new year, each year, in each *MeanTree*~~ the GPP
 409 from the previous year is placed in the transient pool E . Losses from this pool
 410 occur via maintenance respiration (R_M) of leaves, fine roots, sapwood, and
 411 growth respiration. Respired tree carbon returns directly to the atmosphere.
 412 Tissues are also lost at tissue-specific ~~rates due to senescence senescence rates~~.
 413 When senescing biomass leaves the *MeanTree*, the associated carbon in the
 414 labile storage pool (C_L, C_R , or C_S) returns to the transient pool E , where
 415 it becomes available again for allocation during the subsequent year. ~~The~~

416 structural carbon of senescing biomass becomes input for the soil module.

417 Thinning and cutting events reduce the number of trees (N_i) represented
418 by a *MeanTree* i . Part of the carbon stored in the harvested biomass is turned
419 into short- (WP_S) or long-lasting (WP_L) wood products (SI, Section A.5)
420 ~~, while the with the partitioning depending on dimensions of the harvested~~
421 ~~trunk wood. The~~ cutting residues are either left on site ~~(litter input for soil~~
422 ~~module) and provide litter or coarse woody debris input for the soil module~~
423 or can become short-lasting bioenergy (part of WP_S).

424 The ~~amount of~~ carbon available for allocation after the annual mainte-
425 nance respiration is $C_{\text{alloc}} \Delta t := E - R_M \Delta t$, where $\Delta t = 1 \text{ yr}$. When the tree
426 is healthy, its allocation to labile storage, tissue growth, and growth respira-
427 tion is based on species-specific statistical ~~models describing the dependence~~
428 ~~of allometric relationships linking~~ the *MeanTree* organs' biomasses ~~on to~~
429 its diameter at breast height (dbh) (SI, Section A.3.1). ~~These data-driven~~
430 ~~dynamic relationships~~). These dynamic relationships are based on forest
431 inventory data (Repola, 2009, Repola and Ahnlund Ulvcrona, 2014, Lehtonen, 2005)
432 ~~and~~ overcome a limitation of the original ACGCA model, where the tree al-
433 lometries were defined by time-invariant ~~parameter values~~ parameters (SI,
434 Section A.3.2). For simplicity, the species-specific fine root-to-leaf biomass
435 ratio (ρ_{RL}) is assumed constant.

436 With the allometrically-based information on tree organ biomasses based
437 on dbh, we apply an iterative root-search algorithm to identify the annual
438 radial growth Δdbh such that all available carbon ($C_{\text{alloc}} \Delta t$) is used to re-
439 grow tissue lost by senescence and to grow new tissue. The density ρ_W of
440 newly produced sapwood and the sapwood to heartwood ratio are determined
441 dynamically for each year, so that the trunk biomass follows the external al-
442 lometric relationships.

443 The carbon allocated to leaves is split ~~in into~~ three components, tissue
444 growth (B_L), transfer into the labile storage pool (C_L), and growth respira-
445 tion (G_L), so that the ratio of labile storage to leaf structural biomass remains

446 constant (δ_L). The same approach is applied to fine roots (B_R , C_R , δ_R). Conversely, for “other” and trunk, who share a common labile storage pool (C_S),
447 the ratio of labile storage to structural biomass is variable and depends on
448 the density of newly produced sapwood (ρ_W) and species-dependent sapwood
449 parameters (SI, Tables A.3 and A.4). ~~Additional carbon fluxes within the~~
450 ~~MeanTree are related to labile storage returning to the transient pool when~~
451 ~~associated structural biomass is lost due to senescence.~~

452 Should the available photosynthetic carbon input be low, the tree reverts
453 to a “static” physiological state (see SI, Section A.4), in which the regrowth
454 of senescent leaves and fine roots is prioritized, and with tissue is prioritized
455 ($\Delta\text{dbh} = 0$). The regrowth of lost sapwood and heartwood of coarse
456 roots and branches exploits carbon resources from the labile storage pool
457 C_S . If $C_{\text{alloc}} \Delta t$ is insufficient to cover the costs of replacement of senescing
458 leaves and fine roots, the tree switches to a “shrinking” state, where the tree
459 it loses leaf and fine root biomass proportionally to the needs, while “other”
460 organs are regrown from the labile storage. If in subsequent years $C_{\text{alloc}} \Delta t$
461 is again returns to being sufficient to cover all the carbon needs (e.g., due to
462 stand management or favorable environmental conditions), the tree reverts
463 directly to the “healthy” state. If instead the GPP remains low, and the
464 labile carbon storage C_S depletes, the MeanTree dies.

466 2.3.3. Soil module

467 The soil module (Fig. 1; SI, Section A.7) describes soil carbon dynamics
468 based on three pools: fast decomposing litter (Litter), slowly decomposing
469 coarse woody debris (CWD), and soil organic carbon (SOC). We included a
470 single only one soil organic carbon pool because we focus on carbon in the
471 topsoil. Our interest in yearly to decadal timescales limits the need for
472 a separation into fast and slow decomposing soil organic carbon pools slowly
473 decomposing SOC (Manzoni and Porporato, 2009). The carbon input from
474 the MeanTrees’ senescing leaves and fine roots enters the soil module as litter
475 fall through provides input to the Litter pool, while sapwood and heartwood

476 carbon due to senescence enters the coarse woody debris pool (CWD).
477 Further soil carbon input occurs from cutting residues that are not removed
478 from the ecosystem and are partitioned similarly to litter fall from living
479 trees (see SI, Section A.5).

480 For simplicity, the decay rates and transfer coefficients between pools are
481 set constant, i.e., we currently neglect the role of inter-annual climatic vari-
482 ability. Decomposing Annually decomposing carbon from Litter and CWD
483 is partly directly respiration to the atmosphere and partly moved to SOC, from
484 where it is eventually respiration.

485 *2.3.4. Management and wood-product module*

486 The forest management module defines the management actions applied
487 to *MeanTrees* in the stand. Management includes i) initial planting of new
488 *MeanTrees* of given species and initial size (dbh_i) at a density N_i ; ii) thinning
489 (i.e., partial reduction of a *MeanTree*'s N_i); iii) cutting (complete removal of
490 the *MeanTree*), and iv) potential replanting of a new *MeanTree* after cutting.
491 The cutting can be planned or caused by the death of the *MeanTree*, which
492 happens when in the “shrinking” state the labile storage pool (C_S) is depleted.

493 When a tree in a stand is removed by thinning or cutting, the tree carbon
494 is transferred to the soil and to short- and long-term wood-product pools
495 depending on the tree's species, size, and its taper curve (see SI, Section A.5).
496 The carbon transferred to wood-product pools is removed from the stand.

497 *2.3.5. Mathematical formulation of the model*

498 The model can mathematically be represented as a compartmental system
499 (Anderson, 1983, Jaquez and Simon, 1993, Luo and Weng, 2011, Sierra and Müller, 2015, Sierra
500 and described by a d -dimensional system of nonlinear and nonautonomous

501 ordinary differential equations,

$$\frac{d}{dt} \mathbf{x}(t) = \mathbf{B}(\mathbf{x}(t), t) \mathbf{x}(t) + \mathbf{u}(\mathbf{x}(t), t), \quad t > 0,$$
$$\mathbf{x}(0) = \mathbf{x}^0.$$

502 Here $\mathbf{x}(t) \in \mathbb{R}^d$ (gC m^{-2}) is the vector of carbon pools at time $t \geq 0$ (yr),
503 \mathbf{x}^0 gives their initial sizes at time $t = 0$ and the vector-valued function \mathbf{u}
504 ($\text{gC m}^{-2} \text{yr}^{-1}$) represents the gross photosynthetic input to the system ($\text{GPP} = \sum_{i=1}^n \text{GPP}_i$).
505 The matrix-valued function \mathbf{B} (compartmental matrix) governs the internal
506 carbon cycling and the release of carbon from the system to the atmosphere.
507 The matrix entry B_{ij} denotes the rate of carbon transferred from pool j to
508 pool i . The dimension of the equation system is $d = 10n + 3 + 2$, comprising
509 ten pools for each of the n Mean Trees, three soil carbon pools, and two
510 wood-product pools.

511 Fluxes ($\text{gC m}^{-2} \text{yr}^{-1}$) from pool j to pool i at time t are given by

$$F_{ij}(t) = B_{ij}(\mathbf{x}(t), t) x_j(t), \quad t \geq 0.$$

512 By running the (discretely implemented) model and storing all pool sizes and
513 fluxes through time, we can reconstruct the compartmental matrices $\mathbf{B}(t_k)$
514 (Metzler et al., 2020) for all time steps t_k . This allows us to compute the
515 transit times of carbon through the system (Rasmussen et al., 2016, Metzler et al., 2018)
516 and to quantify the climate change mitigation potential of the system (Bolin and Rodhe, 1973, Sierra
517 (see Section 2.2.2)).

518 The solution of Eq. is given by (Brockett, 2015, Theorem 1.6.1)

$$\mathbf{x}(t) = \Phi(t, 0) \mathbf{x}^0 + \int_0^t \Phi(t, \tau) \mathbf{u}(\tau) d\tau,$$

519 where the first term on the right hand side is the remaining legacy carbon

520 at time t and the second term is the amount of carbon that has entered the
521 system and remained since the beginning of the simulation. Legacy carbon,
522 given by \mathbf{x}^0 , is the initial amount in the vegetation biomass, the soil, and
523 the wood products at time $t = 0$. The matrix-valued function Φ denotes
524 the state-transition operator given as the numerical solution of the matrix
525 equation

$$\frac{d}{dt}\Phi(t, s) = \mathbf{B}(t)\Phi(t, s), \quad 0 < s \leq t,$$
$$\Phi(s, s) = \mathbf{I},$$

526 where \mathbf{I} is the identity matrix. For a vector $\mathbf{x}(s)$ of carbon stocks in different
527 pools at time s , the vector $\Phi(t, s)\mathbf{x}(s)$ describes the remaining mass (not yet
528 returned to the atmosphere) and its distribution over the pools at time $t \geq s$.

529

530 2.4. *Performance metrics for Simulations and explored management scenarios*

532 We assess the performance of alternative scenarios by measuring their
533 wood production, carbon sequestration and climate change mitigation potential.

534

535 2.4.1. *Wood production*

536 The short-lasting (Y_S) and long-lasting (Y_L) wood product yields until
537 time T are quantified as the integrated carbon fluxes entering the short-
538 and long-lasting wood product pools (WP_S and WP_L), respectively. Let S
539 and L be the indices of WP_S and WP_L in the carbon content vector \mathbf{x} , i.e.,

540 $x_S = \text{WP}_S$ and $x_L = \text{WP}_L$. Then

$$Y_S(T) = \int_0^T \sum_{j \neq S} B_{Sj}(t) x_j(t) dt \quad \text{and}$$
$$Y_L(T) = \int_0^T \sum_{j \neq L} B_{Lj}(t) x_j(t) dt.$$

541 *2.4.1. Carbon sequestration and climate change mitigation potential*

542 We quantify carbon sequestration and the potential for climate change
543 mitigation via three metrics, measuring the net carbon gain and the time
544 that carbon is held in the system (i.e., away from the atmosphere). We
545 contrast the results relative to the entire system (including wood products)
546 with those for the forest stand only, because the wood products can be a
547 crucial factor for whether a forest stand subject to a specific management
548 scenario is a carbon sink or source (Liski et al., 2001).

549 We measure carbon sequestration via the Integrated Net Carbon Balance
550 (INCB). At time T , INCB(T) quantifies the net gain or loss over a certain
551 time interval $[0, T]$, but without considering *when* the carbon uptake or
552 release have taken place. It is quantified as the integrated carbon inputs
553 to the system minus the integrated outputs from the system over a certain
554 period of time. The INCB can also be described as the total carbon stocks
555 at time T minus the total stocks at time $t = 0$. Hence,

$$\text{INCB}(T) = \int_0^T \|\mathbf{u}(t) - \mathbf{r}(t)\| dt = \|\mathbf{x}(T)\| - \|\mathbf{x}^0\|,$$

556 where the carbon inputs at a generic time t are given by $\|\mathbf{u}(t)\|$, with

557 $\|\mathbf{u}(t)\| = \sum_i |u_i(t)|$, and the carbon outputs from pool j are given by

$$r_j(t) = - \sum_i B_{ij}(t) x_j(t).$$

558 A second metric is the Integrated Inputs Transit Time (IITT, called CS
559 in Sierra et al. 2021). It accounts both for the amount of photosynthetically
560 fixed carbon during the rotation and for the time that this carbon spends
561 outside the atmosphere (i.e., not acting as greenhouse gas), but ignores the
562 storage and release of legacy carbon. The IITT up to time T is given by

$$\text{IITT}(T) = \int_0^T \int_0^t \|\Phi(t, \tau) \mathbf{u}(\tau)\| d\tau dt.$$

563 To overcome the limitation of HTT not considering legacy carbon, we
564 consider a third metric, the Integrated Carbon Stocks (ICS), based on the
565 same concept as HTT, but including also the fate of legacy carbon, which is
566 treated as entering the system at $t = 0$. The ICS is computed as

$$\text{ICS}(T) = \int_0^T \|\Phi(t, 0) \mathbf{x}^0\| dt + \text{IITT}(T) = \int_0^T \|\mathbf{x}(t)\| dt.$$

567 While the dimension of INCB is mass, the dimension of both HTT and
568 ICS is mass \times time, because we integrate a mass over time. All three
569 quantities increase as more carbon enters the system, but only the latter
570 two increase if this carbon spends more time in the system. Consequently,
571 HTT and ICS can be used to effectively assess climate change mitigation
572 potential, while INCB is suitable only to quantify carbon sequestration.

573 *2.5. Simulations and management scenarios*

574 Starting with empty To generate the result below, starting with empty
575 tree carbon pools, a common 160 yr spinup (SI, Section C) 160-yr spinup
576 consisting of a mono-specific mixed-aged pine forest stand made of four
577 *MeanTrees* is run to initialize the stand structure and tree, soil, and wood-
578 product carbon pools (SI, Section C). From this single initial state, we con-
579 sider four sample alternative management scenarios leading to different stand
580 compositions and likely, to different wood production, carbon sequestration,
581 and climate change mitigation potential:

582 • Mixed-aged pine stand

583 We maintain a mixed-aged pine stand with a continuous canopy cover.
584 At the beginning of the rotation, the oldest *MeanTree* from the spinup
585 is cut and replanted a new *MeanTree* seedling is planted. Thereafter,
586 every 20 yr the oldest *MeanTree* is cut and a seedling replanted, thus
587 maintaining four *MeanTrees* of ages ranging from 0 to 80 yr and differ-
588 ing among them by 20 yr.

589 • Even-aged single-species stand (pine or spruce) stands

590 After a clear-cut clear cut of the spinup stand, four *MeanTree* pines (or
591 spruces) are replanted. We use planted. We plant four slightly differ-
592 ently sized *MeanTrees* at planting seedlings (dbh = 1.0, 1.2, 1.4, 1.6 cm)
593 to approximate the initial size distribution. The effects of small initial
594 size differences can compound in time due to unequal access to light.

595 • Even-aged mixed-species (pine and spruce) stand

596 After a clear-cut clear cut of the spinup stand, we plant two pine
597 *MeanTrees* and two spruce *MeanTrees*. For both species the initial
598 dbh dbh values are 1.2 and 1.4 cm.

599 In all even-aged scenarios, the *MeanTree* i initially comprises $N_i = 500 \text{ ha}^{-1}$
600 identical trees, while in the mixed-aged scenario $N_i = 375 \text{ ha}^{-1}$. All scenar-
601 ios start with the same initial condition, last for 80 yr, and end with a final
602 felling of all trees, where all tree carbon is transferred to soil- or wood-product

603 pools. The same environmental forcing is used in all simulations, consisting of
604 re-cycled 20 yr meteorological data from Hyytiälä SMEAR II-research
605 station (61.51°N , 24.00°E) in Southern Finland (Launiainen et al., 2022).

606 In even-aged scenarios, a pre-commercial thinning is executed as soon as
607 the mean tree height reaches 3.0 m. All *MeanTrees* are then equally thinned
608 such that the total stand density is reduced from 2000 to 1500 trees per
609 hectare, which equals the stand density of the mixed-aged scenario. When
610 the stand basal area (SBA) reaches $25 \text{ m}^2 \text{ ha}^{-1}$ during any simulation, all
611 *MeanTrees* are uniformly thinned to reduce SBA to $18 \text{ m}^2 \text{ ha}^{-1}$, resembling
612 current recommendations in Finland (Kellomäki, 2022, Kellomäki et al., 2008,
613 Yrjölä, 2002). Such thinning is, however, skipped if a scheduled cutting
614 partial harvest (in the mixed-aged pine scenario) or the final felling (in all
615 simulations) is planned for within the following 10 yr.

616 In the mixed-aged pine scenario, when a *MeanTree* i is cut, it is replanted
617 at density $N_i = 375$ trees per hectare with a delay of 4 yr. This delay in
618 replanting is implemented because the allometric relationships used here are
619 not valid below dbh = 1.0 cm. Hence, the four years of delay approximate
620 the time that seedlings need to grow to a size of dbh = 1.0 cm.

621 When the forest stand becomes increasingly dense, a *MeanTree* might
622 not gather enough carbon from photosynthesis to sustain maintenance and
623 regrowth of senescent biomass. In this case the growth of the *MeanTree* is
624 reduced, and it uses its labile storage (C_S) to regrow senescent coarse roots
625 and branches (see SI, Section A.4). Upon depletion of C_S , the *MeanTree* dies
626 and is removed from the stand by cutting it down and transferring its carbon
627 to the soil and to wood products. This process resembles self-thinning, and
628 is called *emergency removal* of the *MeanTree*. At the time of an emergency
629 removal of a dying *MeanTree*, the remaining stand is also equally thinned
630 down to $\text{SBA} = 18 \text{ m}^2 \text{ ha}^{-1}$ in order to minimize the number of thinnings
631 and cuttings that have to be executed.

632 3. Results

633 3.1. Dynamics of stand attributes and biomassunder different management
634 scenarios

635 Despite the common starting point at the end of the spinup, the dynamics
636 of stand attributes and carbon pool dynamics pools differ significantly among
637 the sample management scenarios (Fig. 3).

638 All the even-aged scenarios involve an initial clear cut of the spinup trees
639 and replanting. As a result, mean stand dbh dbh, stand basal area (SBA)
640 and tree carbon stocks are low compared with the mixed-aged pine forest at
641 the beginning of the simulation (Fig. 3). The replanted Planted trees then
642 grow until SBA reaches the $25 \text{ m}^2 \text{ ha}^{-1}$ thinning threshold or a *MeanTree*
643 dies due to persistent light limitations and is subsequently cut. Which event
644 occurs first and its timing depends on the scenario. In the even-aged pine
645 scenario (orange lines) the SBA SBA reaches the thinning threshold after 50
646 and 60 yr; the uniform thinning of all four *MeanTrees* reduces stand density
647 to 1056 and further to 740 trees ha⁻¹ per hectare, respectively.

648 In the even-aged spruce scenario, emergency removals due to persis-
649 tent light-limitations light limitations occur after 40 and 49 yr in the sup-
650 pressed (small) spruces. The remaining *MeanTrees* are equally thinned to
651 $\text{SBA} = 18 \text{ m}^2 \text{ ha}^{-1}$. After 61 yr the SBA SBA-dependent thinning threshold
652 is reached and the two remaining *MeanTrees* are equally thinned. After 65 yr
653 another emergency removal occurs, leaving only one *MeanTree* till the end
654 of the rotation, without any additional thinning. The final stand density in
655 the even-aged spruce scenario is 202 trees ha⁻¹ per hectare.

656 In the mixed-species scenario (red lines) SBA SBA reaches the $25 \text{ m}^2 \text{ ha}^{-1}$
657 thinning threshold after 42, 52, and 61 yr; the uniform thinning of all *MeanTrees*
658 subsequently reduces stand density to 1069, 765 and finally to 547 trees
659 ha⁻¹ per hectare. In all scenarios, when thinning occurs, tree density declines
660 and SBA SBA (Fig. 3B) temporarily decreases. In case of an emergency re-
661 moval, mean dbh dbh increases (Fig. 3A) because the smallest (light-limited)

662 *MeanTree* is removed.

663 The mixed-aged pine forest scenario has radically different stand dynam-
664 ics (blue lines in Fig. 3), because only the tallest *MeanTree* is cut down
665 at the beginning of the simulation and one new small *MeanTree* seedling is
666 replanted. The mean ~~dbh dbh~~ (Fig. 3A) decreases at removal of the
667 largest tree and more so when the seedlings are replanted 4 years later,
668 although changes are small compared with even-aged forests. Also ~~the~~
669 ~~stand basal area SBA~~ (Fig. 3B) and the total tree carbon stock (Fig. 3D) drop
670 upon removal of the dominant *MeanTree*. ~~The initial cutting of the oldest~~
671 ~~tree causes a transfer of 2.3 kgC m⁻² from the tree pools to the soil pools~~
672 ~~(Litter and CWD), whereas 3.2 kgC m⁻² are transferred from tree pools to~~
673 ~~wood-product pools (WP_S and WP_L)~~. Every 20 yr the oldest *MeanTree* has
674 a ~~dbh dbh~~ around 20 cm and is cut and substituted by ~~seedlings~~ a seedling,
675 leading to periodicity in ~~SBA~~ SBA.

676 *3.2. Wood production*

677 The mixed-aged pine scenario is the most productive over the 80-yr ro-
678 tation, having the largest ~~cumulative yield of short- and long-term wood~~
679 ~~products total wood product yield~~ ($Y_S + Y_L = 13.6 \text{ kgC m}^{-2}$). Between
680 1.7 and 2.0 kgC m^{-2} are transferred to the soil pools, and between 2.3 and
681 2.7 kgC m^{-2} to the wood-product pools at each cutting. At the end of the
682 rotation, all trees are cut down and 2.7 and 3.0 kgC m^{-2} ~~are transferred move~~
683 to the soil and wood products, respectively. This scenario is used as reference
684 in further comparisons (see values in Fig. 4A and Table 2). In terms of ~~total~~
685 wood products, the even-aged pine scenario ~~ranks second and~~ is about 88 %
686 as productive in total and 94 % and 83 % in terms of short- and long-lasting
687 wood products, respectively. The even-aged spruce scenario ~~is emerges as~~
688 the least productive, with total wood products of 69 % and short- and long-
689 lasting products of 45 % and 83 % of that of the mixed-aged pine.

690 ~~While in both the~~ In both mixed-aged and the even-aged pine stands ca.
691 60 % of the harvested wood met the ~~dbh dbh~~ and length criteria ~~implemented~~

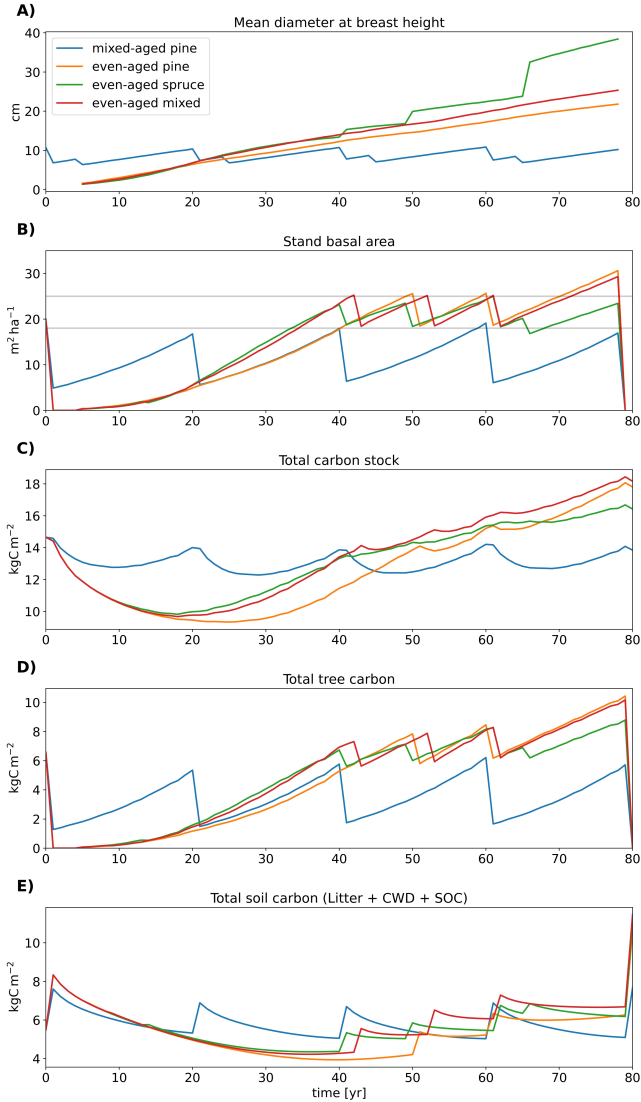


Figure 3: Temporal evolution of key model outputs (panels) for the four management scenarios (colors): A) Tree mean diameter at breast height (cm), averaged over all trees in the stand. B) Stand basal area ($m^2 \text{ha}^{-1}$). Grey lines correspond to $SBA = 25$ and $SBA = 18 \text{m}^2 \text{ha}^{-1}$, i.e., the upper and lower ends of SBA-dependent thinning. C) Total carbon stock including trees, soil, and wood products (kgC m^{-2}). D) Total tree carbon stock (kgC m^{-2}). E) Total soil carbon (Litter + CWD + SOC) (kgC m^{-2}). A detailed attribution of tree carbon to single *MeanTrees* is shown in SI, Fig. E.1.

for long-lasting wood products ~~—additional~~ (SI, Section A.5). Additional mixed-aged pine simulations showed that this percentage strongly increases when ~~stand density decreases, light competition is reduced by decreasing stand density~~ from $N = 2000$ to $N = 1000 \text{ ha}^{-1}$. This, however, reduces the total carbon stock in the system, climate change mitigation potential, and the yield of short-lasting wood products (SI, Fig. E.2).

3.3. Carbon sequestration and climate change mitigation potential

The modelled dynamics of ~~dbh, SBA~~dbh, SBA, carbon stocks, and wood production (Fig. 3) offer insights into the carbon sequestration and the potential for climate change mitigation.

~~The initial clear cut in~~ In the even-aged scenarios, ~~the initial clear cut~~ drastically reduces tree carbon stocks and ~~eecosystem~~stand carbon uptake, while wood-product and soil carbon is continuously lost as CO_2 (Fig. 3D). During the first 18 (spruce and mixed) to 25 yr (pine) the total carbon stock (trees + soil + wood products) in the system decreases by $\approx 5 \text{ gC m}^{-2} \approx 5 \text{ kgC m}^{-2}$, and at the minimum it is less than two thirds of the pre-harvest level. The soil carbon stock is lowest ca. 40 yr after the clear cut, approximately half of the initial value. Later in the rotation, ~~all~~ even-aged ~~pine and mixed species~~ scenarios lead to higher total carbon stock than the continuous-cover scenario (Fig. 3C). About 50 yr ~~in the rotation~~into the rotation, the initial losses are regained (Fig. 3E); ~~this period is referred as to “payback time” in, e.g.,~~ Rolls and Forster (2020).

~~While the differences in total~~ The differences in tree carbon stocks ~~between~~ ~~the three even-aged scenarios are small~~ at the end of the rotation are small among the even-aged scenarios (Fig. 3D), but the total carbon stock is highest in the even-aged ~~mixed pine~~ scenario, followed by even-aged ~~pine mixed~~ and even-aged spruce (Fig. 3C). Conversely, the total carbon stock recovery early in the rotation is most rapid in the fast-growing young spruce stand. In the even-aged ~~management~~ scenarios, it takes ~~42—46 yr~~ 42-46 yr before the total carbon stocks (Integrated Net Carbon Balance, INCB, Fig. 35B) have

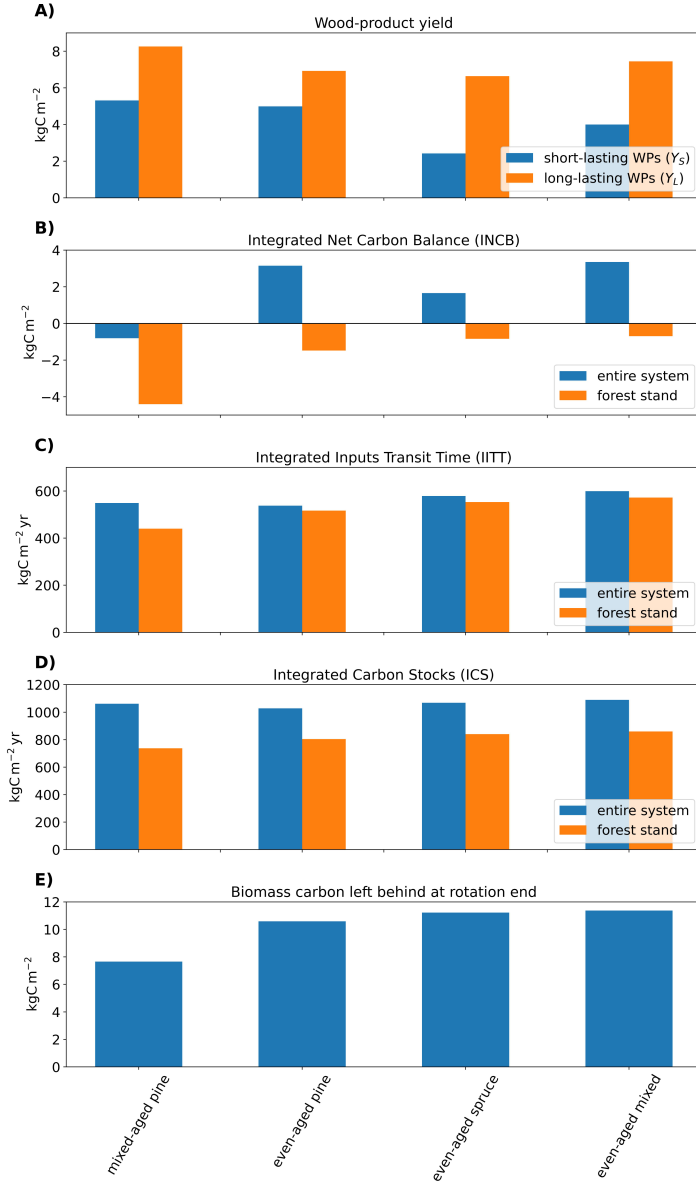


Figure 4: Performance of management scenarios over the ~~whole~~-rotation when wood-product carbon is included (blue bars), and when excluded (forest stand; i.e., tree and soil carbon only; orange bars). Panels refer to the following metrics: A) ~~Integrated wood-product yield as Yield of~~ short-lasting (Y_S) and long-lasting (Y_L) wood-products (Eq. 5). B) Integrated Net Carbon Balance (INCB, Eq. 6). C) Integrated Inputs Transit Time (IITT, Eq. 8). D) Integrated Carbon Stocks (ICS, Eq. 9). E) The carbon left at the site after ~~the clear cut at the end of the rotation~~~~final felling~~; includes carbon in litter, coarse woody debris, and soil organic carbon.

722 recovered from the initial clear-cut loss and are at the level of the mixed-
723 aged (continuous cover) scenario. However, ~~it takes 68 yr in mixed-species~~
724 ~~forest and 70 yr for spruce to compensate the lost climate change mitigation~~
725 ~~potential~~, if considering the time during which carbon is retained from the
726 atmosphere (Integrated Inputs Transit Time, IITT, Fig. 5C), ~~it takes 68 yr~~
727 ~~in the mixed-species and 70 yr for the spruce stand to compensate the lost~~
728 ~~climate change mitigation potential~~. The even-aged pine forest does not
729 ~~compensate for that reach this compensation point~~ within the simulated ~~80 yr~~
730 ~~80-yr~~ rotation.

731 ~~An even more pronounced difference~~ Differences among management sce-
732 ~~narios emerges are even more pronounced~~ when considering also the fate of
733 legacy carbon, i.e., carbon in the system at the beginning of rotation (In-
734 tegrated Carbon Stocks, ICS, Fig. 5D), ~~i.e., the carbon that was in trees,~~
735 ~~soil, or wood products at the beginning of the simulation. Even-aged~~ The
736 ~~even-aged~~ mixed and spruce scenarios are level with the mixed-aged simu-
737 lation only after 72 and 78 yr, respectively. ~~Both IITT and ICS Similar to~~
738 ~~IITT~~ in the even-aged pine scenario ~~fail~~ ICS fails to recover over the entire
739 rotation.

740 ~~When accounting for~~ The absolute values of both IITT and ICS, i.e., the
741 ~~climate change mitigation potential, increase when~~ carbon retention times of
742 wood products ~~are included in the analysis~~ (Table 2, Entire system) instead
743 ~~of considering retention times only in trees and soil~~ (Table 2, Stand only),
744 ~~the absolute values of both IITT and ICS increase~~. Relative increases by
745 including wood products are clearly highest in the mixed-aged pine scenario
746 (IITT: +25 %, ICS: +44 %). Also some rankings of the management scenarios
747 change when ~~including wood products~~ wood products are included (Table 2).

748 In order to assess the effect of different categorization schemes of wood
749 products (FAO, 2022), we additionally assumed wood-product distribution
750 with two extreme wood-product set-ups: short-lasting *only* and long-lasting
751 wood products *only*. This analysis provides the ranges of climate change

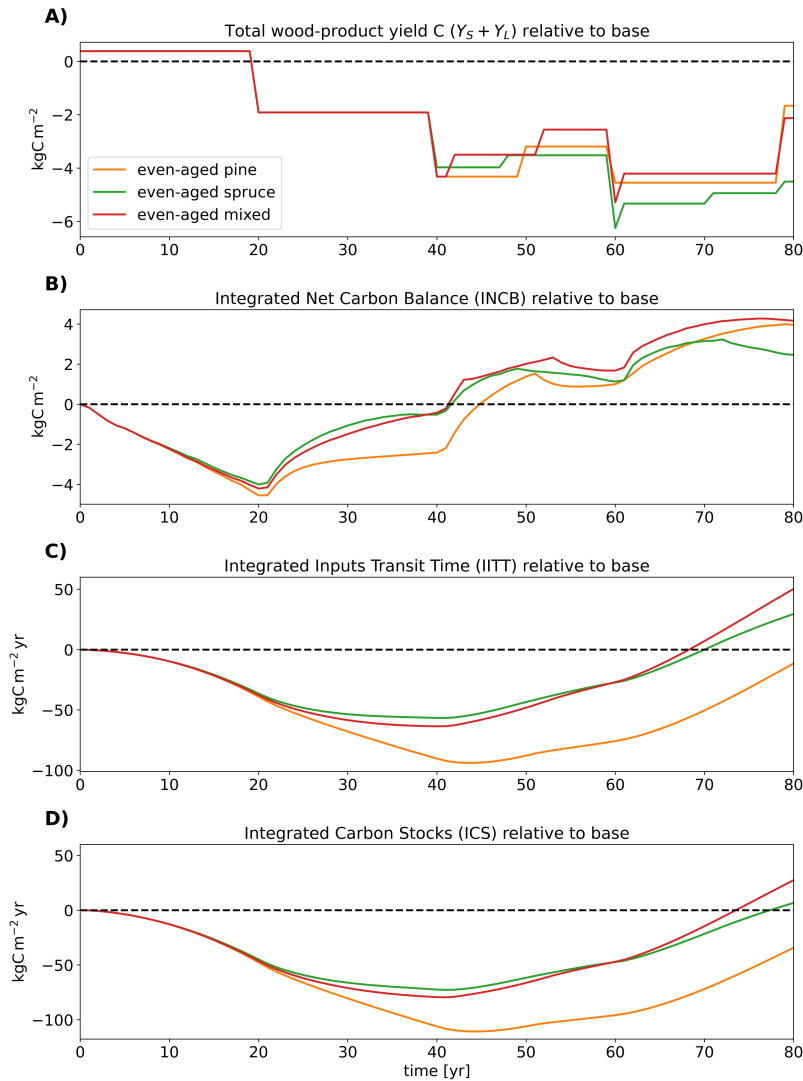


Figure 5:
Temporal evolution Time series of wood production, carbon sequestration, and climate change mitigation potential metrics. A) Total cumulative wood-product yield carbon ($(Y_S + Y_L)$, Eq. 5). B) Integrated Net Carbon Balance (INCB, Eq. 6). C) Integrated Inputs Transit Time (IITT, Eq. 8). D) Integrated Carbon Stocks (ICS, Eq. 9). Values are differences of the even-aged strategies from the mixed-aged scenario.

Metric	Scenario	Entire system		Stand only	
		Rank	Value	Rank	Value
INCB (kgC m ⁻²)	mixed-aged pine	4	-0.8	4	-4.4
	even-aged pine	2	3.2	3	-1.5
	even-aged spruce	3	1.8	2	-0.9
	even-aged mixed	1	3.5	1	-0.6
IITT (kgC m ⁻² yr)	mixed-aged pine	3	549.0	4	440.0
	even-aged pine	4	537.5	3	516.4
	even-aged spruce	2	577.4	2	550.1
	even-aged mixed	1	600.0	1	573.4
ICS (kgC m ⁻² yr)	mixed-aged pine	3	1061.7	4	737.2
	even-aged pine	4	1027.5	3	803.8
	even-aged spruce	2	1067.3	2	837.5
	even-aged mixed	1	1090.0	1	860.8
Y_S (kgC m ⁻²)	mixed-aged pine	1	5.3		
	even-aged pine	2	5.0		
	even-aged spruce	4	2.4		
	even-aged mixed	3	4.0		
Y_L (kgC m ⁻²)	mixed-aged pine	1	8.3		
	even-aged pine	3	6.9		
	even-aged spruce	4	6.9		
	even-aged mixed	2	7.5		
$Y_S + Y_L$ (kgC m ⁻²)	mixed-aged pine	1	13.6		
	even-aged pine	2	11.9		
	even-aged spruce	4	9.4		
	even-aged mixed	3	11.6		

Table 2: Ranking of management scenarios according to carbon sequestration (INCB) and climate change mitigation potential metrics (IITT, ICS), with respect to the entire system (trees, soil, and wood products) and the stand only (trees and soil), and short-lasting (Y_S), long-lasting (Y_L) and combined ($Y_S + Y_L$) wood-product yield. The values correspond to those in Fig. 4

mitigation potential metrics (IITT and ICS) that encompass all potential ways to categorize the harvested wood (Fig. 6). Both IITT (panel A) and ICS (panel B) become more beneficial the more wood is allocated to long-lasting products. Our wood end-use with a short- and a long-lasting pool as described in SI, Section A.5 is located between the two extreme cases (black horizontal lines). In the mixed-aged pine scenario wood end-use has the biggest effect on both IITT and ICS. While wood end-use as short-lasting wood products makes the mixed-aged pine scenario only rank last in terms of climate change mitigation potential, a strong priority on long-lasting wood products lifts the mixed-aged pine scenario to the second rank.

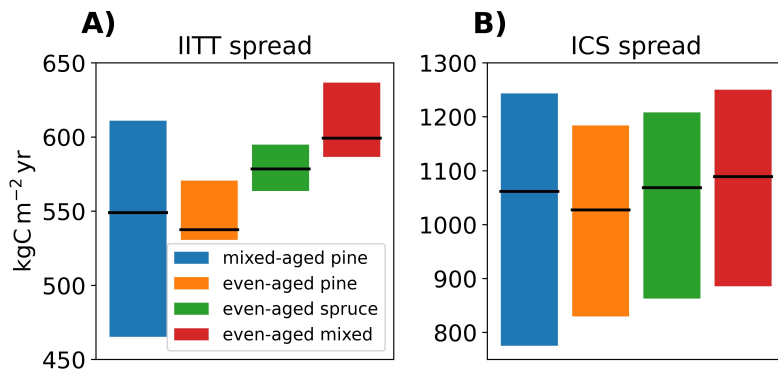


Figure 6: Effect of wood end-use on the climate change mitigation potential metrics in the four different scenarios. The lower end of each bar represents wood end-use as short-lasting wood products only, the upper end long-lasting wood products only. The black horizontal line represents the wood end-use with short- and long-lasting wood products as described in SI, Section A.5. A) Integrated Inputs Transit Time (IITT, Eq. 8). B) Integrated Carbon Stocks (ICS, Eq. 9).

762 4. Discussion

763 4.1. *Methodological considerations*

764 Boreal forest management strategies have commonly been assessed through
765 their economic perspectives

766 The performance of boreal forestry has been commonly assessed through
767 the economic perspectives and wood production over fixed planning hori-
768 zons (e.g., 60—100 yr 60-100-yr rotation cycles). The increasing interest
769 in climate change mitigation by forests and biodiversity conservation (As-
770 trup et al., 2018, Triviño et al., 2023) makes such metrics insufficient. To
771 properly Forest performance needs to be assessed via a combination of metrics
772 describing forest productivity, management and climate change mitigation
773 synergies and trade-offs. In particular, to assess the climate change miti-
774 gation potential of an ecosystem, we must consider the forest management,
775 it is necessary to quantify the amount and timing of carbon fixation, its
776 release and storage dynamics (i.e., the time that carbon spends outside the
777 atmosphere) over the entire rotation and beyond. Contrasting management
778 scenarios thus requires models that can and to track the carbon flow from its
779 photosynthetical fixation, through its use in tree metabolism and growth, to
780 its subsequent transfer to other ecosystem components (e.g., the soil) or to
781 path through the analyzed forest - wood product system until its release via
782 decomposition or the burning of wood products.

783 To address this need, we combined

784 4.1. *Model properties*

785 To quantify metrics of production, carbon sequestration, and climate
786 change mitigation potential at different time scales, we developed a process-based,
787 mass-balanced model that combines an improved version of the Allometri-
788 cally Constrained Growth and Carbon Allocation model (ACGCA, Ogle and
789 Pacala, 2009) with process-based photosynthesis and soil carbon modules,
790 and incorporated harvested wood-product pools. Compared

791 with existing tree and stand-level growth models (see reviews by Hawkes
792 2000, Le Roux et al. 2001, Busing and Mailly 2004) and allocation schemes
793 (see reviews by Ågren and Wikström 1993, Cannell and Dewar 1994, La-
794 cointe 2000), our model has the advantage of resting on a mass-balanced
795 approach described by discretely implemented ordinary differential equa-
796 tions. ~~Our formulation~~ As such, it allows computing the carbon age dis-
797 tributions and transit times directly (Sections 2.1 and 2.2), quantifying not
798 only ~~how much carbon~~ the forest stand ~~stores~~ carbon storage in different
799 pools but also the *avoided* atmospheric radiative warming ~~effect~~ provided by
800 the ~~prolonged~~ storage of carbon ~~in the ecosystem~~ (Sierra et al., 2021) or in
801 (Sierra et al., 2021) in both forest stand and wood products. The quantifi-
802 cation of ~~not only the amount of carbon in the system but also the time~~
803 ~~it spends there storage time~~ is necessary to evaluate the reduction of ~~the~~
804 Global Warming Potential (Shine et al., 1990) ~~for of~~ different management
805 scenarios. ~~We employed a detailed~~ The model developed was necessary to
806 overcome the limitations of the majority of current forest models such as
807 FORMIND (Köhler and Huth, 1998), CABLE (Wang et al., 2010) and 3-PG
808 (Landsberg and Waring, 1997), which either include only tree biomass carbon
809 pools or would require a substantial mathematical reformulation to recast the
810 model as an ordinary differential equation in compartmental form to compute
811 transit times (Section 2.1, Rasmussen et al. 2016, Metzler et al. 2018).

812 The process-based photosynthesis model ~~that~~ quantifies carbon fixation ~~at~~
813 ~~a half-hourly time step~~ for each *MeanTree* (part of APES, Launiainen et al.,
814 2015). ~~In contrast to forest growth models relying on empirical relationships,~~
815 ~~our approach~~, and allows to describe directly the effects of species traits,
816 soil, and climatic conditions, ~~ensuring transferability to other species and~~
817 ~~regions~~. The explicit description of the light environment in the canopy en-
818 ables the consideration of ~~the~~ among-tree competition for light, necessary
819 to simulate mixed-species and mixed-aged forests. As such, we can eval-
820 ate also the prospects of ~~currently uncommon~~ novel management strategies

821 with no or little historical data to rely on. The inclusion of the nonstructural
822 carbohydrate reserve (C_s) allows us to consider the effect of light competition
823 and reduced carbon fixation on tree health and mortality (see SI, Section A.4).
824 The depletion of tree labile carbon storage under prolonged light limitation
825 mimics self-thinning. Indeed, the modelled stand densities in the even-aged
826 spruce and pine scenarios largely follow Reineke's rule (Reineke, 1933), which
827 links tree density and mean dbh (SI, Fig. E.3).

828 A mass-conserving approach is used to compute maintenance and growth
829 respiration and carbon flows based on annually available GPP within each
830 *MeanTree*. This provides a true carbon age distribution for autotrophic
831 respiration, which is comparable with radiocarbon measurements (Carbone et al., 2007, 2013, Muhr
832 . These increasingly available data could support identifying model parameters
833 related to, e.g., nonstructural carbohydrate pools ($\delta_L, \delta_R, \delta_S$) that are otherwise
834 hard to estimate.

835 ~~Process-based descriptions and mass conservation are applied to compute
836 GPP, respiration, and fluxes between system compartments.~~ Carbon allo-
837 cation to tree organs is described via empirical allometric equations , linking
838 tree organ biomass to dbh, derived from species-specific forest inventory
839 data (SI, Section A.3.1). ~~Allometric equations are~~ This is a compromise be-
840 tween a minimalist description and detailed physiology-based functions (Bug-
841 mann, 2001) . ~~At the same time, employing allometries derived from forest~~
842 ~~inventory reduces the effects of internal parameter uncertainties, because they~~
843 ~~ensure that tree carbon allocation is ultimately realistic. The disadvantage~~
844 ~~is that some parameters lack clear ecophysiological meaning and are hard~~
845 ~~to estimate independently and ensures that organ growth follows observed~~
846 ~~allocation patterns in the studied species, while the total biomass growth~~
847 ~~rate is determined by stand structure and environmental conditions. The~~
848 ~~allometric equations are based on even-aged and mostly mono-specific stands~~
849 ~~from Finland (Repola and Ahnlund Ulvcrona, 2014, Repola, 2009, Lehtonen, 2005)~~
850 . Nevertheless, in reality allometries in mixed-species stands can deviate from

851 those of single-species stands (Riofrío et al., 2019). In the current version of
852 the model, allocation does not change with climatic conditions or site fertility
853 - a simplification that could be relaxed by a source-sink based approach as
854 implemented, e.g., in the Quincy model (Thum et al., 2019), which probably
855 amounts to a research project of a size comparable to the one presented
856 here. The species-specific but fixed parameterization of biomass mainte-
857 nance and growth costs and the fine root-to-leaf biomass ratio neglect ~~the~~
858 ~~dynamic behavior of trees in the stand~~
~~tree adaptation to given environmental~~
859 ~~conditions~~. For instance, a reduction in the fine root-to-leaf biomass ratio
860 (ρ_{RL}) ~~leads would lead~~ to reduced carbon allocation to roots and hence more
861 carbon available for ~~stem~~ growth.

862 ~~The detailed description of carbon flows within the *MeanTree* also results~~
863 ~~in allocating carbon from GPP (instead of net primary productivity) to the~~
864 ~~tree organs and to maintenance respiration (Sierra et al., 2022)~~. This is not
865 ~~only more physiologically correct, but provides a true carbon age distribution~~
866 ~~for autotrophic respiration, which is comparable with radiocarbon measurements~~
867 ~~(Carbone et al., 2007, 2013; Muhr et al., 2013)~~. These increasingly available
868 ~~data could support validation or identification of model parameters that are~~
869 ~~otherwise hard to estimate (e.g., those related to nonstructural carbohydrate~~
870 ~~pools – δ_L , δ_R , δ_S).~~

871 ~~The inclusion of the nonstructural carbohydrate pool C_S enables the~~
872 ~~assessment of the tree's health status and its response to external stress~~
873 ~~(Bugmann, 2001)~~, although we employ a simplified description of the transition
874 ~~back to a healthy state~~. This allows us to consider the effects of light
875 ~~limitations and reduced carbon fixation on tree mortality, and of carbon~~
876 ~~release upon competition removal via tree death or different thinning practices~~
877 ~~(see SI, Section A.4)~~. The removal of *MeanTrees* after they have depleted
878 ~~their labile carbon storage under prolonged light limitation mimics self-thinning~~
879 ~~or thinning from below~~. Indeed, the modelled stand density in the even-aged
880 spruce and pine scenarios largely follows Reineke's rule (Reineke, 1933) which

881 links density and mean dbh (SI, Fig. E.3), thus lending support to our
882 resultstrunk growth. We addressed this issue in a sensitivity analysis (see
883 Section 4.1.1).

884 Our model also allows the analysis of single/mixed-species and even/mixed-aged
885 stands. Species and age mixtures are, however, The species- and age-mixtures
886 are considered in a simplified wayneglecting among tree. Among-tree com-
887 petition for water and nutrients and the facilitating effects beyond reduction
888 of competition for light, for instance due to canopy niche complementarity .
889 Furthermore, we assumed that tree allometric relationships are independent
890 of the specific mixture, although in reality mixed-species allometries can
891 deviate from those of single-species stands (Riofrío et al., 2019).-

892 While light, water and temperature limitations are considered, other
893 abiotic and biotic disturbances (e.g., nutrient limitation, pest infestation,
894 wind throw, snow and ice damage) are currently omitted. As such, the
895 estimated carbon sequestration and wood production could be considered a
896 best-case scenario. The are not considered. However, the modular structure
897 of the model ,however, enables additional processes to be easily included or
898 substituted by more detailed descriptions, should data be availableenables
899 easy development of existing modules and inclusion of additional processes.
900 For example, the soil carbon module could be developed to include dynamie
901 deecay rates and transfer coefficients between pools to capture the role of
902 inter-annual climatic variability as in models with more sophisticated structures;
903 such as Roth-C (Jenkinson and Rayner, 1977) or Century (Parton et al., 1987)
904 . Similarly, inclusion of broadleaf species such as birch or other mixtures
905 of three or more species in the simulations is possible. Also understory
906 vegetation, currently omitted, could contribute substantially to the stand
907 carbon dynamics and fill spatial or functional niches. Also the allometric re-
908 lationships could be altered to accommodate forests growing in different and
909 changing conditions, via dynamic rules or competition on water and nutrients
910 among the *MeanTrees*.

911 Sensitivity analysis revealed that growth, stand biomass development,
912 and subsequent tree and soil carbon pool dynamics are most sensitive to
913 parameters relative to sapwood width (SW), wood density (ρ_W), leaf senescence
914 rate (S_L), and maintenance and growth (e.g., R_{mL} , C_{gL} , R_{ms} , C_{gw} ; not
915 shown). This underlines the need for accurate data from field experiments.
916 Another integral part of our model is the description of the tree allometry.
917 Currently, the allometric functions are independent of dynamically changing
918 site properties, such as tree density. The model's generality and applicability
919 could be improved by calibrating the model against growth and yield data
920 from national forest inventory (NFI) plots and introducing tree-density dependent
921 rules, in case data is available. Similarly, the soil carbon module could include
922 dynamic decay rates and transfer coefficients between pools to capture the
923 role of inter-annual climatic variability (e.g., for the dbh-tree height relationship).

924

925 Finally, we note that in this work our primary goal was to illustrate the
926 model capabilities in determining climate change mitigation potential and
927 how that contrasts with other, commonly employed performance metrics.
928 Thus, we considered a single initial state and idealized management scenarios.
929 Nevertheless, whether mixed-aged or even-aged management is more productive
930 might depend on the age structure of the initial stand (Gobakken et al., 2008)
931 as in Roth-C, Jenkinson and Rayner 1977 or Century, Parton et al. 1987).

932 *4.2. Model evaluation and benchmarking*

933 Most of the model's

934 *4.1.1. Benchmarking and sensitivity analysis*

935 We used sub-modules rely based on well-established approaches, which
936 have been extensively tested earlier. For example, the photosynthesis module
937 has already been validated been applied successfully for boreal forests in
938 Fennoscandia (Launiainen et al., 2015, Leppä et al., 2020, Launiainen et al.,
939 2019, 2022). The carbon dynamics of the tree module are is, to a large extent,

940 based on ACGCA, which has previously been successfully used in simulations
941 of tree growth (Fell et al., 2018), gap dynamics (Ogle and Pacala, 2009, Fell
942 and Ogle, 2018), and labile carbon dynamics (Ogle and Pacala, 2009).

943 ~~We~~We further benchmarked the modules against representative observa-
944 tions and data from the literature(see and provide more in-depth tests of
945 the model behavior in SI, Section D).

946 The key model outputswere internally consistent and reasonably in-line
947 with existing data for even-aged single-species forests (such as annual
948 mean diameter growth (SI, Fig. 3; SI, D.1, Repola 2009, Table 3) and total
949 biomass growth rate (Fig. D.1) 3, Berggren Kleja et al. 2007, Fig. 3a) were
950 reasonably well aligned with observations from even-aged single-species forests,
951 lending support to our model and results. The reliable estimates of mean
952 diameter (dbh) growth over 5 yr ensure that also trunk volume growth and
953 resulting yield of short- and long-term wood products are reasonably well
954 simulated over time. Because dbh drives the tree allometry via the external
955 statistical allometries (Lehtonen, 2005, Repola, 2009, Repola and Ahnlund Ulvcrona, 2014)
956 , accordance of modelled mean radial growth with observations lends support
957 to the modelled biomass of the tree organs. Moreover, the mean trunk wood
958 densities ($481 \text{ kg}_{\text{dw}} \text{ m}^{-3}$ for even-aged pine and $385 \text{ kg}_{\text{dw}} \text{ m}^{-3}$ for even-aged
959 spruce) were just outside the ranges observed for pine and spruce forests
960 (Repola 2006, Fig. 4).

961 At stand level and averaged over the rotation, the carbon use efficiency
962 (CUE), i.e., the complement to autotrophic respiration to gross primary pro-
963 ductivity ratio, $(\text{GPP} - R_a)/\text{GPP}$, was comparable (0.49 and 0.32 for even-
964 aged pine and spruce, respectively) with values observed for jack pine (0.34
965 to 0.43) and black spruce (0.29 to 0.39), respectively (Ryan et al., 1997,
966 Table 7). Note that, in order to compare the CUE values with those in
967 literature, we included foliage dark respiration during the day (R_d) in the
968 denominator of the calculated CUE.

969 The modelled total tree biomass carbon for even-aged spruce (6.7 kg C m^{-2}) was

970 within the range observed in 40 yr old forests across Sweden (between 4 and
971 8 kgC m⁻²; Berggren Kleja et al., 2007, Fig. 3a). The mean radial growth
972 over 5 yr of both spruce and pine was in line with forest inventory data
973 (Repola, 2009, Table 3), (SI, Fig. D.1). These reliable estimates of mean
974 radial growth over 5 yr ensure that trunk volume growth is reasonably well
975 simulated over time. Because dbh drives the tree allometry via the external
976 statistical allometries (Lehtonen, 2005, Repola, 2009, Repola and Ahnlund Ulverona, 2014)
977 , accordance of modelled mean radial growth with observations lends support
978 to the modelled biomass of During the process of development and calibration,
979 the model proved most sensitive to four parameters: maintenance respiration
980 rate of leaves (R_{mL}), senescence rate of fine roots (S_R), maximum carboxylation
981 rate at 25°C ($V_{cmax,25}$), and fine root-to-leaf biomass ratio (ρ_{RL}). To analyze
982 whether the parameter uncertainty has major impact on answering the research
983 questions, we ran the four management scenarios by varying the four above
984 mentioned parameters, one at a time, from 90 to 110 % of the values reported
985 in Tables A.1, A.3, and A.4. We computed the relative spread (the tree
986 organs. The mean trunk wood densities (481 kg_{dw} m⁻³ for even-aged pine
987 and 385 kg_{dw} m⁻³ for even-aged spruce) were just outside the ranges emerging
988 from tree inventories (350–460 kg_{dw} m⁻³ difference between the maximum
989 and minimum values divided by the values from simulation with default
990 parameters) of the analyzed metrics, i.e., total carbon stock, total wood-product
991 yield ($Y_S + Y_L$), Integrated Net Carbon Balance (INCB), Integrated Inputs Transit Time (IITT),
992 and Integrated Carbon Stocks (ICS) at the end of the rotation period. The total carbon stock in the even-aged spruce
993 scenario was the most sensitive metric, with particularly high sensitivity
994 to the root-associated parameters S_R and 390–410 kg_{dw} m⁻³ for pine and
995 spruce forests, respectively; Repola 2006, Fig. 4). Deviations possibly arose
996 from discrepancies between literature values for wood density and wood
997 density as derived from allometric relationships, in particular for small trees;
998 and by averaging the wood density over several trees and the entire rotation.

1000 SI, Section D, provides more in-depth tests of the model's biomass predictions.

1001

1002 *4.2. Implications for planning forest management for different goals*

1003 ρ_{RL} (Table E.1). This sensitivity can be explained by the high level of
1004 light competition by shading in dense spruce stands. Any carbon additionally
1005 allocated to roots instead of above-ground biomass growth comes with the
1006 risk of carbon starvation due to low light availability, and mortality of suppressed
1007 trees negatively affects the total amount of carbon in the stand. In general,
1008 the wood-product yield, IITT, and ICS vary less than 15 % when parameter
1009 values of R_{mL} , S_R , and ρ_{RL} vary up to $\pm 10\%$ away from their default values.
1010 All three metrics showed the strongest sensitivity with respect to variations in
1011 leaf-level carbon assimilation capacity (i.e., $V_{cmax,25}$). The sensitivity analysis
1012 showed that, although the values of the different metrics naturally vary with
1013 parameter values, the specific choice and uncertainty of parameter values do
1014 not alter the interpretation of our results and conclusions.

1015 Managed forests need to provide biomass while increasingly supporting
1016 climate change mitigation efforts. These goals are often in contrast (Jandl et al., 2007b; Noormets et
1017 al., 2018), calling for robust approaches and metrics to evaluate benefits and drawbacks
1018 of different management strategies, in support of the scientific and public
1019 debate (Sierra et al., 2021). We developed a model that allows to evaluate
1020 both wood production and

1021 *4.2. Climate change mitigation potential depends on management decisions
1022 and target timescale*

1023 We explored how stand management decisions affect wood-product yield
1024 and alternative climate change mitigation potential of management alternatives
1025 at different timescales. To this aim, the model follows tree-, stand- and
1026 wood-product carbon dynamics and carbon flows from the initial photosynthetic
1027 uptake to the release back into the atmosphere (Fig. 1). We demonstrated
1028 the model capabilities by contrasting metrics under a fixed 80-yr rotation

1029 period. We analyzed four management scenarios that represent idealized
1030 cases of typical management chains in the Nordic countries. The even-aged
1031 single/mixed-species stands scenarios mimic rotational forestry, while the
1032 mixed-aged scenario resembles continuous-cover management.

1033 The results show that, despite the same starting point in terms of
1034 identical initial carbon stocks in trees, soil, and wood products, different
1035 management alternatives lead to drastically different pathways of carbon
1036 stocks and climate change mitigation potential. Regarding metrics (Figs. 3
1037 and 5). Importantly, the ranking of the management scenarios according to
1038 their net carbon sequestration (ICNB) or transit-time based metrics (ITTT
1039 and ICS) depends on the timescale considered (Fig. 5).

1040 We used the mixed-aged pine scenario as a baseline to compare the other
1041 management alternatives. Over the 80-yr rotation, all even-aged scenarios
1042 yield more than the mixed-aged pine after an 80-yr rotation (ICNB, mixed:
1043 +31 %, pine: +29 %, spruce: +19 % lead to higher carbon stock increase
1044 than the mixed-age simulation (ICNB; Fig. 4 ;and Table 2). However,
1045 the initial clear cut and planting at $t = 0$ cause decreasing carbon stocks
1046 during the first ca. 20 yr, and the time for ICNB to reach the level of the
1047 mixed-age scenario is 40–43 yr. In terms of wood products, the mixed-aged
1048 and mixed-species stand management scenarios were the most productive
1049 (Table 2). The high productivity of small-diameter wood in the mixed-aged
1050 and even-aged pine scenarios can support fossil-fuel substitution and climate
1051 change mitigation (Schulze et al., 2020). This is important, given that the
1052 current amount of logging residues in, e.g., Sweden might not suffice in the
1053 future (Börjesson et al., 2017).

1054 While wood Wood production and carbon sequestration are relevant metrics
1055 for forest managers, they are insufficient to quantify for forest owners and
1056 forest industry but insufficient to evaluate the climate impacts of boreal forest
1057 management. For the latter, the time horizon considered, the fate of legacy
1058 carbon (i.e., the carbon initially in the system) and the retention effect of

1059 wood-product carbon are key, as apparent from the differing rankings of
1060 our sample management scenarios. This becomes evident when comparing
1061 the dynamics and scenario-ranking of INCB to those of the transit-time
1062 based metrics IITT and ICS (Table 2 & Fig. 5). Thus, to evaluate
1063 the climate change mitigation potential, the metric ICS (integrated carbon
1064 stocks, including transit times and effects of legacy carbon) is necessary. The
1065 inclusion of retention effects of wood-product carbon into ICS increases the
1066 climate change mitigation potential of the mixed-aged scenario by +44%,
1067 while the In even-aged scenario (pine) with the most increasing scenarios the
1068 decrease in carbon stock and reduced carbon uptake early in the rotation
1069 (Fig. 3C) has a strong negative effect on climate change mitigation poten-
1070 tial improves only by +28%. Our estimated ICS suggests (Fig. 5C, D). The
1071 transit-time based metrics suggest that all the even-aged scenarios are infe-
1072 rior to mixed-aged management, unless the planning horizon is extended to
1073 the end of the 80 yr rotation. The rate at which the even-aged management
1074 scenarios regain their carbon sequestration and climate change mitigation
1075 potential after the clear-cut, compared with the mixed-aged stand (Fig. 5)
1076 or delayed set-a-side management (not considered), must be compared with
1077 the timescales of the climate targets. For instance, Finland aims at carbon
1078 neutrality by 2035 (Huttunen et al., 2022), but our model shows that the
1079 recovery from the initial loss of carbon storage due to clear-cut requires
1080 stand for most part of the rotation period, as it takes almost the entire
1081 80-yr-yr rotation to compensate for the lost climate change mitigation po-
1082 tential. Clear-cut management thus has significant caused by the initial
1083 clear cut. Thus, the climate change mitigation potential of a management
1084 scenario strongly depends on the time scale considered. Long-term effects
1085 and short-term impacts can be in conflict: clear-cut management has nega-
1086 tive effects on short-term (\leq 50 yrs) climate goals (Fig. 5), and can thus
1087 compromise reaching short-term climate targets such as Finland's goal of
1088 reaching carbon neutrality by 2035 (Huttunen et al., 2022).

1089 In addition to wood production, carbon sequestration and Our idealized
1090 scenarios also suggest the higher climate change mitigation potential , there
1091 are other factors (not included in the model) that generally favor mixed-aged
1092 and mixed-species forests Messier et al. (2022). Despite (at least in the short-term)
1093 of mixed-age management does not compromise wood production, in line
1094 with, e.g., Pukkala et al. (2009), Pukkala (2014), Kuuluvainen et al. (2012)
1095 . Similarly, despite lacking an explicit facilitation effect in the model, the
1096 simulated species mixture yielded ca. 9% more total wood products than
1097 a theoretical 50—50 50-50 mix of mono-specific forests (Table 2). Such
1098 slight overyielding is expected (Ruiz-Peinado et al., 2021) overyielding is in
1099 line with Ruiz-Peinado et al. (2021). We can also conclude that pine con-
1100 tributes slightly more than spruce to IITT in the mixed-species simulation
1101 (55 % compared with 45 %). In particular, during the first 50 yr the contri-
1102 bution of pine is much higher than the one of spruce, and later the relative
1103 contribution of spruce increases. However, we cannot disentangle the contri-
1104 butions of different species to INCB and ICS because we cannot attribute the
1105 effects of legacy carbon to a specific species. Moreover, more diverse forests
1106 are less susceptible to biotic and abiotic disturbances such as pest outbreaks
1107 (Jaetel et al., 2021) and extreme weather events (Bauhus et al., 2017), thus
1108 increasing ecosystem stability (Loreau, 2022). Mixed-species forests also
1109 tend to harbor greater biodiversity (Ampoorter et al., 2020) and are also
1110 often more socially accepted (Ribe, 1989, Gundersen and Frivold, 2008). We
1111 emphasize that these results are, however, far from conclusive for making
1112 management decisions because the consequences of age and species diversity
1113 for stand productivity are shown to be highly site- and species-specific in
1114 general (Mikola, 1984, Lähde et al., 2010, Huuskonen et al., 2021, Holmström et al., 2018)
1115 .

1116 4.2.1. Wood end-use is central for climate change mitigation potential
1117 The Food and Agriculture Organization of the United Nations (FAO)
1118 suggests 14 different categories of wood products (FAO, 2022). We considered

here only short-lasting (WP_S) and long-lasting (WP_L) wood products, as this simplification allows us to study the magnitude of the effects of carbon stored in wood products on climate change mitigation potential without delving into economical considerations or wood markets, which would be out of the scope of this manuscript. We attributed harvested trunk wood to WP_S and WP_L according to its diameter and length (SI, Section A.5) to reveal how wood end-use affects the alternative metrics of climate change mitigation potential. Both IITT and ICS increase when carbon retention in wood products is included in the analysis (Table 2, Entire system vs. Stand only), affecting also the ranking of the management scenarios.

We further studied two extreme cases of wood allocation to only short-lasting or only long-lasting wood products. This study allows us to cover the effects of a whole range of potential alternative wood-product categorizations on climate change mitigation potential. Fig. 6 shows that long-lasting wood products have a strong positive effect on climate change mitigation potential. Over the 80-yr horizon considered here, wood end-use has a stronger effect than the differences among stand management scenarios, making it crucial to consider wood end-use and wood-product lifetimes when evaluating climate impacts of forestry (Hurmekoski et al., 2023).

4.3. *Implications for planning climate-smart forest management*

Managed forests need to provide biomass while increasingly supporting climate change mitigation efforts. These goals are often in contrast (Jandl et al., 2007b; Noormets et al., 2014), calling for robust approaches and metrics to evaluate benefits and drawbacks of different management strategies in support of the scientific and public debate (Sierra et al., 2021). While a practically realizable approach to climate-smart forestry needs to take economic aspects into account (Nabuurs et al., 2014; Yousefpour et al., 2018), the theoretical foundation for climate change mitigation requires focus on carbon transit times because the time carbon fixed via photosynthesis remains stored in living plants, residues, soil, or wood products is central to determine the *avoided* global warming effect of carbon sequestration.

1149 Our model makes it possible, for the first time, to contrast boreal forest
1150 stand management with respect to different wood-product (Y_S , Y_L), carbon
1151 sequestration (INCB), and climate change mitigation potential (IITT, ICS)
1152 metrics simultaneously. The INCB (Eq. 6), IITT (Eq. 8) and ICS (Eq. 9)
1153 increase, because more carbon enters the system than is released. However,
1154 only the latter two metrics increase if this carbon spends more time in the
1155 system (and hence outside of the atmosphere). This is because the timing
1156 of carbon uptake and release matters: a large amount of carbon entering
1157 the system towards the end of the rotation has a large impact on INCB,
1158 but contributes little to IITT and ICS. Thus, only the transit-time based
1159 metrics IITT and ICS are measures of climate change mitigation potential.
1160 We emphasize that INCB is suitable only to quantify carbon sequestration,
1161 yet it is often incorrectly used as climate change mitigation potential metric
1162 (Pukkala, 2020). This is likely because computing the explicit transit times,
1163 i.e., using IITT, requires a detailed compartmental model as the one developed
1164 in this study.

1165 Eq. (9) shows that, somewhat surprisingly, ICS is implicitly a transit-time
1166 based metric. The ICS comes with the advantage that its computation does
1167 not explicitly require transit times and the compartmental model, rather just
1168 the time series of total carbon stocks during the rotation. This makes ICS and
1169 equivalent metrics such as rotation-average carbon stocks (Lundmark et al., 2018)
1170 a powerful and widely applicable means to assess climate change mitigation
1171 potential, as long as soil- and wood-product carbon is taken into account.
1172 However, in order to disentangle the effects of legacy carbon and carbon fixed
1173 during the rotation, we need to compute both ICS and IITT, which requires
1174 a detailed compartmental model in the background.

1175 Both the explored boreal forest management scenarios and the newly
1176 developed model act on the level of a single forest stand. It is the fundamental
1177 unit at which management operations are done and also the scale on which
1178 virtually all forest growth models, carbon balance models, and forest simulators

1179 supporting decision making such as MOTTI (Hynynen et al., 2005) or Heureka
1180 (Lämä et al., 2023) operate. Therefore, the stand level was also the natural
1181 scale to analyze and interpret the differences in carbon sequestration and
1182 climate change mitigation potential metrics in this study. We acknowledge
1183 that addressing climate change mitigation potential of forest management
1184 and its trade-offs, e.g., with wood production within a given region and
1185 timescale, depends on the initial stand attributes, site type distribution, and
1186 management history (Hiltunen et al., 2021). Therefore, scenario simulations
1187 to broadly address climate change mitigation potential of forest management
1188 requires, at minimum, simulating representative sub-samples from the true
1189 distribution of forest stands in the region of interest (e.g., Lehtonen et al. 2023, Matala et al. 2009
1190). Our results show that the integrated carbon stocks (ICS), i.e., the integrated
1191 effect of carbon storage over time, is a powerful metric for such an analysis
1192 because of its simple computation and its implicit transit-time dependence.
1193 The proposed process-based model framework can also provide support for
1194 scenario analyses under changing demands, management methods, and climate
1195 conditions not well covered by the commonly used statistical-empirical forest
1196 simulators. To leverage the full capability of the proposed model requires
1197 extensive evaluation and parameter optimization against, e.g., National Forest
1198 Inventory data and growth experiments, to obtain parameter values and
1199 allometric equations for specific species mixtures (Riofrío et al., 2019, Ruiz-Peinado et al., 2021)
1200 and for sites located on a large geographical grid to investigate carefully the
1201 averaged performance metrics on a larger scale (Lemprière et al., 2013).

1202 Upon availability of physiological parameters and allocation rules, inclusion
1203 of broadleaf species such as birch or other mixtures of three or more species in
1204 the simulations is possible. Also understory vegetation, currently neglected
1205 in the model, could contribute substantially to the stand carbon dynamics
1206 and fill spatial or functional niches.

1207 **5. Conclusions**

1208 We developed a forest growth model. Boreal forests are increasingly expected to
1209 cater to different, often contrasting goals, from biomass production to climate
1210 change mitigation. We illustrated how conclusions regarding the performance
1211 of forest stands depend on the metric used, even when considering the same
1212 goal, like climate change mitigation potential. To that end, we developed a
1213 novel forest growth and carbon-balance model that is capable of tracking the
1214 carbon path through the system. The model combines process-based mod-
1215 ules for gross-primary productivity as well as autotrophic and heterotrophic
1216 respiration with mass-conserving statistical carbon allocation in a tree. The
1217 model allows to track It allows to compute the age distribution of carbon in
1218 the tree-soil-wood product system, enabling the quantification of both wood
1219 production, wood production, carbon sequestration, and climate change miti-
1220 gation potential of different forest management scenarios across an entire
1221 rotation. The model was tested and its capabilities demonstrated for four
1222 idealized management scenarios resembling even-aged and continuous-cover
1223 forestry in Fennoscandia of single- or mixed-species stands.

1224 Using the model, we considered four metrics of performance: wood production,
1225 mass-only based carbon sequestration as expressed by the Integrated Net
1226 Carbon Balance (INCB), and transit-time based climate change mitigation
1227 potential as expressed by the Integrated Inputs Transit Time (IITT) and the
1228 Integrated Carbon Stocks (ICS).

1229 Over the 80 yr Our results clearly show that wood production, transit-time
1230 based climate change mitigation potential, and mass-based only carbon sequestration
1231 provide different information and hence ranks of management scenario performances.
1232 For example, when comparing four sample management scenarios over an
1233 80-yr rotation, the wood production was highest in the mixed-aged pine
1234 scenario for both short- and long-lasting wood products. Nevertheless, in
1235 terms of carbon sequestration, all, while carbon sequestration was higher
1236 in the even-aged scenarios were more effective than the mixed-aged strategy,
1237 although. However, the even-aged scenarios show a clearly had lower cli-

1238 mate change mitigation potential for most of the rotation compared ~~with to~~
1239 the mixed-aged scenario. The ~~inclusion of legacy carbon and wood-product~~
1240 ~~retention effects emphasized the advantage of the mixed-aged pine scenario~~
1241 ~~over initial clear-cut based scenarios.~~ While ~~effects on carbon stocks were~~
1242 ~~compensated after 42 – 45 yr, and ultimately even-aged scenarios were sequestering~~
1243 ~~sequestered more carbon over the rotation cycle, the initial clear-cut effects~~
1244 ~~on carbon stocks (INCB) were compensated only after about 42 to 45 yr (i.e.,~~
1245 ~~had higher INCB).~~ However, ~~a the transit-time based metric including metrics,~~
1246 ~~accounting for the retention time of carbon away from the atmosphere (ICS)~~
1247 ~~shows , HTT), show that it takes almost a typical rotation of a typical 80 yr~~
1248 ~~(or longer) rotation or more~~ to compensate for the lost climate regulation
1249 caused by an initial clear cut. It is thus necessary to select the evaluation
1250 metrics based on the desired goal and its time scales and to consider the
1251 fate of the legacy and wood-product carbon, i.e., clearly define the system
1252 boundaries.

1253 These results clearly show that transit-time based ~~When evaluating~~ cli-
1254 mate change mitigation ~~potential and pure carbon sequestration provide~~
1255 ~~different information and hence ranks of management scenario performances.~~
1256 Further, options of forest management, we conclude that it is necessary
1257 to consider also the fate of the legacy carbon and wood-products when
1258 addressing resort to transit-based metrics to determine the avoided radiative
1259 effects of greenhouse gasses in the atmosphere. Nevertheless, an effective
1260 metric of climate change mitigation ~~potential of forestry.~~ It is thus imperative
1261 to select the evaluation metrics based on the desired goal and clearly specify
1262 the timescales of interest when evaluating does not necessarily need to rest on
1263 tracking the path of carbon in the system. We show that ICS is implicitly a
1264 transit-time based metric as it accounts for both the amount and storage time
1265 of carbon uptake in the system (Eq. 9). The computation of ICS requires only
1266 time series of total carbon stocks during the rotation. Therefore, ICS and
1267 equivalent metrics such as rotation-average carbon stocks (Lundmark et al., 2018)

1268 emerge as widely applicable and powerful metrics to assess climate change
1269 mitigation potential of forest management, as long as soil- and wood-product
1270 carbon is taken into account. The in-depth understanding of the different
1271 metrics provides support to future applications.

1272 Author contributions

1273 **Holger Metzler:** methodology, software, validation, formal analysis,
1274 investigation, data curation, writing(~~original draft~~), visualization; **Samuli
1275 Launiainen:** conceptualization, software (photosynthesis module), valida-
1276 tion, writing(~~review & editing~~), funding acquisition; **Giulia Vico:** concep-
1277 tualization, validation, writing (~~review & editing~~), supervision, project ad-
1278 ministration, funding acquisition

1279 Acknowledgements

1280 Funding was provided by the Swedish Research Council for Sustainable
1281 Development FORMAS, under grant (grant number 2018-01820, and), the
1282 Research Council of Finland (grant no. number 348102), and the Knut and
1283 Alice Wallenberg Foundation (grant number 2018.0259). We thank Carlos A.
1284 Sierra, Henrik Hartmann, and David Herrera from Max Planck Institute for
1285 Biogeochemistry Jena, Germany, for fruitful discussions and input, and are
1286 particularly grateful to Carlos A. Sierra for providing access to computing
1287 facilities. We also thank two anonymous reviewers for their constructive
1288 suggestions which allowed us to significantly improve the manuscript.

1289 Supplementary Information

1290 Part A Detailed model description

1291 Photosynthetically fixed carbon enters the the *MeanTrees* as glucose and
1292 is distributed to the single trees represented by the *MeanTree*. Single tree
1293 carbon dynamics are based on ACGCA (Ogle and Pacala, 2009). The glucose
1294 carbon is allocated to tree organs as part of tissues (g_{dw}) and to labile storage
1295 (g_{gluc}). In order to describe single-tree carbon dynamics in units of gC, we
1296 need to convert g_{dw} and g_{gluc} to gC using the two conversion constants

$$\zeta_{dw} := 0.5 \frac{gC}{g_{dw}} \quad \text{and} \quad \zeta_{gluc} := \frac{72}{180.15} \frac{gC}{g_{gluc}}. \quad (\text{A.1})$$

1297 On single-tree level, the carbon cycling is then described in units of gC and
1298 on *MeanTree* level, in the soil, and in wood products in units of gC m^{-2} .

1299 A.1 Photosynthesis module

1300 The photosynthesis module computes gross-primary productivity (GPP_i)
1301 of each *MeanTree* at a half-hourly time step, and accumulates it to annual
1302 GPP_i for the tree module. It uses established approaches to compute needle
1303 level photosynthesis (Farquhar-model with co-limitation, (Farquhar et al.,
1304 1980, Launiainen et al., 2022)) and stomatal conductance (USO, (Medlyn
1305 et al., 2012)). The short-wave radiation, leaf gas-exchange and seasonal
1306 cycle sub-modules are adopted from the multi-layer APES-model (Launiainen
1307 et al., 2015, Leppä et al., 2020) (see summary of parameters in Table A.1).

1308 Rainfall and snow interception, snowpack dynamics and soil water balance
1309 (a bucket model) are based on the SpaFHy -model (Launiainen et al., 2019).

1310 The forest stand consists of one or several *MeanTrees*, whose dimensions
1311 (height and leaf-area density distribution, LAD_i) are updated in the begin-
1312 ning of each year. The stand LAD is computed as the sum of LAD_i s and
1313 determines radiation and wind attenuation in the canopy. The transmittance

1314 and absorption of photosynthetically active radiation (PAR) and fraction of
1315 sunlit foliage at each canopy layer (here 30) are computed following Zhao and
1316 Qualls (2005), with adaptations to coniferous canopy described in Launiainen
1317 et al. (2015). The photosynthesis and transpiration rates are subsequently
1318 computed separately for sunlit and shaded needles of each *MeanTree* and
1319 canopy layer, assuming the leaves are at the air temperature. The leaf-level
1320 rates are then integrated over the leaf-area density and time to provide annual
1321 GPP_t and transpiration of each *MeanTree*.

1322 The response of leaf gas-exchange to limited soil water availability is ac-
1323 counted for by decreasing the USO model parameter g_1 (proportional to
1324 inverse of marginal water use efficiency) and maximum carboxylation rate
1325 ($V_{cmax,25}$) at 25°C whenever relative plant available water (REW) is be-
1326 low a critical threshold. The non-linear response is formulated as $x =$
1327 $x_{ww} \times (\frac{REW}{b_0})^{b_1}$, where x_{ww} is the property ($g_1, V_{cmax,25}$ etc.) in well-watered
1328 conditions, and parameters b_t are fitted based on pine shoot gas-exchange
1329 data from Hyytiälä SMEAR II-site in Southern Finland. For details, see
1330 Launiainen et al. (2022, 2015). A standard approach is used for the tem-
1331 perature response of the Farquhar-model parameters (Medlyn et al., 2002,
1332 Kattge and Knorr, 2007), while the seasonal cycle of photosynthetic capacity
1333 is accounted for by making $V_{cmax,25}$ a function of delayed air temperature
1334 (Kolari et al., 2007). For details, see Supplementary material of Launiainen
1335 et al. (2015) and Launiainen et al. (2022).

1336 The soil water content (θ) is solved with a two-layer bucket model (Lau-
1337 niainen et al., 2019). The top layer resembles organic litter/moss and acts
1338 as a rainfall interception storage, and the lower layer represents the plant
1339 root zone (here depth $D = 0.5$ m), whose hydraulic properties are described
1340 using Van Genuchten's (1980) approach. The snow accumulation and melt
1341 is modelled using the degree-day approach, and rainfall interception is com-
1342 puted assuming the canopy behaves as a single big leaf with one effective
1343 water storage. For details, see Launiainen et al. (2019).

1344 The used needle gas-exchange, radiation and water balance sub-models
 1345 have been tested independently and as part of the evaluation of a multi-layer
 1346 ecosystem model (APES, Launiainen et al., 2015) against observed ecosystem
 1347 level eddy-covariance-based carbon, water and energy fluxes at several boreal
 1348 coniferous forests (Launiainen et al., 2015, Leppä et al., 2020). Moreover, the
 1349 approach has shown to well reproduce the observed non-linear response of
 1350 stand-level GPP and evapotranspiration (ET) to stand leaf-area index (LAI)
 1351 across several boreal forest sites (Launiainen et al., 2015, 2016).

1352 For this work, we further tested that our simplified vertically-resolved
 1353 model, omitting the air temperature and humidity gradients within the canopy
 1354 simulated by APES, predicted the expected non-linear response of ecosystem
 1355 GPP and ET to LAI. We also compared simulated annual ~~GPP~~GPP and
 1356 its inter-annual variability with the long-term ~~time-series~~time series from
 1357 Hyytiälä coniferous forest in Southern Finland (Launiainen et al., 2022) with
 1358 satisfactory results (not shown). The benchmarking lends support that the
 1359 *MeanTree*'s annual GPP_i and its dependency on stand structure, i.e., light
 1360 competition via stand LAD and *MeanTree* LAD profiles, and weather con-
 1361 ditions are adequately described.

Parameter	Value	Description
$V_{cmax,25}$	60 (pine), 50 (spruce) $\text{mol m}^{-2} \text{s}^{-1}$	maximum carboxylation rate at 25°C
$J_{max,25}$	$1.97 \times V_{cmax,25}$	maximum electron transport rate at 25°C, Kattge and Knorr (2007)
$R_{d,25}$	$0.5 \text{ mol m}^{-2} \text{s}^{-1}$	dark respiration rate at 25°C
α	0.3 (-)	quantum efficiency parameter, Launiainen et al. (2022)
θ	0.7 (-)	curvature parameter
β	0.95 (-)	co-limitation parameter
g_1	$2.6 \text{ kPa}^{0.5}$	USO model parameter, Launiainen et al. (2015), Leppä et al. (2020)
g_0	$0.001 \text{ mol m}^{-2} \text{s}^{-1}$	USO model, residual conductance for H_2O , Launiainen et al. (2015)
a_0, a_1	0.39, 0.83	g_1 response to plant available water, Launiainen et al. (2022)
b_0, b_1	0.39, 0.83	$V_{cmax,25}$ response to plant available water, Launiainen et al. (2022)
α_p	0.1 (-)	shoot and ground PAR albedo, Launiainen et al. (2015)
f_{clump}	0.7 (-)	foliage clumping factor, (Launiainen et al., 2015)
W_{max}	$0.2 \text{ kg H}_2\text{O LAI}^{-1}$	canopy interception storage, Launiainen et al. (2019)
D	0.5 m	root zone depth
θ_s	$0.50 \text{ m}^3 \text{m}^{-3}$	porosity
θ_r	$0.03 \text{ m}^3 \text{m}^{-3}$	residual water content
α_s	0.06 m^{-1}	air-entry potential
n	1.35 (-)	pore size distribution parameter

Table A.1: Photosynthesis and water balance model parameters.

1362 *A.2 Tree module*

1363 The tree module represents the dynamics of carbon stocks (in units of
1364 grams of carbon, gC) within each single tree represented by a *MeanTree*.
1365 The *MeanTree* i represents N_i identical single trees per ground area and we
1366 consider the stocks per *MeanTree* in units of gC m⁻².

1367 Each tree's transient pool E receives GPP _{i} (gC) based on the previous
1368 year's photosynthesis. Part of this leaves E to the atmosphere as maintenance
1369 respiration $R_M = M_L + M_R + M_S$, consisting of leaf maintenance (M_L), fine
1370 root maintenance (M_R) and sapwood maintenance (M_S) costs. Sapwood
1371 maintenance M_S is combined for coarse roots and branches ("other") and the
1372 trunk.

1373 The remaining carbon, $C_{\text{alloc}} \Delta t = E - R_M \Delta t$, with $\Delta t = 1$ yr, becomes
1374 available for allocation to tree organs, according to the rules specified below.
1375 The carbon allocated to the tree organs is subsequently used for sapwood
1376 transformation to heartwood ("other" and trunk), for growth of tissues (in-
1377 cluding replacement of tissue turnover and growth of new tissue), growth
1378 respiration, and for labile carbon associated to newly created tissue. The la-
1379 bile carbon (C_L, C_R, C_S) associated to tissue lost due to senescence returns
1380 to the transient pool E . Labile carbon (C_S) associated to sapwood (B_{TS} ,
1381 B_{OS}) that is transformed to heartwood (B_{TH}, B_{OH}) is incorporated into the
1382 heartwood.

1383 The following sections describe the external and internal fluxes of different
1384 tree organs (leaves, fine roots, coarse roots and branches, trunk). Planting
1385 a tree introduces carbon to the forest stand that is part of a new tree as
1386 external input flux, and fluxes caused by forest harvesting are described in
1387 SI, Section A.5.

1388 *A.2.1 Leaves and fine roots*

1389 A schematic for the leaf pools and fluxes is shown in Fig. A.1. The carbon
1390 dynamics in fine roots is analogous. The external input flux to the transient

1391 pool is indicated by \searrow , external output fluxes by \nearrow , and fluxes between
 1392 pools inside the model by \rightarrow .

1393 Leaf maintenance respiration is given by

$$M_L = R_{mL} B_L \frac{\zeta_{gluc}}{\zeta_{dw}}, \quad (A.2)$$

1394 where R_{mL} is the species-specific leaf maintenance respiration rate ($g_{gluc} g_{dw}^{-1} \text{yr}^{-1}$).

1395 The fraction f_L of $C_{alloc} \Delta t$ is allocated to leaves and split in three com-
 1396 ponents: leaf tissue growth (B_L), transfer into the leaf labile storage pool
 1397 (C_L), and growth respiration (G_L). Leaf tissue construction comes at costs
 1398 C_{gL} ($g_{gluc} g_{dw}^{-1}$) and induces growth respiration

$$G_L = \frac{C_{gL}}{C_{gL} + \delta_L} (1 - \eta_L) f_L C_{alloc} \Delta t, \quad (A.3)$$

1399 where

$$\eta_L = \frac{1}{C_{gL}} \frac{\zeta_{dw}}{\zeta_{gluc}} \quad (A.4)$$

1400 is the carbon use efficiency during leaf tissue growth (regrowth and net
 1401 growth). Allocation to leaf tissue (B_L), including regrowth of senescent
 1402 tissues and net growth (net biomass increase), and associated labile stor-
 1403 age (C_L) are balanced such that the ratio of labile storage to leaf structural
 1404 biomass carbon remains constant (δ_L , $g_{gluc} g_{dw}^{-1}$).

1405 Leaf tissue is lost due to senescence at a species-specific senescence rate
 1406 S_L (yr^{-1}), generating a loss ($S_L B_L$). The labile storage carbon ($S_L C_L$)
 1407 associated to this tissue loss returns to the tree's common transient pool
 1408 (E).

1409 A.2.2 Trunk

1410 A schematic for the trunk component is shown in Fig. A.2. The trunk
 1411 consists of the tissue pools B_{TS} and B_{TH} and shares one labile storage pool
 1412 (C_S) with coarse roots and branches (“other”). Carbon allocated to the trunk

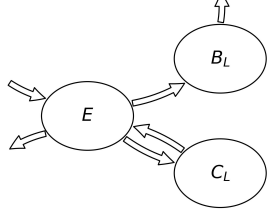


Figure A.1: Leaf carbon stocks and fluxes.

External input fluxes

- $\searrow E$: GPP

External output fluxes

- $E \nearrow M_L + G_L$

Internal fluxes

- $E \rightarrow B_L: f_L \cdot \frac{C_{gL}}{C_{gL} + \delta_L} \cdot \eta_L \cdot C_{alloc}$
- $E \rightarrow C_L: f_L \cdot \frac{\delta_L}{C_{gL} + \delta_L} \cdot C_{alloc}$
- $C_L \rightarrow E: S_L \cdot C_L$
- $B_L \rightarrow \text{Litter}: S_L \cdot B_L$

comes from the transient pool E . The combined maintenance respiration of trunk sapwood and “other” sapwood is given by

$$M_S = R_{ms} \cdot B_S^* \zeta_{gluc}. \quad (\text{A.5})$$

Here R_{ms} is the species-specific sapwood maintenance respiration rate ($\text{g}_{gluc} \text{ g}_{dw}^{-1} \text{ yr}^{-1}$) and B_S^* is the biomass of living sapwood in g_{dw} (Ogle and Pacala, 2009, SI, Eq. (29)).

The amount $f_T C_{alloc} \Delta t$ is allocated to the trunk and is split up in three components: sapwood growth (B_{TS}), transfer into the labile storage pool (C_S), and growth respiration (G_{TS}). Trunk sapwood construction from transient pool carbon comes at costs C_{gw} ($\text{g}_{gluc} \text{ g}_{dw}^{-1}$) and induces growth respiration

$$G_{TS} = \frac{C_{gw}}{C_{gw} + \delta_W} (1 - \eta_W) f_T C_{alloc} \Delta t. \quad (\text{A.6})$$

Trunk tissue is not lost due to senescence.

Depending on heartwood volume growth (ΔB_{TH}), a fraction of trunk

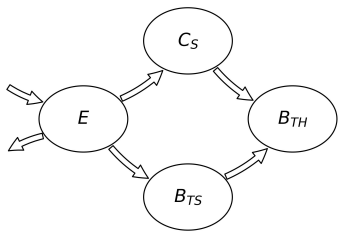


Figure A.2: Trunk carbon stocks and fluxes.

External input fluxes

- $\searrow E$: GPP

External output fluxes

- $E \nearrow M_S + G_{TS}$

Internal fluxes

- $E \rightarrow B_{TS}$: $f_T \cdot \frac{C_{gW}}{C_{gW} + \delta_W} \cdot \eta_W \cdot C_{alloc}$
- $E \rightarrow C_S$: $f_T \cdot \frac{\delta_W}{C_{gW} + \delta_W} \cdot C_{alloc}$
- $B_{TS} \rightarrow B_{TH}$: $v_T \cdot B_{TS}$
- $C_S \rightarrow B_{TH}$: $v_T \cdot \eta_{HW} \cdot \frac{B_{TS}}{B_S} \cdot C_S$

1425 sapwood ($v_T B_{TS}$) is converted to heartwood with heartwood construction
 1426 rate v_T given by Eq. (A.29). The associated labile storage ($v_T C_S B_{TS}/B_S$,
 1427 $B_S = B_{OS} + B_{TS}$), is directly incorporated into heartwood biomass at no
 1428 costs. If the tree is in “static” or “shrinking” state, then no new heartwood is
 1429 being constructed, i.e., $v_T = 0$.

1430 *A.2.3 Coarse roots and branches (“other”)*

1431 A schematic for the coarse roots and branches (“other”) component is
 1432 shown in Fig. A.3. This tree component consists of the tissue pools B_{OS} and
 1433 B_{OH} , while it shares the labile storage pool (C_S) with the trunk. As for other
 1434 organs, the carbon allocated to the coarse roots and branches comes from the
 1435 transient pool E . The combined maintenance respiration of trunk sapwood
 1436 and “other” sapwood is given by Eq. (A.5).

1437 The amount $f_O C_{alloc}, \Delta t$ of C is allocated to coarse roots and branches
 1438 and is split up in three components: sapwood growth (B_{OS}), transfer into
 1439 the labile storage pool (C_S), and growth respiration ($G_{OS,E}$). Sapwood con-

¹⁴⁴⁰ struction comes at costs C_{gw} ($\text{g}_{\text{gluc}} \text{ g}_{\text{dw}}^{-1}$) and induces growth respiration

$$G_{\text{OS},E} = \frac{C_{\text{gw}}}{C_{\text{gw}} + \delta_W} (1 - \eta_W) f_O C_{\text{alloc}} \Delta t, \quad (\text{A.7})$$

¹⁴⁴¹ where

$$\eta_W = \frac{1}{C_{\text{gw}}} \frac{\zeta_{\text{dw}}}{\zeta_{\text{gluc}}} \quad (\text{A.8})$$

¹⁴⁴² is the carbon use efficiency during sapwood tissue production, and δ_W is the
¹⁴⁴³ maximum labile storage capacity of newly produced sapwood.

¹⁴⁴⁴ In contrast to the trunk, coarse roots and branches are lost due to senes-
¹⁴⁴⁵ cence. This senescence provides input to the coarse woody debris pool
¹⁴⁴⁶ (CWD) of the soil module and concerns both sapwood ($S_O B_{\text{OS}}$) and heart-
¹⁴⁴⁷ wood ($S_O B_{\text{OH}}$), where S_O (yr^{-1}) is the species-specific senescence rate. The
¹⁴⁴⁸ labile storage carbon associated to sapwood lost by senescence, $S_O C_S B_{\text{OS}} / B_S$,
¹⁴⁴⁹ returns to the transient pool E . Heartwood loss needs to be regrown from
¹⁴⁵⁰ sapwood (including the associated labile storage from C_S), and the induced
¹⁴⁵¹ sapwood loss needs to be regrown from carbon coming from the transient
¹⁴⁵² pool E , considering growth costs and associated labile storage to C_S . The
¹⁴⁵³ rate v_O of sapwood conversion to heartwood is determined such that heart-
¹⁴⁵⁴ wood losses are compensated and the tree meets the external statistically
¹⁴⁵⁵ derived allometries (Eq. (A.43)). The labile storage carbon ($v_O C_S B_{\text{OS}} / B_S$)
¹⁴⁵⁶ associated to sapwood converted to heartwood is directly incorporated into
¹⁴⁵⁷ heartwood biomass with efficiency $\eta_{\text{HW}} = 1$. If the tree is in “static” or
¹⁴⁵⁸ “shrinking” state, then the newly constructed sapwood biomass based on the
¹⁴⁵⁹ available transient carbon is not sufficient to make up for senescence losses
¹⁴⁶⁰ and heartwood production from sapwood. The missing amount of carbon to
¹⁴⁶¹ keep sapwood biomass unchanged is supplied by the labile pool C_S and given
¹⁴⁶² by $f_{C_S} C_S$ as described in Eq. (A.44). The flux $f_{C_S} C_S$ also induces growth
¹⁴⁶³ respiration, which is given by

$$G_{\text{OS},C_S} = f_{C_S} (1 - \eta_W) C_S. \quad (\text{A.9})$$

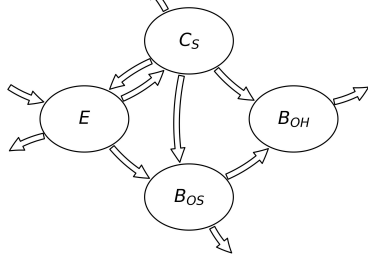


Figure A.3: Coarse root and branch carbon stocks and fluxes.

External input fluxes

- $\searrow E$: GPP

External output fluxes

- $E \nearrow: M_S + G_{OS,E}$
- $C_S \nearrow: G_{OS,C_S}$

Internal fluxes

- $E \rightarrow B_{OS}: f_O \cdot \frac{C_{gw}}{C_{gw} + \delta_W} \cdot \eta_W \cdot C_{alloc}$
- $E \rightarrow C_S: f_O \cdot \frac{\delta_W}{C_{gw} + \delta_W} \cdot C_{alloc}$
- $C_S \rightarrow E: S_O \cdot \frac{B_{OS}}{B_S} \cdot C_S$
- $C_S \rightarrow B_{OS}: f_{CS} \cdot \eta_W \cdot C_S$
- $B_{OS} \rightarrow B_{OH}: v_O \cdot B_{OS}$
- $C_S \rightarrow B_{OH}: v_O \cdot \eta_{HW} \cdot \frac{B_{OS}}{B_S} \cdot C_S$
- $B_{OS} \rightarrow CWD: S_O \cdot B_{OS}$
- $B_{OH} \rightarrow CWD: S_O \cdot B_{OH}$

1464 In contrast to sapwood construction by carbon coming from the transient
 1465 pool E , sapwood construction from the labile storage pool C_S does not lead to
 1466 additional storage in labile carbon associated to the newly produced sapwood,
 1467 as the supplied carbon already comes from the labile pool. This allows a
 1468 depletion of the labile storage.

1469 *A.3 Carbon allocation in the tree*

1470 *A.3.1 Tree allometric relationships*

1471 All tree allometry rules are based on the *MeanTree*'s diameter at breast
 1472 height (dbh, cm) and some additionally on the *MeanTree*'s height (H , m).

¹⁴⁷³ Tree height is computed as

$$H = 1.3 + \frac{\text{dbh}^k}{(a + b \text{dbh})^k} \quad (\text{A.10})$$

¹⁴⁷⁴ based on the Näslund height model (Näslund, 1936) parameterized for 155
¹⁴⁷⁵ stands in southern Finland (Siipilehto, 2000). Since dynamic radial growth
¹⁴⁷⁶ is (internally) computed at the *MeanTree*'s radius at trunk base (r , m), it is
¹⁴⁷⁷ necessary to compute r from dbh and H . The computation of r differs be-
¹⁴⁷⁸ tween small and larger trees. For dbh < 3.0 cm, Laasasenaho (1982) suggests
¹⁴⁷⁹ the diameter at trunk base to be

$$r = 2 + 1.25 \frac{\text{dbh}}{200}. \quad (\text{A.11})$$

¹⁴⁸⁰ For dbh \geq 3.0 cm, we use the tree radius at breast height ($r_{\text{BH}} = 1/2 \text{dbh}$)
¹⁴⁸¹ to identify r through the current trunk-shape based relation as expressed in
¹⁴⁸² Ogle and Pacala (2009, SI, Eq. (24)).

¹⁴⁸³ We describe the allometrically derived biomass of leaves (m_L), stem wood
¹⁴⁸⁴ (m_{SW}), stem bark (m_{SB}), living branches (m_{LB}), stump (m_S), and (coarse)
¹⁴⁸⁵ roots (m_{CR}) in kg_{dw} based on the *MeanTree*'s diameter at breast height (dbh,
¹⁴⁸⁶ cm) and its height (H , m) via the empirical relations based on tree inventory
¹⁴⁸⁷ data. The allometric equations for leaves, stem wood, stem bark, living
¹⁴⁸⁸ branches, stump and (coarse) roots for large trees come from Repola (2009).
¹⁴⁸⁹ Trees are considered large if their dbh is at least the critical value, which is
¹⁴⁹⁰ defined as mean dbh minus one standard deviation of the forest inventory
¹⁴⁹¹ data used to derive the allometric relationships. According to Repola (2009,
¹⁴⁹² Table 3) pines are considered large if dbh \geq (13.1 – 5.3) cm and spruces if
¹⁴⁹³ dbh \geq (11.2 – 4.0) cm.

¹⁴⁹⁴ The allometric equations have the general form

$$\ln m_Y = \text{intercept} + b_1 \frac{\text{dbh}}{\text{dbh} + n} + b_2 \frac{H}{H + m} + b_3 \log(H) + b_4 H, \quad (\text{A.12})$$

1495 where the $b_i b_l$ s are empirical coefficients depending on the type of biomass
 1496 Y , and a variance-correction term is added to the intercept to correct for the
 1497 bias due to the logarithmic transformation:

$$\text{intercept} = b_0 + \frac{1}{2} (\sigma_u^2 + \sigma_e^2). \quad (\text{A.13})$$

1498 For small trees, the coefficients in Eq. (A.12) for stem wood and living
 1499 branches were taken from Repola and Ahnlund Ulvcrona (2014). Empirical
 1500 coefficients were not reported for stem bark, stump, and (coarse) roots
 1501 of small trees. So we use the according coefficients for large trees here. The
 1502 biomass equation for leaves in small trees is given by

$$m_L = a \text{dbh}^b H^c \quad (\text{A.14})$$

1503 with coefficients for pine and spruce provided in Lehtonen (2005, Table 4).

1504 The vertical distribution of leaf biomass in the crown follows Tahvanainen
 1505 and Forss (2008, Table 8), based on the tree' crown base heights which derived
 1506 from Tahvanainen and Forss (2008, Fig. 4).

1507 To ensure continuity, the biomass curves of small trees are scaled such
 1508 that they match the biomass curves of taller trees at the critical dbh . .

1509 A.3.2 Routines for carbon allocation within a single tree

1510 Each year we identify a new $\text{dbh}^* = \text{dbh}(t + \Delta t)$ so that the tree organs'
 1511 new biomasses match the external allometric constraints as defined by dbh^*
 1512 and Eq. A.12. Identifying dbh^* requires writing a carbon balance for each tree
 1513 organ, i.e., for leaves (SI, Section A.3.3), for fine roots (SI, Section A.3.4),
 1514 for the trunk (SI, Section A.3.5), and for coarse roots and branches (SI,
 1515 Section A.3.6). The allocation fractions f_X (yr^{-1}) across organs must satisfy

$$f_L + f_R + f_T + f_O = 1 \text{ yr}^{-1}, \quad (\text{A.15})$$

1516 where f_X is the fraction of the newly available carbon ($C_{\text{alloc}} \Delta t$) allocated to
 1517 tree organ X . The new diameter at breast height (dbh *) appears in each f_X ,
 1518 via the relations linking the change in biomass of X to the fluxes in and out
 1519 X , which are described next for each organ. The according species-dependent
 1520 parameter values are shown in Tables A.3 and A.4. When the newly fixed
 1521 carbon is insufficient to meet the demands imposed by replacement of biomass
 1522 losses via senescence, the tree reverts to the “static” or “shrinking” state (SI,
 1523 Section A.4).

1524 *A.3.3 Leaves*

1525 Each year, new carbon allocated from $C_{\text{alloc}} \Delta t$ to leaves is required for net
 1526 growth of new leaf biomass (ΔB_L), to balance leaf biomass lost via senescence
 1527 ($S_L B_L \Delta t$), for tissue growth costs (C_{gL}) and a fixed share of associated labile
 1528 storage (δ_L) Ogle and Pacala (2009, SI, Eq. (1A)). Hence,

$$f_L C_{\text{alloc}} \Delta t = (\Delta B_L + S_L B_L \Delta t) (C_{gL} + \delta_L) \frac{\zeta_{\text{gluc}}}{\zeta_{\text{dw}}}, \quad (\text{A.16})$$

1529 where both sides of the equation are in gC. The dependence of f_L on dbh *
 1530 comes through its dependence on the net biomass growth

$$\Delta B_L = B_L^* - B_L = B_L(\text{dbh}^*) - B_L. \quad (\text{A.17})$$

1531 We assume that labile carbon associated to leaves (C_L) is actually stored
 1532 within the leaves. Hence, we require the new leaf biomass carbon and labile
 1533 pool to equal the leaf biomass carbon imposed by the allometric relationship
 1534 (Eq. (A.12)). In formulas,

$$B_L^* + C_L^* = 10^3 m_L^* \zeta_{\text{dw}}, \quad (\text{A.18})$$

1535 where $m_L^* := m_L(\text{dbh}^*, H^*)$ is the biomass from the allometric model (Eq. (A.12))
 1536 applied to leaves (in g_{dw}), and ζ_{dw} transforms g_{dw} into gC. C_L is calculated
 1537 as a fraction of the biomass carbon itself, as $C_L^* = \delta_L B_L^* \zeta_{\text{gluc}} \zeta_{\text{dw}}^{-1}$. By rear-

1538 ranging the terms, we obtain

$$B_L^* = \frac{10^3 m_L^*}{1 + \delta_L \frac{\zeta_{\text{gluc}}}{\zeta_{\text{dw}}}} \zeta_{\text{dw}}. \quad (\text{A.19})$$

1539 *A.3.4 Fine roots*

1540 Similarly to leaves, the fine root fraction is given by (Ogle and Pacala,
1541 2009, SI, Eq. (1B)),

$$f_R C_{\text{alloc}} \Delta t = (\Delta B_R + S_R B_R \Delta t) (C_{\text{gR}} + \delta_L) \frac{\zeta_{\text{gluc}}}{\zeta_{\text{dw}}}. \quad (\text{A.20})$$

1542 The new fine root biomass is computed as a constant fraction of the new leaf
1543 biomass, $B_R^* = \rho_{\text{RL}} B_L^*$.

1544 *A.3.5 Trunk*

1545 Carbon allocated to the trunk is used for net sapwood growth ($\rho_W \Delta V_T$)
1546 involving sapwood construction costs (C_{gW}) and a labile storage fraction
1547 (δ_W). The formula given by Ogle and Pacala (2009, SI, Eq. (31C)),

$$f_T C_{\text{alloc}} \Delta t = \left(\rho_W \Delta V_T \zeta_{\text{dw}} - \frac{\delta_S}{C_{\text{gHW}}} v_T B_{\text{TS}} \Delta t \right) \cdot (C_{\text{gW}} + \delta_W) \frac{\zeta_{\text{gluc}}}{\zeta_{\text{dw}}}, \quad (\text{A.21})$$

1548 allows ρ_W to become negative for slowly growing trunk volumes. Further-
1549 more, we assume labile carbon associated to the trunk to be part of the trunk
1550 volume. Consequently, we adapt this formula and compute f_T from

$$f_T C_{\text{alloc}} \Delta t = \rho_W \Delta V_T \zeta_{\text{dw}} \cdot (C_{\text{gW}} + \delta_W) \frac{\zeta_{\text{gluc}}}{\zeta_{\text{dw}}}. \quad (\text{A.22})$$

1551 Because of sapwood transformation to heartwood ($v_T B_{\text{TS}} \Delta t$) with unitary
1552 efficiency ($C_{\text{gHW}} = 1.00 \text{ g}_{\text{gluc}} \text{ g}_{\text{dw}}^{-1}$), the labile storage fraction

$$\delta_S := \frac{C_S}{B_S} \frac{\zeta_{\text{dw}}}{\zeta_{\text{gluc}}} \text{ with } B_S := B_{\text{TS}} + B_{\text{OS}} \quad (\text{A.23})$$

1553 associated to transformed sapwood becomes becomes integrated into heart-
 1554 wood.

1555 Once f_T is identified, according to Ogle and Pacala (2009, SI, Eqs. (1C)
 1556 and (1D)), we determine

$$\Delta B_{\text{TS}} = \frac{f_T C_{\text{alloc}} \Delta t}{C_{\text{gW}} + \delta_W} - v_T B_{\text{TS}} \Delta t \quad (\text{A.24})$$

1557 and

$$\Delta B_{\text{TH}} = \left(1 + \frac{\delta_S}{C_{\text{gHW}}}\right) v_T B_{\text{TS}} \Delta t. \quad (\text{A.25})$$

1558 In order to determine f_T from Eq. (A.22), we need to identify the density of
 1559 newly produced sapwood (ρ_W), the sapwood to heartwood conversion rate
 1560 of the trunk (v_T), and the maximum labile carbon storage capacity of newly
 1561 produced sapwood (δ_W). Since δ_W depends on ρ_W , and both ρ_W and v_T
 1562 depend on the new heartwood volume $V_{\text{TH}}^* = V_{\text{TH}}(\text{dbh}^*, \text{SW}^*)$, which in
 1563 turn depends on the new sapwood width $\text{SW}^* = \text{SW}(\text{dbh}^*)$, we first describe
 1564 how to identify SW^* and then how we derive V_{TH}^* from it. The density of
 1565 newly produced sapwood $\rho_W = \rho_W(\text{dbh}^*)$ is then dynamically chosen such
 1566 that the modelled trunk biomass follows the external allometries.

1567 *Sapwood width.* We compute SW^* (m) such that the ratio of sapwood to
 1568 heartwood width (HW^* , m) follows Sellin (1994). From Eq. [2] we get

$$\text{SW}_{\text{Sellin}} = \frac{\text{SW}_a d^*}{d^* + \text{SW}_d} \quad (\text{A.26})$$

1569 in cm and from Fig. 1 we get

$$\text{HW}_{\text{Sellin}} = \text{HW}_{\text{slope}} d^*, \quad (\text{A.27})$$

1570 where $d^* = 200 r^*$ is the new diameter at trunk base in cm. Then we obtain

$$\text{SW}^* = \frac{\text{SW}_{\text{Sellin}}}{\text{SW}_{\text{Sellin}} + \text{HW}_{\text{Sellin}}} r^*. \quad (\text{A.28})$$

1571 *Trunk heartwood volume.* The new trunk heartwood volume V_{TH}^* in m^3 is
1572 computed as in Ogle and Pacala (2009, SI, Eq. (14)) with a mathematical
1573 correction of the formula for heartwood height (SI, Eq. (13)).

1574 *Sapwood to heartwood conversion rate of trunk.* The sapwood to heartwood
1575 conversion rate of the trunk, $v_T = v_T(V_{\text{TH}}^*)$ in yr^{-1} , is given as in Ogle and
1576 Pacala (2009, SI, Eq. (2)) by

$$v_T = \frac{\Delta V_{\text{TH}}}{V_{\text{TS}} \Delta t}, \quad (\text{A.29})$$

1577 where $\Delta V_{\text{TH}} = V_{\text{TH}}^* - V_{\text{TH}}$. The trunk sapwood volume is denoted by $V_{\text{TS}} =$
1578 $V_T - V_{\text{TH}}$, and the trunk volume $V_T = V_T(\text{dbh})$ is given by Ogle and Pacala
1579 (2009, SI, Eq. (9)).

1580 *Density of newly produced sapwood.* While sapwood converted to heartwood
1581 does not change the trunk volume, new sapwood is needed for radial trunk
1582 growth. The allometrically derived trunk biomass is given by

$$m_T := m_{\text{SW}} + m_{\text{SB}} + m_S, \quad (\text{A.30})$$

1583 consisting of stem wood, stem bark, and the stump as given by Eq. (A.12).
1584 The trunk biomass carbon is given by

$$B_T = B_{\text{TH}} + B_{\text{TS}} + \frac{B_{\text{TS}}}{B_S} C_S, \quad (\text{A.31})$$

1585 assuming that labile carbon associated to trunk sapwood is actually stored
1586 in the trunk. In order to match the allometrically derived trunk biomass by
1587 modelled biomass, we strive for $B_T^* = m_T^*$, which leads to the goal of

$$\Delta B_T = m_T^* - B_T. \quad (\text{A.32})$$

1588 Considering growth costs, we have

$$\Delta B_T = f_T C_{\text{alloc}} \Delta t \frac{1 + \delta_W}{C_{gW} + \delta_W}. \quad (\text{A.33})$$

1589 We combine Eq. (A.33) with Eq. (A.22), and obtain ρ_W from

$$\rho_W = \frac{m_T^* - B_T}{\Delta V_T (1 - \delta_W)} \quad (\text{A.34})$$

1590 under the additional conditions that

$$\rho_{W_{\min}} \leq \rho_W \leq \rho_{W_{\max}}. \quad (\text{A.35})$$

1591 *Maximum labile carbon storage capacity of newly produced sapwood.* We com-
1592 pute the maximum labile carbon storage capacity of newly produced sapwood
1593 as in Ogle and Pacala (2009, SI, Eq. (6)) by

$$\delta_W = \frac{\gamma_C (1 - \gamma_X - \gamma_W \rho_W)}{\rho_W}. \quad (\text{A.36})$$

1594 A.3.6 Coarse roots and branches (“other”)

1595 Carbon allocated to “other” is needed for net sapwood biomass growth
1596 (ΔB_{OS}) and to balance losses of sapwood to senescence ($S_O B_{OS} \Delta t$) and to
1597 heartwood production ($v_O B_{OS} \Delta t$). For each term, there are sapwood con-
1598 struction costs (C_{gW}) and an associated labile storage fraction (δ_W) involved.
1599 Hence, following Ogle and Pacala (2009, SI, Eq. (1E)),

$$f_O C_{\text{alloc}} \Delta t = [\Delta B_{OS} + (S_O + v_O) B_{OS} \Delta t] \cdot (C_{gW} + \delta_W) \frac{\zeta_{\text{gluc}}}{\zeta_{\text{dw}}}. \quad (\text{A.37})$$

1600 In order to determine f_O from Eq. (A.37), we need to identify the net sapwood
1601 biomass carbon change (ΔB_{OS}) and the sapwood to heartwood conversion
1602 rate of “other” (v_O). First, we compute ΔB_{OS} , then we compute the net
1603 heartwood biomass carbon change of “other” (ΔB_{OH}) and use it to identify

₁₆₀₄ v_O .

₁₆₀₅ *Net sapwood biomass carbon change of “other”.* The new sapwood biomass
₁₆₀₆ carbon of “other” (B_{OS}^*) is allometrically defined as

$$B_{OS}^* = \lambda_S^* \cdot B_{TS}^*, \quad (\text{A.38})$$

₁₆₀₇ where

$$\lambda_S^* = \frac{m_O^*}{m_T^*} \quad (\text{A.39})$$

₁₆₀₈ is the ratio of “other” biomass to trunk biomass as derived from external
₁₆₀₉ allometries. Allometric “other” biomass is computed as the sum of biomasses
₁₆₁₀ of living branches and (coarse) roots in Eq. (A.12), i.e.,

$$m_O := m_{LB} + m_{CR}. \quad (\text{A.40})$$

₁₆₁₁ Obviously, $\Delta B_{OS} = B_{OS}^* - B_{OS}$.

₁₆₁₂ *Heartwood biomass carbon change of “other”.* The new heartwood biomass
₁₆₁₃ carbon of “other” (B_{OH}^*) is allometrically defined as

$$B_{OH}^* = \lambda_H^* \cdot B_{TH}^*, \quad (\text{A.41})$$

₁₆₁₄ where

$$\lambda_H^* = \lambda_S^* = \frac{m_O^*}{m_T^*} \quad (\text{A.42})$$

₁₆₁₅ is the ratio of “other” biomass to trunk biomass as derived from external
₁₆₁₆ allometries. Obviously, $\Delta B_{OH} = B_{OH}^* - B_{OH}$.

₁₆₁₇ *Sapwood to heartwood conversion rate of “other”.* Heartwood production must
₁₆₁₈ satisfy net heartwood biomass growth (ΔB_{OH}) and make up for senescence
₁₆₁₉ losses ($S_O B_{OH} \Delta t$), while carbon supply is provided by the sapwood pool
₁₆₂₀ ($v_O B_{OS} \Delta t$) and by the labile storage pool ($v_O \delta_S B_{OS} \Delta t$) at no heartwood
₁₆₂₁ construction costs ($C_{gHW} = 1.00 \text{ g}_{\text{gluc}} \text{ g}_{\text{dw}}^{-1}$). Consequently, following (Ogle

1622 and Pacala, 2009, SI, Eq. (1F)),

$$v_O \left(1 + \frac{\delta_S}{C_{\text{gHW}}} \right) B_{\text{OS}} \Delta t = \Delta B_{\text{OH}} + S_O B_{\text{OH}} \Delta t. \quad (\text{A.43})$$

1623 *A.4 Physiological tree states*

1624 In case a *MeanTree* is subject to excessive competition for light and its
 1625 annual photosynthetic carbon uptake is insufficient to sustain maintenance
 1626 respiration and biomass regrowth caused by senescence in leaves, fine roots,
 1627 and coarse roots and branches (“other”), the *MeanTree* changes its physio-
 1628 logical status from “healthy” to “static”. In the “static” state, the *MeanTree*
 1629 has no radial trunk growth but only regrows the senescent biomass in leaves
 1630 and fine roots from $C_{\text{alloc}} \Delta t$. The amount of carbon insufficient to regrow
 1631 all lost sapwood and heartwood “other” is extracted from the labile storage
 1632 pool (C_S) and can be computed by

$$f_{C_S} C_S = (S_O + v_O) B_{\text{OS}} \Delta t C_{\text{gW}} \frac{\zeta_{\text{gluc}}}{\zeta_{\text{dw}}} - C_{\text{alloc}} \Delta t (1 - f_L - f_R) \frac{C_{\text{gW}}}{C_{\text{gW}} + \delta_W}. \quad (\text{A.44})$$

1633 In “healthy” trees, $f_{C_S} = 0 \text{ yr}^{-1}$. The first part of the right hand side is the
 1634 hypothetical amount of carbon required for sapwood regrowth at costs C_{gW}
 1635 because of senescence and heartwood construction if all carbon for that came
 1636 from C_S . Recall that, other than from $C_{\text{alloc}} \Delta t$, sapwood construction from
 1637 C_S does not involve an additional share (δ_W) to be stored in labile carbon
 1638 (C_S). Some carbon included in the first part of the right hand side, however,
 1639 is already provided by $C_{\text{alloc}} \Delta t$ and is represented by the second part of the
 1640 right hand side. This amount does not need to be provided by C_S . By using
 1641 $f_{C_S} C_S$ from the labile storage pool, $\Delta B_{\text{OH}} = \Delta B_{\text{OS}} = 0$ and the tree can
 1642 potentially survive in the “static” state for a few years after which the light
 1643 situation might improve and allow the tree to return to the “healthy” state.
 1644 Labile storage carbon from C_S cannot be used for regrowth of leaves and fine

1645 root biomass.

1646 If $C_{\text{alloc}} \Delta t$ is not even enough to regrow senescence losses from leaves and
1647 fine roots only, then the tree switches to the “shrinking” state. In this state,
1648 leaves, fine roots, and “other” receive carbon from photosynthesis proportional
1649 to their respective demand in the “healthy” state for regrowth such that
1650 all captured carbon is used up. This means that the *MeanTree* loses biomass
1651 of leaves and fine roots, while the biomass in coarse roots and branches is re-
1652 grown with the support from labile storage in C_S . When C_S becomes empty,
1653 the *MeanTree* dies and is removed from the stand. However, if before death
1654 the light situation improves, the *MeanTree* switches back to the “healthy”
1655 physiological state with no delay.

1656 *A.5 Carbon transfers via thinning and cutting and short- and long-lasting*
1657 *wood products*

1658 When a *MeanTree* in a stand is subject to thinning (partial removal) or
1659 cutting (complete removal), some tree carbon is transferred to the soil and
1660 wood products. Wood products with two different mean life times are con-
1661 sidered: pulpwood or bioenergy (WP_S), represented via a short-lasting pool
1662 with fast turnover rate (0.3 yr^{-1}); and long-lasting wood products (WP_L),
1663 represented by a pool with slow turnover rate ($0.02, \text{yr}^{-1}$). At the end of the
1664 wood product’s lifetime, carbon returns from the wood-product module to
1665 the atmosphere as CO_2 emission. The turnover rates are taken from Pukkala
1666 (2014, Table 4).

1667 The allocation of carbon from trees to soil and wood products depends on
1668 the tree’s species and size and hence its stem shape (taper curve) (Laasase-
1669 naho, 1982, Eq. (33.1), parameters (41.1)). The stem is partitioned into saw
1670 log, fibre and cutting residues depending on stem dimensions. We set the
1671 minimum diameter and length for saw logs as 16.0 cm and 4 m, respectively,
1672 while the minimum dimensions for fibre wood are 8 cm in diameter and 3 m
1673 in length. The lowest 0.2 m of the stem is considered as stump.

1674 The carbon in saw logs is considered as long-lasting wood product and
1675 is transferred to WP_L , while fibre is considered a short-lasting wood prod-
1676 uct and is transferred to WP_S . All other material (residue, stump) from
1677 “other” and the trunk is transferred to the CWD pool in the soil. The de-
1678 cision not to consider harvesting of cutting residues to bioenergy might not
1679 always be in line with current forestry practices and could be easily changed
1680 to include part of residue carbon into the short-lasting wood products (W_S).
1681 While labile storage carbon associated to coarse roots and branches sapwood
1682 ($C_S \text{Bos}/B_S$) is transferred to CWD, labile storage associated to trunk sap-
1683 wood ($C_S \text{Bos}/B_S$) is split up between WP_L , WP_S analogous to B_{TS} . All
1684 carbon in leaves and fine roots (including associated labile storage) and car-
1685 bon from the transient pool is transferred to the Litter pool.

1686 A.6 MeanTree state variables and parameters

Symbol	Unit	Description	Source
r	m	tree radius at trunk base	Section A.3.1
Δr	m	change of tree radius at trunk base	dynamically solved for
r_{BH}	m	radius at breast height	Ogle and Pacala (2009, SI, Eq. (24))
dbh	cm	tree radius at breast height	Section A.3.1
H	m	tree height	Eq. (A.10), Näslund (1947), Siipilehto and Kangas (2015)
GPP	gCyr^{-1}	carbon uptake by photosynthesis	-
C_{alloc}	gCyr^{-1}	available gC/yr for allocation to tree organs	$E/\Delta t - R_M$
R_M	gCyr^{-1}	whole plant maintenance respiration	$M_L + M_R + M_S$
M_L	gCyr^{-1}	maintenance respiration leaves	Eq. (A.2)
M_R	gCyr^{-1}	maintenance respiration fine roots	analogous to M_L
M_S	gCyr^{-1}	maintenance respiration sapwood	Eq. (A.5)
G_L	gCyr^{-1}	growth respiration leaves	Eq. (A.3)
G_R	gCyr^{-1}	growth respiration fine roots	analogous to G_L
$G_{OS,E}$	gCyr^{-1}	growth respiration sapwood from transient carbon	Eq. (A.7)
$G_{OS,CS}$	gCyr^{-1}	growth respiration sapwood from labile storage carbon	Eq. (A.9)
η_L		CUE during leaf tissue growth	Eq. (A.4)
η_R		CUE during fine root tissue growth	analogous to η_L
η_W		CUE during sapwood production	Eq. (A.8)
η_{HW}		CUE during heartwood production	fixed to 1
H_{TH}	m	height of trunk heartwood section	Ogle and Pacala (2009, SI, Eq. (9)), corrected and introduced capturing of equalities
LA	m^2	total leaf area	$SLA B_L$
V_T	m^3	trunk volume	Ogle and Pacala (2009, SI, Eq. (9))
V_{TH}	m^3	volume of trunk heartwood section	Ogle and Pacala (2009, SI, Eq. (14)), introduced capturing of equalities
V_{TS}	m^3	volume of trunk sapwood	Ogle and Pacala (2009, SI, Eq. (15))
SW	m	width (or depth) of sapwood at trunk base	Section A.3.5, Helmisäari et al. (2007), Sellin (1994)
C_S^*	ggluc	maximum amount of labile carbon stored in sapwood	Ogle and Pacala (2009, SI, Eq. (5))
B_S^*	gdw	biomass of 'living' sapwood	Ogle and Pacala (2009, SI, Eq. (29))
B_S	gC	biomass of bulk sapwood	$B_{OS} + B_{TS}$
δ_S	$\frac{\text{ggluc}}{\text{gdw}}$	concentration of labile carbon storage of bulk sapwood	Eq. (A.23), Ogle and Pacala (2009, SI, Eq. (7))
ρ_W	$\frac{\text{gdw}}{\text{m}^3}$	density of newly produced sapwood	Eq. (A.34)
δ_W	$\frac{\text{ggluc}}{\text{gdw}}$	maximum labile carbon storage capacity of newly produced sapwood	Eq. (A.36), Ogle and Pacala (2009, SI, Eq. (6))
B_T	gC	biomass of trunk	$B_{TH} + B_{TS} + \frac{B_{TS}}{B_S} C_S$
m_X	gdw	allometrically derived biomass of tree organ X	based on Eq. (A.12)
λ_S		ratio of "other" sapwood to trunk sapwood	Eq. (A.39)
λ_H		ratio of "other" heartwood to trunk heartwood	Eq. (A.39)
v_T	yr^{-1}	sapwood to heartwood conversion rate of trunk	Eq. (A.29), Ogle and Pacala (2009, SI, Eq. (2))
v_O	yr^{-1}	sapwood to heartwood conversion rate of coarse roots and branches	Eq. (A.43), Ogle and Pacala (2009, SI, Eq. (1F))
f_L		partitioning from transient pool to leaves	Section A.3.3, Ogle and Pacala (2009, SI, Eq. (1A))
f_R		partitioning from transient pool to fine roots	Section A.3.4, Ogle and Pacala (2009, SI, Eq. (1B))
f_T		partitioning from transient pool to trunk	Section A.3.5, Ogle and Pacala (2009, SI, Eq. (31C))
f_O		partitioning from transient pool to coarse roots and branches	Section A.3.6, Ogle and Pacala (2009, SI, Eq. (1E))
f_{CS}		fraction of C_S used to regrow "other" sapwood	Eq. (A.44)

Table A.2: Tree module variables. Units are per single tree.

Scots pine

Symbol	Value	Unit	Description	Source
SLA	6.162	$\frac{\text{m}^2}{\text{kg}_{\text{dw}}}$	specific leaf area	Goude et al. (2019)
R_{mL}	0.950	$\frac{\text{g}_{\text{gluc}}}{\text{g}_{\text{dw}}} \text{ yr}^{-1}$	maintenance respiration rate of leaves	Ogle and Pacala (2009, Table 2)
R_{mR}	0.750	$\frac{\text{g}_{\text{gluc}}}{\text{g}_{\text{dw}}} \text{ yr}^{-1}$	maintenance respiration rate of fine roots	Ogle and Pacala (2009, Table 2)
R_{mS}	0.063	$\frac{\text{g}_{\text{gluc}}}{\text{g}_{\text{dw}}} \text{ yr}^{-1}$	maintenance respiration rate of sapwood	Lavigne and Ryan (1997, Table 5, northern)
S_L	0.200	yr^{-1}	senescence rate of leaves	Muukkonen (2005, Table 3)
S_R	0.811	yr^{-1}	senescence rate of fine roots	Pukkala (2014, Table 2)
S_O	0.040	yr^{-1}	senescence rate of coarse roots and branches	Vanninen and Mäkelä (2005, Table 1); also following simulations for coarse roots, Eq. (10) leads to 0.06 for branches, we took one of the two Pukkala (2014, Table 2)
ρ_{RL}	0.670		fine root-to-leaf biomass ratio	Ogle and Pacala (2009, Table 2)
η_B	0.045		relative height at which trunk transitions from a neiloid to a paraboloid	Ogle and Pacala (2009, Table 2)
η_C	0.710		relative height at which trunk transitions from a paraboloid to a cone	Ogle and Pacala (2009, Table 2, called η)
γ_X	0.620		xylem conducting area to sapwood area ratio	Ogle and Pacala (2009, Table 2)
γ_C	2.650e+05	$\frac{\text{g}_{\text{gluc}}}{\text{m}^3}$	maximum storage capacity of living sapwood cells	Ogle and Pacala (2009, Table 2)
γ_W	6.670e-07	$\frac{\text{m}^3}{\text{g}_{\text{dw}}}$	(inverse) density of sapwood structural tissue	Ogle and Pacala (2009, Table 2)
SW_a	18.800		numerator parameter for sapwood width model	Sellin (1994, Eq. 2)
SW_b	60.0		denominator parameter for sapwood width model	Sellin (1994, Eq. 2)
HWslope	0.480		slope value for heartwood width line	Sellin (1994, Fig. 1)
$\rho_{W\text{max}}$	5.500e+05	$\frac{\text{g}_{\text{dw}}}{\text{m}^3}$	maximum density of newly produced sapwood	computed to keep δ_W positive
$\rho_{W\text{min}}$	2.800e+05	$\frac{\text{g}_{\text{dw}}}{\text{m}^3}$	minimum wood density	empirical parameter after some testing
dbh_M	4.0	cm	for $\text{dbh} < \text{dbh}_M$ the allometrically derived wood density is assumed to be useless	empirical parameter after some testing
δ_L	0.110	$\frac{\text{g}_{\text{gluc}}}{\text{g}_{\text{dw}}}$	labile carbon storage capacity of leaves	Ogle and Pacala (2009, Table 2)
δ_R	0.080	$\frac{\text{g}_{\text{gluc}}}{\text{g}_{\text{dw}}}$	labile carbon storage capacity of fine roots	Ogle and Pacala (2009, Table 2)
C_{gL}	2.442	$\frac{\text{g}_{\text{gluc}}}{\text{g}_{\text{dw}}}$	construction costs of producing leaves	Ryan et al. (1997, p.878) states that leaf construction costs were 28/15 · 0.25 (of leaf NPP)
C_{gR}	1.597	$\frac{\text{g}_{\text{gluc}}}{\text{g}_{\text{dw}}}$	construction costs of producing fine roots	Ryan et al. (1997, Table 4) and some empirical adaptation
C_{gHW}	1.0	$\frac{\text{g}_{\text{gluc}}}{\text{g}_{\text{dw}}}$	construction costs of converting heartwood from labile sapwood (actually: no costs)	missing in Ogle and Pacala (2009) (causing a unit mismatch)
C_{gW}	1.558	$\frac{\text{g}_{\text{gluc}}}{\text{g}_{\text{dw}}}$	construction costs of producing sapwood	Lavigne and Ryan (1997, Table 5, northern), we add 1.0 because for us growth is not part of the factor to multiply with

Table A.3: Scots pine parameters.

Norway spruce

Symbol	Value	Unit	Description	Source
SLA	5.020	$\frac{m^2}{kg_{dw}}$	specific leaf area	Goude et al. (2019)
R_{mL}	0.950	$\frac{g_{gluc}}{g_{dw}} \text{ yr}^{-1}$	maintenance respiration rate of leaves	Ogle and Pacala (2009, Table 2)
R_{mR}	0.750	$\frac{g_{gluc}}{g_{dw}} \text{ yr}^{-1}$	maintenance respiration rate of fine roots	Ogle and Pacala (2009, Table 2)
R_{mS}	0.077	$\frac{g_{gluc}}{g_{dw}} \text{ yr}^{-1}$	maintenance respiration rate of sapwood	Lavigne and Ryan (1997, Table 5, northern)
S_L	0.100	yr^{-1}	senescence rate of leaves	Muukkonen and Lehtonen (2004)
S_R	0.868	yr^{-1}	senescence rate of fine roots	Pukkala (2014, Table 2)
S_O	0.013	yr^{-1}	senescence rate of coarse roots and branches	Muukkonen and Lehtonen (2004)
ρ_{RL}	0.250		fine root-to-leaf biomass ratio	Pukkala (2014, Table 2)
η_B	0.045		relative height at which trunk transitions from a neiloid to a paraboloid	Ogle and Pacala (2009, Table 2) (pine parameter)
η_C	0.710		relative height at which trunk transitions from a paraboloid to a cone	Ogle and Pacala (2009, Table 2, called η) (pine parameter)
γ_X	0.620		xylem conducting area to sapwood area ratio	Ogle and Pacala (2009, Table 2) (pine parameter)
γ_C	2.650e+05	$\frac{g_{gluc}}{m^3}$	maximum storage capacity of living sapwood cells	Ogle and Pacala (2009, Table 2) (pine parameter)
γ_W	6.670e-07	$\frac{m^3}{g_{dw}}$	(inverse) density of sapwood structural tissue	Ogle and Pacala (2009, Table 2) (pine parameter)
SW_a	18.800		numerator parameter for sapwood width model	Sellin (1994, Eq. 2)
SW_b	60.0		denominator parameter for sapwood width model	Sellin (1994, Eq. 2)
$H_W\text{slope}$	0.480		slope value for heartwood width line	Sellin (1994, Fig. 1)
$\rho_{W\max}$	5.500e+05	$\frac{g_{dw}}{m^3}$	maximum density of newly produced sapwood	computed to keep δ_W positive
$\rho_{W\min}$	2.800e+05	$\frac{g_{dw}}{m^3}$	minimum wood density	empirical parameter after some testing
dbh_M	4.0	cm	for $dbh < dbh_M$ the allometrically derived wood density is assumed to be useless	empirical parameter after some testing
δ_L	0.110	$\frac{g_{gluc}}{g_{dw}}$	labile carbon storage capacity of leaves	Ogle and Pacala (2009, Table 2) (pine parameter)
δ_R	0.080	$\frac{g_{gluc}}{g_{dw}}$	labile carbon storage capacity of fine roots	Ogle and Pacala (2009, Table 2) (pine parameter)
C_{gL}	2.442	$\frac{g_{gluc}}{g_{dw}}$	construction costs of producing leaves	Ryan et al. (1997, p.878) states that leaf construction costs were 28/15 · 0.25 (of leaf NPP)
C_{gR}	1.601	$\frac{g_{gluc}}{g_{dw}}$	construction costs of producing fine roots	Ryan et al. (1997, Table 4) and some empirical adaptation
C_{gHW}	1.0	$\frac{g_{gluc}}{g_{dw}}$	construction costs of converting heartwood from labile sapwood (actually: no costs)	missing in Ogle and Pacala (2009) (causing a unit mismatch)
C_{gw}	2.202	$\frac{g_{gluc}}{g_{dw}}$	construction costs of producing sapwood	Lavigne and Ryan (1997, Table 5, northern), we add 1.0 because for us growth is not part of the factor to multiply with

Table A.4: Norway spruce parameters.

1687 *A.7 Soil module*

1688 As described in Section 2.3.3, the soil module describes soil carbon dy-
1689 namics in a minimalist way, using a three-pool model representing a fast
1690 decomposing litter pool (Litter), a slowly decomposing coarse woody debris
1691 pool (CWD), and a soil organic carbon pool (SOC) with fixed decomposi-
1692 tion and fraction parameters (Table A.5) derived from Hyvönen and Ågren
1693 (2001), Peltoniemi et al. (2004) and Koven et al. (2013). A schematic of the
1694 soil component is shown in Fig. A.4 and next to it is a description of the
1695 associated natural fluxes, not caused by management actions. The turnover
1696 rate of Litter is set to 0.43 yr^{-1} and 50 % of the decomposed carbon is trans-
1697 ferred to SOC, while the other 50 % return as heterotrophic respiration to the
1698 atmosphere. The CWD pool behaves similarly with a turnover rate equal to
1699 0.056 yr^{-1} with 50 % transfer to SOC and 50 % respiration. Decomposition
1700 of SOC by heterotrophs happens at a rate equal to 0.023 yr^{-1} in order to
1701 match SOC stocks in Peltoniemi et al. (2004, Table 5), and contributes to
1702 CO_2 emissions to the atmosphere.

Symbol	Value	Unit	Description	Source
k_{Litter}	0.438	yr^{-1}	total Litter turnover rate	Hyvönen and Ågren (2001, Table 2)
f_{Litter}	0.500	yr^{-1}	Litter respiration fraction	Koven et al. (2013, Fig. 2)
k_{CWD}	0.056	yr^{-1}	total CWD turnover rate	Hyvönen and Ågren (2001, Table 2)
f_{CWD}	0.500	yr^{-1}	CWD respiration fraction	Koven et al. (2013, Fig. 2)
k_{SOC}	0.023	yr^{-1}	respiration rate SOC	defined to match SOC stocks in Peltoniemi et al. (2004, Table 5)

Table A.5: Soil module parameters.

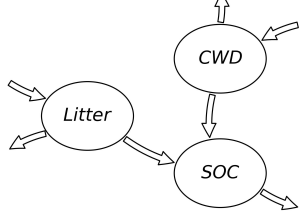


Figure A.4: The soil carbon module.

External output fluxes

- Litter \nearrow : $f_{\text{Litter}} \cdot k_{\text{Litter}} \cdot \text{Litter}$
- CWD \nearrow : $f_{\text{CWD}} \cdot k_{\text{CWD}} \cdot \text{CWD}$
- SOC \nearrow : $k_{\text{SOC}} \cdot \text{SOC}$

Internal fluxes

- $\sum_i S_{L,i} \cdot B_{L,i} + S_{R,i} \cdot B_{R,i} \rightarrow \text{Litter}$
- $\sum_i S_{O,i} \cdot (B_{OS,i} + B_{OH,i}) \rightarrow \text{CWD}$
- Litter \rightarrow SOC: $(1 - f_{\text{Litter}}) \cdot k_{\text{Litter}} \cdot \text{Litter}$
- CWD \rightarrow SOC: $(1 - f_{\text{CWD}}) \cdot k_{\text{CWD}} \cdot \text{CWD}$

1703 Part B Model parameterization and forcing

1704 B.1 Environmental conditions

1705 Climatic conditions refer to those for the years from 2000 to 2019 for
 1706 Hyttiälä SMEAR II-station (retrieved from avaa-database, located in
 1707 `data/forcing/FIHy_forcing_1997_2019.dat`, retrieval date 03/11/2020),
 1708 after removal of the linear trends. The conditions are repeated to cover the
 1709 whole spinup and simulation periods.

1710 B.2 Carbon dynamics parameters

1711 Parameters for the photosynthesis module, the soil module, and the wood
 1712 products were taken from literature (Table A.1, Table A.5, Section A.5). The
 1713 species-specific parameters are listed in Tables A.3 and A.4. When species-
 1714 specific parameters for spruce were not available, values for pines were used
 1715 also for spruce (e.g., labile storage capacities of leaves (δ_L) and roots (δ_R), and

the sapwood parameters γ). A small number of species-specific parameters were subject to numerical investigation. Construction costs for producing fine roots were based Ryan et al. (1997, Table 4) and adjusted to make the model match annual radial growth from literature (Repola 2009, Table 3; see Fig. D.1), which is possible because lower root respiration makes more carbon available for trunk growth. Parameters associated to the density of newly grown sapwood ($\rho_{W_{\min}}$, $\rho_{W_{\max}}$, dbh_M) were empirically chosen to keep the overall wood density close to values reported in (Repola, 2006, Fig. 4), while making sure that the maximum labile carbon storage capacity (δ_W) is nonnegative at all times. The ratio of fine roots to leaves biomass (ρ_{RL}) generally depends on soil fertility. The chosen values (Pukkala, 2014, Table 2) were subject to major investigation in order to match annual radial trunk growth (Repola 2009, Table 3; see Fig. D.1) and indicate, at least for pine, a rather low soil fertility (Vanninen and Mäkelä, 2005, Table 1).

1730 **Part C Model spinup**

1731 Model spinup initializes the stand structure and tree, soil and wood prod-
1732 uct pools for use in the management scenarios. We used a three-stage spinup
1733 to reach reasonable equilibrium pool sizes. First, a uniform pine stand with
1734 one *MeanTree* was initiated assuming empty tree, soil and wood-product
1735 pools. Initial tree dbh = 1.0 cm and $N = 2000 \text{ ha}^{-1}$. As the *MeanTree*
1736 reached a height of 3.0 m, a pre-commercial thinning was performed, to re-
1737 duce N to 1500 ha^{-1} . When the stand basal area (SBA) reached $25 \text{ m}^2 \text{ ha}^{-1}$,
1738 the stand was thinned to SBA = $18 \text{ m}^2 \text{ ha}^{-1}$. A clear cut was done after 80 yr,
1739 the trees in the stand were replanted and the same simulation ran for another
1740 80 yr. After the second clear cut at ~~160-yr~~160-yr, the average of photosyn-
1741 thetically derived carbon input, fluxes between the pools, and the pool sizes
1742 relative to the last 50 yr were used to compute a pseudo-equilibrium of the
1743 carbon stocks in the system (Metzler and Sierra, 2018). These values then
1744 served as initial stocks (soil and wood products) for the second identical
1745 160 yr spinup. The subsequent pseudo-equilibrium soil and wood-product
1746 stocks were then used as the starting point for the third and last spinup
1747 stage, and carbon age distributions were computed from another pseudo-
1748 equilibrium based on the last 50 yr. The last spinup stage runs for another
1749 160 yr and starts with four pine *MeanTrees*, each with dbh = 1.0 cm and rep-
1750 resenting $N_i = 375$ trees per hectare (i.e., a stand density of $N = 1500 \text{ ha}^{-1}$).
1751 The first *MeanTree* was cut and replanted after 20 yr and 100 yr, the sec-
1752 ond one after 40 yr and 120 yr, the third one after 60 yr and 140 yr, and the
1753 fourth one after 80 yr. This creates a mixed-aged pine forest, whose carbon
1754 stocks are in a reasonable equilibrium with a net carbon balance close to zero
1755 (-0.8 kgC m^{-2}), as can be seen from Fig. 3C and Table 2 (INCB, mixed-aged
1756 pine, Entire system). The final conditions are used as the common starting
1757 point for all management scenarios.

1758 **Part D Model benchmarking**

1759 For a more in-depth test of the model's biomass predictions, we compare
1760 it to the external allometric functions based on dbh. The statistical allo-
1761 metric relationships for the biomasses of tree organs depend on one single
1762 dbh value. The different presented management scenarios, however, consist
1763 of differently sized *MeanTrees* with the external allometric relations applied
1764 to each of them separately. Consequently, we ran two ad hoc single-species
1765 (pine, spruce) simulations with a single *MeanTree* each, comparing the tree
1766 organs' biomasses from the two simulations with its associated external statis-
1767 tical allometries. In this way we guarantee that leaf biomass follows perfectly
1768 the observations (Fig. D.2A), which is expected because the *MeanTree*'s leaf
1769 biomass is directly defined by the allometric equation depending on its diam-
1770 eter at breast height. Fine root biomass is perfectly defined by a fixed fine
1771 root-to-leaf biomass ratio (ρ_{RL}). We test discrepancies in the modelled and
1772 observed biomasses of other organs.

1773 The density of newly produced sapwood is dynamically adapted in the
1774 model in order to follow the predicted trunk wood biomass, and we can see
1775 a perfect match Fig. D.2B. Because the biomass of coarse roots and living
1776 branches is linked to trunk biomass via a dynamic factor λ (Eq. A.39), this
1777 perfect match carries over to the biomass of living branches and coarse roots
1778 ("other", Fig. D.2C) and in turn to total tree biomass (Fig. D.2D, without
1779 fine roots).

Radial growth ($\text{dbh}/2$) over 5 years averaged over all trees

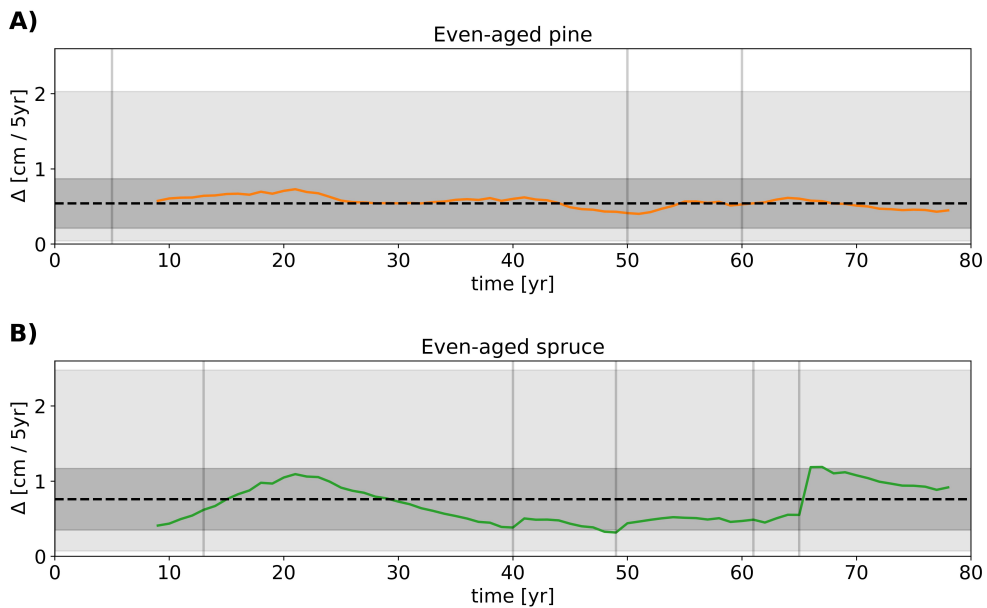


Figure D.1: Radial growth of the two even-aged single-species scenarios. The dark solid graph indicates the radial growth ($\Delta \text{dbh}/2$) over the last five years, averaged over all trees in the stand according to the respective management scenario. The dashed horizontal line marks the mean value, the dark gray area the standard deviation around the mean, and the light gray area the range between the minimum and maximum values of the stand inventory data described in Repola (2009, Table 3).

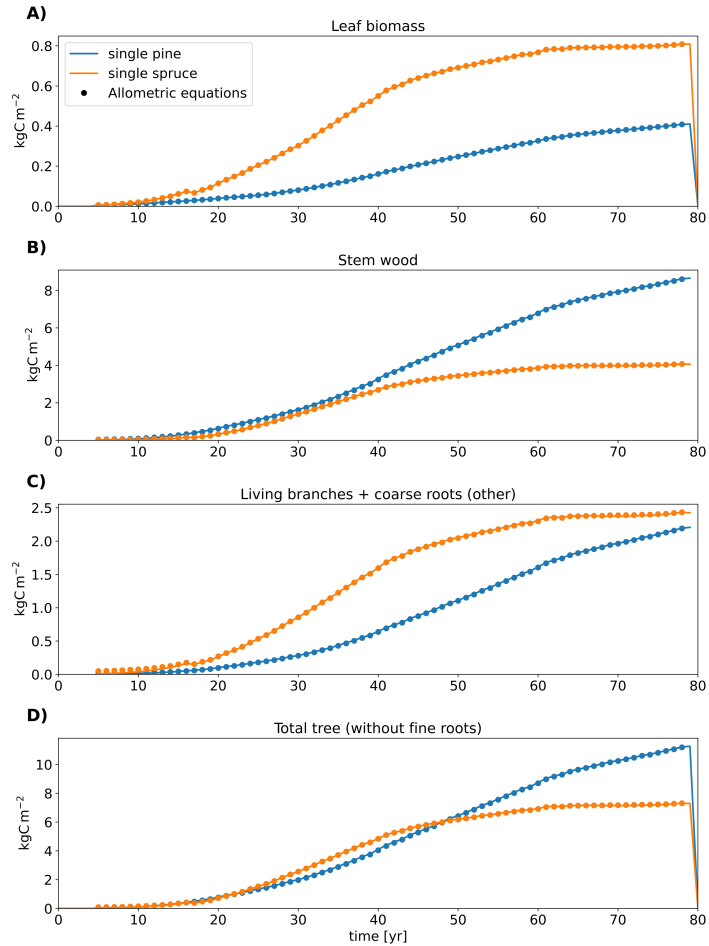


Figure D.2: Model accuracy with respect to external allometries. Different tree organs' carbon content over time (solid lines) and their statistical counterparts as derived from Repola and Ahnlund Ulvcrona (2014), Repola (2009) and Lehtonen (2005) (dots), based on the diameter at breast height of the single-tree simulations for benchmarking.

1780 Part E Supplementary figures and tables

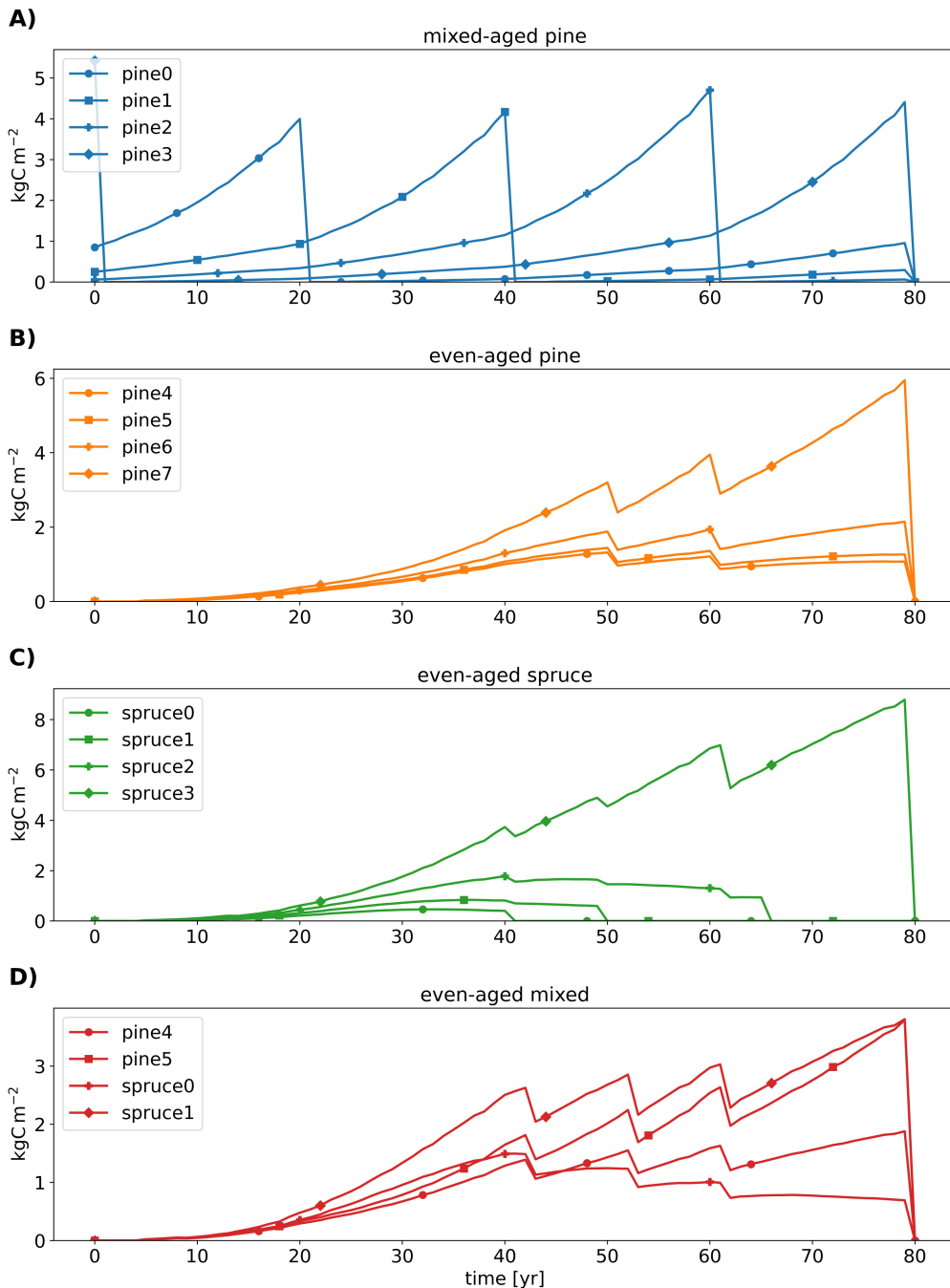


Figure E.1: Time series of carbon in *MeanTrees*. Different panels show different management scenarios.

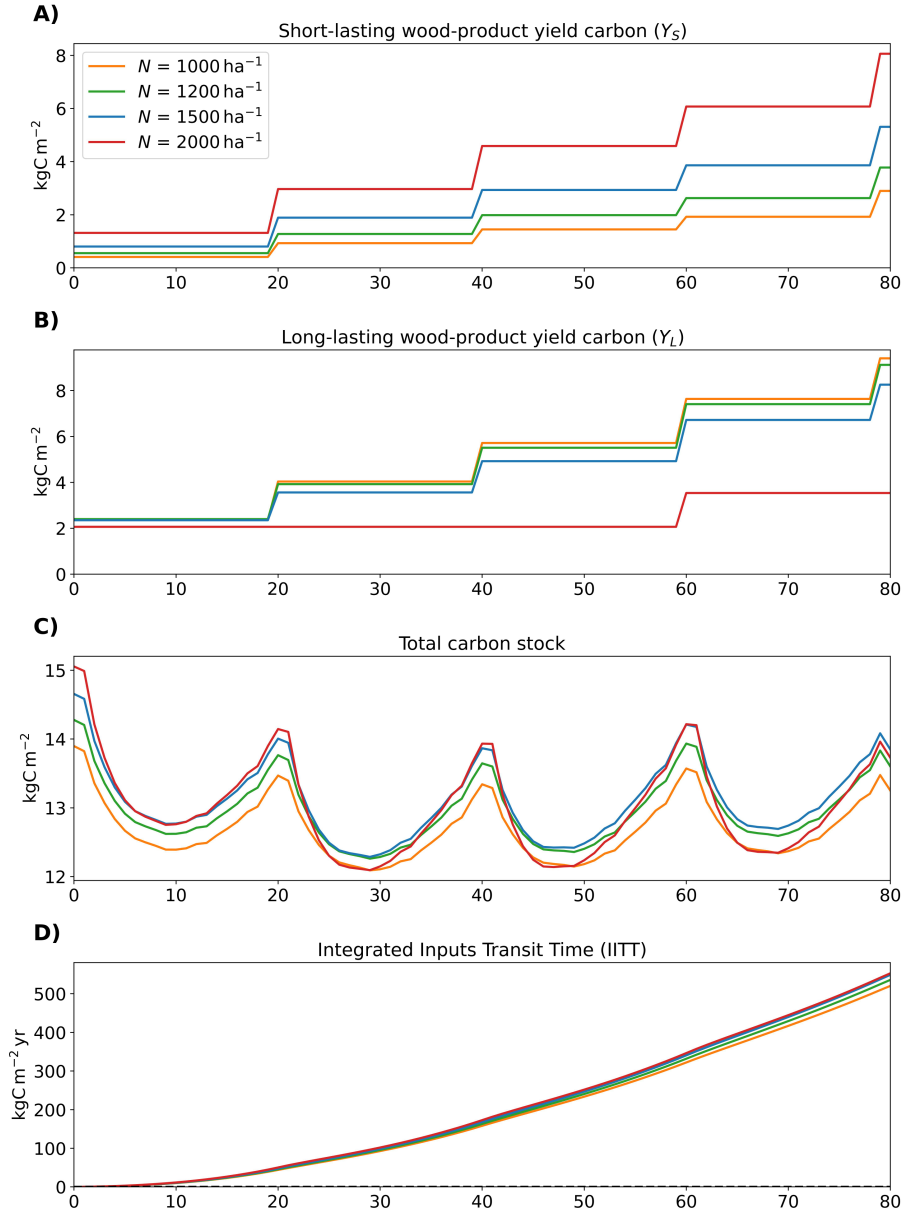


Figure E.2: Temporal evolution of short-lasting and long-lasting wood production, carbon sequestration and climate change mitigation potential metrics for mixed-aged pine scenarios with different tree densities (N). A) Cumulative short-lasting Short-lasting wood-product yield carbon (Y_S , Eq. (5)). B) Cumulative long-lasting Long-lasting wood-product yield carbon (Y_L , Eq. (5)). C) Total carbon stock including trees, soil, and wood products. D) Integrated Inputs Transit Time (IITT, Eq. (8)).

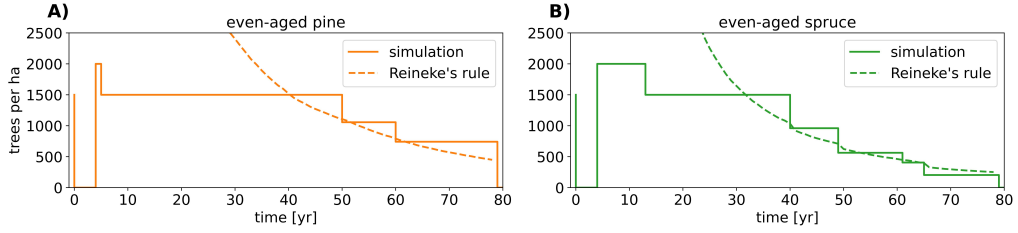


Figure E.3: Reineke's rule self-thinning rule (dashed lines) and the thinning in different management scenarios (solid lines). A) even-aged pine, B) even-aged spruce.

Parameter	Scenario	total carbon	$Y_S + Y_L$	IITT	ICS
R_{mL}	mixed-aged pine ¹	9.39	8.07	8.81	9.41
	mixed-aged pine ²	4.52	6.40	4.17	6.97
	mixed-aged pine ³	8.24	11.43	6.88	8.32
	mixed-aged pine ⁴	9.85	6.17	6.50	8.09
S_R	mixed-aged pine	6.82	7.42	6.21	6.77
	even-aged pine	5.25	8.55	1.91	4.37
	even-aged spruce	30.36	6.96	5.04	3.01
	even-aged mixed	2.81	6.96	1.45	3.99
$V_{cmax,25}$	mixed-aged pine	19.95¹	16.41	18.19	19.93
	even-aged pine	9.74	13.66	12.37	17.27 ²
	even-aged spruce	11.85	18.15	11.47	16.58
	even-aged mixed	10.10	12.69⁴	12.64	17.12
ρ_{RL}	mixed-aged pine	12.29	12.31	11.29	12.26
	even-aged pine	4.84	13.11	4.79	8.78
	even-aged spruce	32.40³	4.09	4.96	4.66
	even-aged mixed	5.69	12.21	3.81	7.99

Table E.1: Parameter sensitivity table showing the relative spread in % from the mean when a specific parameter was varied $\pm 10\%$ from its default value. Bold values mark the highest relative spread per parameter (block), italic values mark the highest relative spread per metric (column), and superscripts mark the highest relative spread per management scenario. The columns represent the parameter subject to change, the management scenario considered, total carbon stock in the system, wood-product yield ($Y_S + Y_L$), Integrated Inputs Transit Time (IITT), and Integrated Carbon Stocks (ICS).

1781 **References**

- 1782 Evy Ampoorter, Luc Barbaro, Hervé Jactel, Lander Baeten, Johanna
1783 Boberg, Monique Carnol, Bastien Castagneyrol, Yohan Charbonnier,
1784 Seid Muhie Dawud, Marc Deconchat, et al. Tree diversity is key for pro-
1785 moting the diversity and abundance of forest-associated taxa in Europe.
1786 *Oikos*, 129(2):133–146, 2020.
- 1787 David H Anderson. *Compartmental modeling and tracer kinetics*, volume 50.
1788 Springer Science & Business Media, 1983.
- 1789 Rasmus Astrup, Pierre Y Bernier, Hélène Genet, David A Lutz, and Ryan M
1790 Bright. A sensible climate solution for the boreal forest. *Nature Climate
1791 Change*, 8(1):11–12, 2018.
- 1792 Dennis Baldocchi, Francis M Kelliher, T Aet Black, and Paul Jarvis. Climate
1793 and vegetation controls on boreal zone energy exchange. *Global Change
1794 Biology*, 6(S1):69–83, 2000.
- 1795 Jürgen Bauhus, David I Forrester, Barry Gardiner, Hervé Jactel, Ramon
1796 Vallejo, and Hans Pretzsch. Ecological stability of mixed-species forests.
1797 In *Mixed-species forests*, pages 337–382. Springer, 2017.
- 1798 Yves Bergeron, Mike Flannigan, Sylvie Gauthier, Alain Leduc, and Patrick
1799 Lefort. Past, current and future fire frequency in the Canadian boreal
1800 forest: implications for sustainable forest management. *Ambio*, 33(6):356–
1801 360, 2004.
- 1802 Dan Berggren Kleja, Magnus Svensson, Hooshang Majdi, Per-Erik Jansson,
1803 Ola Langvall, Bo Bergkvist, Maj-Britt Johansson, Per Weslien, Laimi Tru-
1804 usb, Anders Lindroth, and Göran I Ågren. Pools and fluxes of carbon in
1805 three Norway spruce stands along a climatic gradient in Sweden. *Biogeo-
1806 chemistry*, 2007.

- 1807 Bert Bolin and Henning Rodhe. A note on the concepts of age distribution
1808 and transit time in natural reservoirs. *Tellus*, 25(1):58–62, 1973.
- 1809 Gordon B Bonan. Forests and climate change: forcings, feedbacks, and the
1810 climate benefits of forests. *Science*, 320(5882):1444–1449, 2008.
- 1811 Pál Börjesson, Julia Hansson, and Göran Berndes. Future demand for forest-
1812 based biomass for energy purposes in Sweden. *Forest Ecology and Man-
1813 agement*, 383:17–26, 2017.
- 1814 Hannes Böttcher, Annette Freibauer, Michael Obersteiner, and Ernst-Detlef
1815 Schulze. Uncertainty analysis of climate change mitigation options in the
1816 forestry sector using a generic carbon budget model. *ecological modelling*,
1817 213(1):45–62, 2008a.
- 1818 Hannes Böttcher, Werner A Kurz, and Annette Freibauer. Accounting of
1819 forest carbon sinks and sources under a future climate protocol—factoring
1820 out past disturbance and management effects on age-class structure. *En-
1821 vironmental Science & Policy*, 11(8):669–686, 2008b.
- 1822 Roger W Brockett. *Finite Dimensional Linear Systems*, volume 74. SIAM,
1823 2015.
- 1824 Harald Bugmann. A review of forest gap models. *Climatic Change*, 51(3):
1825 259–305, 2001.
- 1826 Richard T Busing and Daniel Mailly. Advances in spatial, individual-based
1827 modelling of forest dynamics. *Journal of Vegetation Science*, 15(6):831–
1828 842, 2004.
- 1829 MGR Cannell and RC Dewar. Carbon allocation in trees: a review of con-
1830 cepts for modelling. *Advances in ecological research*, 25:59–104, 1994.
- 1831 Mariah S Carbone, Claudia I Czimczik, Kelsey E McDuffee, and Susan E
1832 Trumbore. Allocation and residence time of photosynthetic products in a

- 1833 boreal forest using a low-level ^{14}C pulse-chase labeling technique. *Global*
1834 *Change Biology*, 13(2):466–477, 2007.
- 1835 Mariah S Carbone, Claudia I Czimczik, Trevor F Keenan, Paula F Mu-
1836 rakami, Neil Pederson, Paul G Schaberg, Xiaomei Xu, and Andrew D
1837 Richardson. Age, allocation and availability of nonstructural carbon in
1838 mature red maple trees. *New Phytologist*, 200(4):1145–1155, 2013.
- 1839 FS Chapin III, AD McGuire, J Randerson, R Pielke, Dennis Baldocchi,
1840 SE Hobbie, Nigel Roulet, W Eugster, E Kasischke, EB Rastetter, et al.
1841 Arctic and boreal ecosystems of western North America as components of
1842 the climate system. *Global Change Biology*, 6(S1):211–223, 2000.
- 1843 FAO. Classification of forest products. *Scientific reports*, 2022. doi: 10.4060/
1844 cb8216en.
- 1845 G D Farquhar, S V Caemmerer, and J A Berry. A biochemical model for
1846 photosynthetic CO_2 assimilation in leaves of C_3 species. *Planta*, 149(1):
1847 78–90, 1980.
- 1848 Michael Fell and Kiona Ogle. Refinement of a theoretical trait space for
1849 North American trees via environmental filtering. *Ecological Monographs*,
1850 88(3):372–384, 2018.
- 1851 Michael Fell, Jarrett Barber, Jeremy W Lichstein, and Kiona Ogle. Multidi-
1852 mensional trait space informed by a mechanistic model of tree growth and
1853 carbon allocation. *Ecosphere*, 9(1):e02060, 2018.
- 1854 Terje Gobakken, Nils L Lexerød, and Tron Eid. T: A forest simulator for
1855 bioeconomic analyses based on models for individual trees. *Scandinavian*
1856 *Journal of Forest Research*, 23(3):250–265, 2008.
- 1857 Martin Goude, Urban Nilsson, and Emma Holmström. Comparing direct
1858 and indirect leaf area measurements for Scots pine and Norway spruce

- 1859 plantations in Sweden. *European Journal of Forest Research*, 138(6):1033–
1860 1047, 2019.
- 1861 Andrei Gromtsev. Natural disturbance dynamics in the boreal forests of
1862 European Russia: a review. *Silva Fennica*, 36(1):41–55, 2002.
- 1863 Vegard Sverre Gundersen and Lars Helge Frivold. Public preferences for
1864 forest structures: A review of quantitative surveys from Finland, Norway
1865 and Sweden. *Urban Forestry & Urban Greening*, 7(4):241–258, 2008.
- 1866 Corinna Hawkes. Woody plant mortality algorithms: description, problems
1867 and progress. *Ecological Modelling*, 126(2-3):225–248, 2000.
- 1868 Heljä-Sisko Helmisaari, John Derome, Pekka Nöjd, and Mikko Kukkola. Fine
1869 root biomass in relation to site and stand characteristics in Norway spruce
1870 and Scots pine stands. *Tree Physiology*, 27(10):1493–1504, 2007.
- 1871 M Hiltunen, H Strandman, and A Kilpeläinen. Optimizing forest manage-
1872 ment for climate impact and economic profitability under alternative initial
1873 stand age structures. *Biomass and Bioenergy*, 147:106027, 2021.
- 1874 P Höglberg, LA Ceder, R Astrup, D Binkley, L Dalsgaard, G Egnell, A Fil-
1875 ipchuk, H Genet, A Ilintsev, WA Kurz, et al. Sustainable boreal forest
1876 management challenges and opportunities for climate change mitigation.
1877 2021.
- 1878 Emma Holmström, Martin Goude, Oscar Nilsson, Annika Nordin, Tomas
1879 Lundmark, and Urban Nilsson. Productivity of Scots pine and Norway
1880 spruce in central Sweden and competitive release in mixtures of the two
1881 species. *Forest Ecology and Management*, 429:287–293, 2018.
- 1882 Elias Hurmekoski, Janni Kunttu, Tero Heinonen, Timo Pukkala, and Heli
1883 Peltola. Does expanding wood use in construction and textile markets
1884 contribute to climate change mitigation? *Renewable and Sustainable En-*
1885 *ergy Reviews*, 174:113152, 2023.

- 1886 Riku Huttunen, Petteri Kuuva, Markku Kinnunen, Bettina Lemström, and
1887 Petri Hirvonen. Carbon neutral Finland 2035 - national climate and energy
1888 strategy. 2022.
- 1889 Saija Huuskonen, Timo Domisch, Leena Finér, Jarkko Hantula, Jari Hynynen,
1890 Juho Matala, Jari Miina, Seppo Neuvonen, Seppo Nevalainen, Pentti
1891 Niemistö, et al. What is the potential for replacing monocultures with
1892 mixed-species stands to enhance ecosystem services in boreal forests in
1893 Fennoscandia? *Forest ecology and management*, 479:118558, 2021.
- 1894 Jari Hynynen, Risto Ojansuu, Hannu Hökkä, Jouni Siipilehto, Hannu Salmi-
1895 nen, and Pekka Haapala. *Models for predicting stand development in*
1896 *MELA system*. Metsätutkimuslaitos, 2002.
- 1897 Jari Hynynen, Anssi Ahtikoski, Juha Siitonan, Risto Sievänen, and Jari Liski.
1898 Applying the MOTTI simulator to analyse the effects of alternative man-
1899 agement schedules on timber and non-timber production. *Forest Ecology*
1900 and Management, 207(1-2):5–18, 2005.
- 1901 Riitta Hyvönen and Göran I Ågren. Decomposer invasion rate, decomposer
1902 growth rate, and substrate chemical quality: how they influence soil or-
1903 ganic matter turnover. *Canadian Journal of Forest Research*, 31(9):1594–
1904 1601, 2001.
- 1905 John A Jacquez and Carl P Simon. Qualitative theory of compartmental
1906 systems. *Siam Review*, 35(1):43–79, 1993.
- 1907 Hervé Jactel, Xoaquín Moreira, and Bastien Castagneyrol. Tree diversity
1908 and forest resistance to insect pests: patterns, mechanisms, and prospects.
1909 *Annual Review of Entomology*, 66:277–296, 2021.
- 1910 Robert Jandl, Marcus Lindner, Lars Vesterdal, Bram Bauwens, Rainer
1911 Baritz, Frank Hagedorn, Dale W Johnson, Kari Minkkinen, and Kenneth A

- 1912 Byrne. How strongly can forest management influence soil carbon sequestration? *Geoderma*, 137(3-4):253–268, 2007a.
- 1913
- 1914 Robert Jandl, Lars Vesterdal, Mats Olsson, Oliver Bens, Franz Badeck, and
1915 J Roc. Carbon sequestration and forest management. *CABI Reviews*,
1916 (2007):16–pp, 2007b.
- 1917 DS Jenkinson and JH Rayner. The turnover of soil organic matter in some of
1918 the Rothamsted classical experiments. *Soil science*, 123(5):298–305, 1977.
- 1919 Jens Kattge and Wolfgang Knorr. Temperature acclimation in a biochemical
1920 model of photosynthesis: a reanalysis of data from 36 species. *Plant, cell
& environment*, 30(9):1176–1190, 2007.
- 1921
- 1922 Seppo Kellomäki. *Management of Boreal Forests: Theories and Applications
for Ecosystem Services*. Springer Nature, 2022.
- 1923
- 1924 Seppo Kellomäki, Heli Peltola, Tuula Nuutinen, Kari T Korhonen, and Harri
1925 Strandman. Sensitivity of managed boreal forests in Finland to climate
1926 change, with implications for adaptive management. *Philosophical Transactions of the Royal Society B: Biological Sciences*, 363(1501):2339–2349,
1927 2008.
- 1928
- 1929 Peter Köhler and Andreas Huth. The effects of tree species grouping in
1930 tropical rainforest modelling: simulations with the individual-based model
1931 FORMIND. *Ecological Modelling*, 109(3):301–321, 1998.
- 1930
- 1932 Pasi Kolari, Hanna K Lappalainen, Heikki HäNninen, and Pertti Hari. Re-
1933 lationship between temperature and the seasonal course of photosynthesis
1934 in Scots pine at northern timberline and in southern boreal zone. *Tellus
B: Chemical and Physical Meteorology*, 59(3):542–552, 2007.
- 1935
- 1936 Taneli Kolström. Modelling the development of an uneven-aged stand of
1937 *Picea abies*. *Scandinavian Journal of Forest Research*, 8(1-4):373–383,
1938 1993.

- 1939 CD Koven, WJ Riley, ZM Subin, JY Tang, MS Torn, WD Collins, GB Bonan,
1940 DM Lawrence, and SC Swenson. The effect of vertically resolved soil
1941 biogeochemistry and alternate soil C and N models on C dynamics of
1942 CLM4. *Biogeosciences*, 10(11):7109–7131, 2013.
- 1943 Timo Kuuluvainen, Tuomas Aakala, et al. Natural forest dynamics in boreal
1944 Fennoscandia: a review and classification. *Silva Fennica*, 45(5):823–841,
1945 2011.
- 1946 Timo Kuuluvainen, Olli Tahvonen, and Tuomas Aakala. Even-aged and
1947 uneven-aged forest management in boreal Fennoscandia: a review. *Ambio*,
1948 41(7):720–737, 2012.
- 1949 Jouko Laasasenaho. *Taper curve and volume functions for pine, spruce and*
1950 *birch*. Metsäntutkimuslaitos, 1982.
- 1951 André Lacointe. Carbon allocation among tree organs: a review of basic
1952 processes and representation in functional-structural tree models. *Annals*
1953 *of Forest Science*, 57(5):521–533, 2000.
- 1954 Erkki Lähde, Olavi Laiho, and C Julian Lin. Silvicultural alternatives in an
1955 uneven-sized forest dominated by Picea abies. *Journal of forest research*,
1956 15(1):14–20, 2010.
- 1957 Tomas Lämås, Lars Sängstuvall, Karin Öhman, Johanna Lundström,
1958 Jonatan Årevall, Hampus Holmström, Linus Nilsson, Eva-Maria Nord-
1959 ström, Per-Erik Wikberg, Peder Wikström, et al. The multi-faceted
1960 Swedish Heureka forest decision support system: context, functionality,
1961 design, and 10 years experiences of its use. *Frontiers in Forests and Global*
1962 *Change*, 6:1163105, 2023.
- 1963 JJ Landsberg and RH Waring. A generalised model of forest productivity
1964 using simplified concepts of radiation-use efficiency, carbon balance and
1965 partitioning. *Forest ecology and management*, 95(3):209–228, 1997.

- 1966 Jørgen Bo Larsen, Per Angelstam, Jürgen Bauhus, João Fidalgo Carvalho,
1967 Jurij Daci, Dorota Dobrowolska, Anna Gazda, Lena Gustafsson, Frank
1968 Krumm, Thomas Knoke, et al. *Closer-to-Nature Forest Management.*
1969 *From Science to Policy* 12., volume 12. EFI European Forest Institute,
1970 2022.
- 1971 Samuli Launiainen, Gabriel G Katul, Ari Lauren, and Pasi Kolari. Coupling
1972 boreal forest CO₂, H₂O and energy flows by a vertically structured forest
1973 canopy – soil model with separate bryophyte layer. *Ecological Modelling*,
1974 312:385–405, 2015.
- 1975 Samuli Launiainen, Gabriel G Katul, Pasi Kolari, Anders Lindroth, Annalea
1976 Lohila, Mika Aurela, Andrej Varlagin, Achim Grelle, and Timo Vesala. Do
1977 the energy fluxes and surface conductance of boreal coniferous forests in
1978 Europe scale with leaf area? *Global Change Biology*, 22(12):4096–4113,
1979 2016.
- 1980 Samuli Launiainen, Mingfu Guan, Aura Salmivaara, and Antti-Jussi
1981 Kieloaho. Modeling boreal forest evapotranspiration and water balance
1982 at stand and catchment scales: a spatial approach. *Hydrology and Earth
1983 System Sciences*, 23(8):3457–3480, 2019.
- 1984 Samuli Launiainen, Gabriel G Katul, Kersti Leppä, Pasi Kolari, Toprak
1985 Aslan, Tiia Grönholm, Lauri Korhonen, Ivan Mammarella, and Vesala
1986 Timo. Does increasing atmospheric CO₂ explain increasing carbon sink of
1987 a boreal coniferous forest? *Global Change Biology*, 2022.
- 1988 MB Lavigne and MG Ryan. Growth and maintenance respiration rates of as-
1989 pen, black spruce and jack pine stems at northern and southern BOREAS
1990 sites. *Tree Physiology*, 17(8-9):543–551, 1997.
- 1991 Xavier Le Roux, André Lacointe, Abraham Escobar-Gutiérrez, and Séver-
1992 ine Le Dizès. Carbon-based models of individual tree growth: a critical
1993 appraisal. *Annals of Forest Science*, 58(5):469–506, 2001.

- 1994 Aleksi Lehtonen. Estimating foliage biomass in Scots pine (*Pinus sylvestris*)
1995 and Norway spruce (*Picea abies*) plots. *Tree Physiology*, 25(7):803–811,
1996 2005.
- 1997 Aleksi Lehtonen, Kyle Eyyvindson, Kari Häkkinen, Kersti Leppä, Aura Salmi-
1998 vaara, Mikko Peltoniemi, Olli Salminen, Sakari Sarkkola, Samuli Launi-
1999 ainen, Paavo Ojanen, et al. Potential of continuous cover forestry on
2000 drained peatlands to increase the carbon sink in finland. *Scientific Re-
2001 ports*, 13(1):15510, 2023.
- 2002 TC Lemprière, WA Kurz, EH Hogg, C Schmoll, GJ Rampley, D Yemshanov,
2003 DW McKenney, R Gilsean, A Beatch, D Blain, et al. Canadian boreal
2004 forests and climate change mitigation. *Environmental Reviews*, 21(4):293–
2005 321, 2013.
- 2006 Timothy M Lenton, Hermann Held, Elmar Kriegler, Jim W Hall, Wolfgang
2007 Lucht, Stefan Rahmstorf, and Hans Joachim Schellnhuber. Tipping ele-
2008 ments in the Earth’s climate system. *Proceedings of the national Academy
2009 of Sciences*, 105(6):1786–1793, 2008.
- 2010 Kersti Leppä, Mika Korkiakoski, Mika Nieminen, Raija Laiho, Juha-Pekka
2011 Hotanen, Antti-Jussi Kieloaho, Leila Korpela, Tuomas Laurila, Annalea
2012 Lohila, Kari Minkkinen, Raisa Mäkipää, Paavo Ojanen, Meeri Pearson,
2013 Timo Penttilä, Juha-Pekka Tuovinen, and Samuli Launiainen. Vegeta-
2014 tion controls of water and energy balance of a drained peatland forest:
2015 Responses to alternative harvesting practices. *Agricultural and Forest Me-
2016 teorology*, 295:108198, 2020.
- 2017 Jari Liski, Ari Pussinen, Kim Pingoud, Raisa Mäkipää, and Timo Kar-
2018 jalainen. Which rotation length is favourable to carbon sequestration?
2019 *Canadian Journal of Forest Research*, 31(11):2004–2013, 2001.
- 2020 Michel Loreau. Biodiversity and ecosystem stability: New theoretical in-

- 2021 sights. *The Ecological and Societal Consequences of Biodiversity Loss*,
2022 pages 145–166, 2022.
- 2023 Tomas Lundmark, Bishnu Chandra Poudel, Gustav Stål, Annika Nordin,
2024 and Johan Sonesson. Carbon balance in production forestry in relation to
2025 rotation length. *Canadian journal of forest research*, 48(6):672–678, 2018.
- 2026 Yiqi Luo and Ensheng Weng. Dynamic disequilibrium of the terrestrial car-
2027 bon cycle under global change. *Trends in Ecology & Evolution*, 26(2):
2028 96–104, 2011.
- 2029 Sebastiaan Luyssaert, E Schulze, Annett Börner, Alexander Knöhl, Dominik
2030 Hessenmöller, Beverly E Law, Philippe Ciais, John Grace, et al. Old-
2031 growth forests as global carbon sinks. *Nature*, 455(7210):213–215, 2008.
- 2032 Joachim Maes, Camino Liquete, Anne Teller, Markus Erhard, Maria Luisa
2033 Paracchini, José I Barredo, Bruna Grizzetti, Ana Cardoso, Francesca
2034 Somma, Jan-Erik Petersen, et al. An indicator framework for assessing
2035 ecosystem services in support of the EU Biodiversity Strategy to 2020.
2036 *Ecosystem services*, 17:14–23, 2016.
- 2037 Annikki Mäkelä. A carbon balance model of growth and self-pruning in trees
2038 based on structural relationships. *Forest Science*, 43(1):7–24, 1997.
- 2039 Stefano Manzoni and Amilcare Porporato. Soil carbon and nitrogen mineral-
2040 ization: Theory and models across scales. *Soil Biology and Biochemistry*,
2041 41(7):1355–1379, 2009.
- 2042 Ole Martin Bollandsås, Joseph Buongiorno, and Terje Gobakken. Predicting
2043 the growth of stands of trees of mixed species and size: A matrix model for
2044 Norway. *Scandinavian Journal of Forest Research*, 23(2):167–178, 2008.
- 2045 Juho Matala, Leena Kärkkäinen, Kari Häkkinen, Seppo Kellomäki, and Tu-
2046 ula Nuutinen. Carbon sequestration in the growing stock of trees in finland

- 2047 under different cutting and climate scenarios. *European Journal of Forest*
2048 *Research*, 128:493–504, 2009.
- 2049 BE Medlyn, Erwin Dreyer, D Ellsworth, M Forstreuter, PC Harley, MUF
2050 Kirschbaum, Xavier Le Roux, Pierre Montpied, J Strassemeyer, A Wal-
2051 croft, et al. Temperature response of parameters of a biochemically based
2052 model of photosynthesis. II. a review of experimental data. *Plant, Cell &*
2053 *Environment*, 25(9):1167–1179, 2002.
- 2054 Belinda E. Medlyn, Remko A. Duursma, Derek Eamus, David S. Ellsworth,
2055 I. Colin Prentice, Craig V. M. Barton, Kristine Y. Crous, Paolo De Angelis,
2056 Michael Freeman, and Lisa Wingate. Reconciling the optimal and empirical
2057 approaches to modelling stomatal conductance. *Global Change Biology*, 18
2058 (11):3476–3476, 2012.
- 2059 Christian Messier, Jürgen Bauhus, Rita Sousa-Silva, Harald Auge, Lander
2060 Baeten, Nadia Barsoum, Helge Bruehlheide, Benjamin Caldwell, Jeannine
2061 Cavender-Bares, Els Dhiedt, et al. For the sake of resilience and multi-
2062 functionality, let's diversify planted forests! *Conservation Letters*, 15(1):
2063 e12829, 2022.
- 2064 Holger Metzler and Carlos A Sierra. Linear autonomous compartmental mod-
2065 els as continuous-time Markov chains: Transit-time and age distributions.
2066 *Mathematical Geosciences*, 50(1):1–34, 2018.
- 2067 Holger Metzler, Markus Müller, and Carlos A Sierra. Transit-time and age
2068 distributions for nonlinear time-dependent compartmental systems. *Pro-
2069 ceedings of the National Academy of Sciences*, 115:201705296, 01 2018. doi:
2070 10.1073/pnas.1705296115.
- 2071 Holger Metzler, Qing Zhu, William Riley, Alison Hoyt, Markus Müller, and
2072 Carlos A Sierra. Mathematical reconstruction of land carbon models from
2073 their numerical output: Computing soil radiocarbon from ^{12}C dynamics.
2074 *Journal of Advances in Modeling Earth Systems*, 12(1), 2020.

- 2075 P Mikola. Selection forestry. *Silva Fennica*, 18:293–301, 1984.
- 2076 MEA Millennium Ecosystem Assessment. *Ecosystems and human well-being*,
2077 volume 5. Island press Washington, DC, 2005.
- 2078 Jan Muhr, Alon Angert, Robinson I Negrón-Juárez, Waldemar Alegria
2079 Muñoz, Guido Kraemer, Jeffrey Q Chambers, and Susan E Trumbore.
2080 Carbon dioxide emitted from live stems of tropical trees is several years
2081 old. *Tree Physiology*, 33(7):743–752, 2013.
- 2082 Petteri Muukkonen. Needle biomass turnover rates of Scots pine (*Pinus*
2083 *sylvestris* L.) derived from the needle-shed dynamics. *Trees*, 19(3):273–
2084 279, 2005.
- 2085 Petteri Muukkonen and Aleksi Lehtonen. Needle and branch biomass
2086 turnover rates of Norway spruce (*Picea abies*). *Canadian Journal of Forest
Research*, 34(12):2517–2527, 2004.
- 2088 Gert-Jan Nabuurs, Mart-Jan Schelhaas, Christophe Orazio, Geerten
2089 Hengeveld, Margarida Tome, and Edward P Farrell. European perspective
2090 on the development of planted forests, including projections to 2065. In
2091 *New Zealand Journal of Forestry Science*, volume 44, pages 1–7. Springer,
2092 2014.
- 2093 Manfred Näslund. Skogsförsöksanstaltens gallringsförsök i tallskog. 1936.
- 2094 Manfred Näslund. Funktioner och tabeller för kubering av stående träd. 36
2095 (3):1–81, 1947.
- 2096 Asko Noormets, Daniel Epron, Jean-Christophe Domec, SG McNulty, T Fox,
2097 G Sun, and JS King. Effects of forest management on productivity and
2098 carbon sequestration: A review and hypothesis. *Forest Ecology and Man-
agement*, 355:124–140, 2015.

- 2100 Kiona Ogle and Stephen W Pacala. A modeling framework for inferring tree
2101 growth and allocation from physiological, morphological and allometric
2102 traits. *Tree Physiology*, 29(4):587–605, 2009.
- 2103 Stephen W Pacala, Charles D Canham, John Saponara, John A Silander Jr,
2104 Richard K Kobe, and Eric Ribbens. Forest models defined by field measure-
2105 ments: estimation, error analysis and dynamics. *Ecological monographs*,
2106 66(1):1–43, 1996.
- 2107 Yude Pan, Richard A Birdsey, Jingyun Fang, Richard Houghton, Pekka E
2108 Kauppi, Werner A Kurz, Oliver L Phillips, Anatoly Shvidenko, Simon L
2109 Lewis, Josep G Canadell, et al. A large and persistent carbon sink in the
2110 world’s forests. *Science*, 333(6045):988–993, 2011.
- 2111 William J Parton, David S Schimel, C Vernon Cole, and Dennis S Ojima.
2112 Analysis of factors controlling soil organic matter levels in Great Plains
2113 grasslands. *Soil Science Society of America Journal*, 51(5):1173–1179,
2114 1987.
- 2115 Mikko Peltoniemi, Raisa Mäkipää, Jari Liski, and Pekka Tamminen. Changes
2116 in soil carbon with stand age—an evaluation of a modelling method with
2117 empirical data. *Global Change Biology*, 10(12):2078–2091, 2004.
- 2118 Tähti Pohjanmies, María Triviño, Eric Le Tortorec, Adriano Mazziotta, Tord
2119 Snäll, and Mikko Mönkkönen. Impacts of forestry on boreal forests: An
2120 ecosystem services perspective. *Ambio*, 46(7):743–755, 2017.
- 2121 Timo Pukkala. Does biofuel harvesting and continuous cover management
2122 increase carbon sequestration? *Forest Policy and Economics*, 43:41–50,
2123 2014.
- 2124 Timo Pukkala. Calculating the additional carbon sequestration of Finnish
2125 forestry. *Journal of Sustainable Forestry*, pages 1–18, 2020.

- 2126 Timo Pukkala, Erkki Lähde, and Olavi Laiho. Growth and yield models for
2127 uneven-sized forest stands in Finland. *Forest Ecology and Management*,
2128 258(3):207–216, 2009.
- 2129 Göran I Ågren and J Fredrik Wikström. Modelling carbon allocation — a
2130 review. *NZJ For. Sci*, 23:343–353, 1993.
- 2131 JT Randerson, FS Chapin III, JW Harden, JC Neff, and ME Harmon. Net
2132 ecosystem production: a comprehensive measure of net carbon accumula-
2133 tion by ecosystems. *Ecological applications*, 12(4):937–947, 2002.
- 2134 Martin Rasmussen, Alan Hastings, Matthew J. Smith, Folashade B. Agusto,
2135 Benito M. Chen-Charpentier, Forrest M. Hoffman, Jiang Jiang, Katherine
2136 E. O. Todd-Brown, Ying Wang, Ying-Ping Wang, and Yiqi Luo. Transit
2137 times and mean ages for nonautonomous and autonomous compartmental
2138 systems. *Journal of Mathematical Biology*, 73(6-7):1379–1398, apr 2016.
2139 doi: 10.1007/s00285-016-0990-8.
- 2140 Lester Henry Reineke. Perfection a stand-density index for even-aged forest.
2141 *Journal of Agricultural Research*, 46:627–638, 1933.
- 2142 Jaakko Repola. Models for vertical wood density of Scots pine, Norway
2143 spruce and birch stems, and their application to determine average wood
2144 density. 2006.
- 2145 Jaakko Repola. Biomass equations for Scots pine and Norway spruce in
2146 Finland. 2009.
- 2147 Jaakko Repola and Kristina Ahnlund Ulvcrona. Modelling biomass of young
2148 and dense Scots pine (*Pinus sylvestris* L.) dominated mixed forests in
2149 northern Sweden. 2014.
- 2150 Robert G Ribe. The aesthetics of forestry: what has empirical preference
2151 research taught us? *Environmental management*, 13(1):55–74, 1989.

- 2152 José Riofrío, Miren del Río, Douglas A Maguire, and Felipe Bravo. Species
2153 mixing effects on height–diameter and basal area increment models for
2154 Scots pine and Maritime pine. *Forests*, 10(3):249, 2019.
- 2155 Will Rolls and Piers M Forster. Quantifying forest growth uncertainty on
2156 carbon payback times in a simple biomass carbon model. *Environmental*
2157 *Research Communications*, 2(4):045001, 2020.
- 2158 Ricardo Ruiz-Peinado, Hans Pretzsch, Magnus Löf, Michael Heym, Kamil
2159 Bielak, Jorge Aldea, Ignacio Barbeito, Gediminas Brazaitis, Lars Drössler,
2160 Kšištof Godvod, Aksel Granhus, Stig-Olof Holm, Aris Jansons, Ekaterina
2161 Makrickienė, Marek Metslaid, Sandra Metslaid, Arne Nothdurft, Ditlev
2162 Otto Juel Reventlow, Roman Sitko, Gintarė Stankevičienė, and Miren del
2163 Río. Mixing effects on Scots pine (*Pinus sylvestris* L.) and Norway spruce
2164 (*Picea abies* L. Karst.) productivity along a climatic gradient across Eu-
2165 rope. *Forest Ecology and Management*, 482:118834, 2021. ISSN 0378-
2166 1127. doi: <https://doi.org/10.1016/j.foreco.2020.118834>. URL <https://www.sciencedirect.com/science/article/pii/S0378112720316030>.
- 2168 Michael G Ryan, Michael B Lavigne, and Stith T Gower. Annual carbon
2169 cost of autotrophic respiration in boreal forest ecosystems in relation to
2170 species and climate. *Journal of Geophysical Research: Atmospheres*, 102
2171 (D24):28871–28883, 1997.
- 2172 Ernst Detlef Schulze, Carlos A Sierra, Vincent Egenolf, Rene Woerdehoff,
2173 Roland Irslinger, Conrad Baldamus, Inge Stupak, and Hermann Spell-
2174 mann. The climate change mitigation effect of bioenergy from sustainably
2175 managed forests in Central Europe. *GCB Bioenergy*, 12(3):186–197, 2020.
- 2176 Arne Sellin. Sapwood–heartwood proportion related to tree diameter, age,
2177 and growth rate in *Picea abies*. *Canadian Journal of Forest Research*, 24
2178 (5):1022–1028, 1994.

- 2179 KP Shine, RG Derwent, DJ Wuebbles, and JJ Morcrette. Radiative forcing of
2180 climate in climate change: The IPCC scientific assessment, report prepared
2181 for the Intergovernmental Panel on Climate Change by working group 1,
2182 1990.
- 2183 Ekaterina Shorohova, Timo Kuuluvainen, Ahto Kangur, and Kalev Jõgiste.
2184 Natural stand structures, disturbance regimes and successional dynamics
2185 in the Eurasian boreal forests: a review with special reference to Russian
2186 studies. *Annals of Forest Science*, 66(2):1–20, 2009.
- 2187 Carlos A Sierra and Markus Müller. A general mathematical framework for
2188 representing soil organic matter dynamics. *Ecological Monographs*, 85(4):
2189 505–524, 2015. doi: 10.1890/15-0361.1.
- 2190 Carlos A Sierra, Markus Müller, Holger Metzler, Stefano Manzoni, and Su-
2191 san E Trumbore. The muddle of ages, turnover, transit, and residence
2192 times in the carbon cycle. *Global Change Biology*, 23(5):1763–1773, 2017.
- 2193 Carlos A Sierra, Verónica Ceballos-Núñez, Holger Metzler, and Markus
2194 Müller. Representing and understanding the carbon cycle using the theory
2195 of compartmental dynamical systems. *Journal of Advances in Modeling
2196 Earth Systems*, 2018. doi: 10.1029/2018MS001360.
- 2197 Carlos A Sierra, Susan E Crow, Martin Heimann, Holger Metzler, Ernst-
2198 Detlef Schulze, et al. The climate benefit of carbon sequestration. *Biogeosciences*, 2021.
- 2200 Carlos A Sierra, V Ceballos-Núñez, . Hartmann, D Herrera-Ramírez, and
2201 H Metzler. Ideas and perspectives: Allocation of carbon from net primary
2202 production in models is inconsistent with observations of the age of respired
2203 carbon. *EGUphere*, 2022:1–19, 2022. doi: 10.5194/egusphere-2022-
2204 34. URL <https://egusphere.copernicus.org/preprints/egusphere-2022-34/>.

- 2206 Jouni Siipilehto. A comparison of two parameter prediction methods for
2207 stand structure in Finland. 2000.
- 2208 Jouni Siipilehto and Annika Kangas. Näslundin pituuskäyrä ja siihen perus-
2209 tutvia malleja läpimitan ja pituuden välisestä riippuvuudesta suomalaisissa
2210 talousmetsissä. 2015.
- 2211 Frank F Sterck, Marleen AE Vos, S Emilia SE Hannula, Steven SPC
2212 de Goede, Wim W de Vries, Jan J den Ouden, Gert-Jan GJ Nabuurs,
2213 Wim WH van der Putten, and Ciska GF Veen. Optimizing stand density
2214 for climate-smart forestry: A way forward towards resilient forests with
2215 enhanced carbon storage under extreme climate events. *Soil Biology and*
2216 *Biochemistry*, 162:108396, 2021.
- 2217 Timo Tahvanainen and Eero Forss. Individual tree models for the crown
2218 biomass distribution of Scots pine, Norway spruce and birch in Finland.
2219 *Forest ecology and management*, 255(3-4):455–467, 2008.
- 2220 Tea Thum, Silvia Calderaru, Jan Engel, Melanie Kern, Marleen Pallandt,
2221 Reiner Schnur, Lin Yu, and Sönke Zaehle. A new model of the coupled car-
2222 bon, nitrogen, and phosphorus cycles in the terrestrial biosphere (QUINCY
2223 v1.0; revision 1996). *Geoscientific Model Development*, 12(11):4781–4802,
2224 2019.
- 2225 María Triviño, Alejandra Morán-Ordoñez, Kyle Eyvindson, Clemens Blat-
2226 tert, Daniel Burgas, Anna Repo, Tähti Pohjanmies, Lluís Brotons, Tord
2227 Snäll, and Mikko Mönkkönen. Future supply of boreal forest ecosystem
2228 services is driven by management rather than by climate change. *Global*
2229 *Change Biology*, 29(6):1484–1500, 2023.
- 2230 M Th Van Genuchten. A closed-form equation for predicting the hydraulic
2231 conductivity of unsaturated soils. *Soil science society of America journal*,
2232 44(5):892–898, 1980.

- 2233 Heidi Vanhanen, Ragnar Jonsson, Yuri Gerasimov, Olga Krankina, Christian
2234 Messieur, et al. Making boreal forests work for people and nature. 2012.
- 2235 Petteri Vanninen and Annikki Mäkelä. Carbon budget for Scots pine trees:
2236 effects of size, competition and site fertility on growth allocation and pro-
2237 duction. *Tree Physiology*, 25(1):17–30, 2005.
- 2238 Petteri Vihervaara, Timo Kumpula, Ari Tanskanen, and Benjamin Burkhard.
2239 Ecosystem services—A tool for sustainable management of human–
2240 environment systems. Case study Finnish Forest Lapland. *Ecological com-*
2241 *plexity*, 7(3):410–420, 2010.
- 2242 YP Wang, RM Law, and Bernard Pak. A global model of carbon, nitrogen
2243 and phosphorus cycles for the terrestrial biosphere. *Biogeosciences*, 7(7):
2244 2261–2282, 2010.
- 2245 Thomas Wutzler. Effect of the aggregation of multi-cohort mixed stands on
2246 modeling forest ecosystem carbon stocks. *Silva Fennica*, 42(4):535–553,
2247 2008.
- 2248 Rasoul Yousefpour, Andrey Lessa Derci Augustynczik, Christopher PO
2249 Reyer, Petra Lasch-Born, Felicitas Suckow, and Marc Hanewinkel. Re-
2250 alizing mitigation efficiency of European commercial forests by climate
2251 smart forestry. *Scientific reports*, 8(1):1–11, 2018.
- 2252 Tiia Yrjölä. *Forest management guidelines and practices in Finland, Sweden*
2253 *and Norway*. European Forest Institute, 2002.
- 2254 W. G. Zhao and R. J. Qualls. A multiple-layer canopy scattering model
2255 to simulate shortwave radiation distribution within a homogeneous plant
2256 canopy. *Water Resources Research*, 41(8):A08409, 2005.